UNIVERSITY OF CAPE TOWN

FACULTY OF SCIENCE

DEPARTMENT OF ENVIRONMENTAL AND GEOGRAPHICAL SCIENCE

Research Dissertation for the Degree of:

Master of Science

Environmental and Geographical Sciences

An analysis of nature-based treatment processes for cleaning contaminated surface water runoff from an informal settlement: a case study of the Stiebeuel River catchment, Franschhoek, South Africa

By Emily Nicklin

Supervisor: Dr Kevin Winter

DECLARATION

1. I know that plagiarism is a serious form of academic dishonesty.

2. I have read the document about avoiding plagiarism, I am familiar with its contents, and I have avoided all forms of plagiarism mentioned there.

3. Where I have used the words of others, I have indicated this using quotation marks.

4. I have referenced all quotations and other ideas borrowed from others.

5. I have not and shall not allow others to plagiarise my work.

NAME: _____Emily Nicklin_____

SIGNATURE: Signed by candidate

DATE: _____8 September 2021_____

ACKNOWLEDGEMENTS

ABSTRACT

Contaminated surface water runoff from inadequate drainage and sanitation systems in informal settlements threaten the quality of available freshwater and can negatively impact both human and environmental health. Biofiltration systems (biofilters) provide water pollution controls without inputs of additional energy and chemicals, placing them in the overall context of the need for affordable and sustainable stormwater infrastructure in informal settlements. In addition, cleaned waters from biofilters may be suitable for some reuse applications if they are well-designed and maintained. However, most research is conducted in developed countries where heavy metals are the main surface water pollutant. Consequently, little is known about the extent to which biofilters can be used to meet the water quality targets in conditions likely to be found in informal settlements. In addition, no attempts have been made to recover or reuse the surface water runoff from informal settlements, despite its high nutrient loadings. This study analyses the extent to which biofilters can be used to clean and reuse contaminated surface water runoff from informal settlements. The objectives are threefold: (i) to analyse the performance of two field-scale biofiltration cells (one vegetated and one non-vegetated) that are batch-fed with surface water runoff from an upstream informal settlement; (ii) to determine the effects of varying operating, design and environmental parameters on the performance of the cells; and (iii) to develop a model which predicts the outflow pollutant concentrations under varying conditions. Both cells effectively reduced ammonia (NH_3), Total Phosphate (TP) and *Escherichia coli* (*E. coli*) concentrations, but leached nitrate (NO_3^-) and nitrite (NO_2^-). The treated waters were suitable for irrigational reuse, however, additional disinfection was required to reduce faecal contamination in some cases. Correlation analyses showed that inflow water quality significantly influenced cell performance, with the vegetated cell outperforming the non-vegetated cell under higher inflow pollutant concentrations. Multiple regression models also investigated several parameters influencing outflow NH_3 and showed that inflow pH, temperature and NH_3 concentration can be used to determine the outflow NH_3 concentration of the cells. These models are important for predicting cell performance and thus can be used to improve the design and/or operation of the cells for varying inflow water quality conditions.

CONTENTS

LIST OF FIGURES

LIST OF TABLES

CHAPTER 1: INTRODUCTION

1.1. Overview

Engineering natural processes to clean contaminated surface water runoff has emerged as a passive, low-cost and publicly accepted approach to reduce environmental pollutants (Oral et al., 2020). This approach is broadly placed under the umbrella concept of 'Nature-based Solutions (NBS)', which the European Commission defines as "solutions that are inspired and supported by nature, which are cost-effective, simultaneously provide environmental, social and economic benefits and help build resilience" (European Commission, 2015). Similarly, the International Union for Conservation (IUCN) describes NBS as "actions to protect, sustainably manage and restore natural or modified ecosystems that address societal challenges effectively and adaptively, simultaneously providing human well-being and biodiversity benefits" (Cohen-Shacham et al., 2016). These descriptions highlight the role of NBS in improving biodiversity and facilitating the delivery of ecosystem services, however, they also recognise the plurality of social, economic and environmental benefits provided by NBS (Dumitru and Wendling, 2021).

At present, the most effective way to implement NBS is through 'blue-green infrastructure' (BGI), which Brears (2018) describes as "a strategically planned network of high-quality natural and semi-natural features that are designed to deliver a wide range of ecosystem services and protect biodiversity". The concept of BGI builds on traditional stormwater management (Fletcher et al., 2014) and has become fundamental to the integration of landscape multifunctionality in policy and planning (Pappalardo et al., 2017). It is based on the fundamental concept of mimicking the natural hydrology of the area and therefore follows the basic principles and objectives of low impact development (LID). These include reducing runoff volumes, minimising peak flows, recharging groundwater and increasing evapotranspiration (Hunt et al., 2008).

In addition to hydrologic control, BGI provides water quality treatment by reducing the mass of pollutants entering surface and groundwater bodies without inputs of additional energy and chemicals (Oral et al., 2020). This is achieved by mimicking natural wetland systems and therefore involves interactions among plants, substrate, biofilm, nutrients and atmosphere (Boano et al., 2020). These interactions favour different pollutant removal mechanisms, for

example, physical removal processes (e.g., filtration and sedimentation), chemical removal processes (e.g., adsorption and precipitation) and biological removal processes (e.g., plant uptake and microbiological degradation) (Arden and Ma, 2018). Therefore, the removal mechanisms influence the pollutant removal efficiencies of BGI and are ultimately responsible for improving the quality of surface water runoff.

BGI also create innovative opportunities to use water more efficiently and effectively. Previous research has shown that BGI has the potential to recover resources from urban water runoff (Kisser et al., 2020). These recoverable resources range widely from reclaimed water for agricultural (e.g., crop fertigation and irrigation), residential (e.g., sanitary flushing), industrial (e.g., cooling water) and urban (e.g., park irrigation and crop production) purposes to groundwater recharge (Masi et al., 2018). Therefore, BGI has the potential to promote resource circularity by slowing, closing and narrowing material loops, thereby minimising resource inputs and waste (Pappalardo et al., 2017). This can encourage the sustainable use of natural resources and support sustainable development objectives (Pearlmutter et al., 2020), which has broader implications for climate change mitigation and adaptation (Pappalardo et al., 2017; Oral et al., 2020; Pearlmutter et al., 2020).

Although the benefits of BGI are being increasingly recognised, their success ultimately depends on the adaptation of BGI to local conditions. This sentiment is shared among several researchers who argue that most BGI research is based in developed countries and therefore has little applicability in the context of developing countries (Kivaisi, 2001; Milandri et al., 2012; Zhang et al., 2014). Consequently, more research is needed to support the application of NBS for cleaning and reusing surface water runoff in developing countries.

Arguments for advancing BGI in developing countries usually recognise the need for low-cost infrastructure that is passive and is easy to construct, operate and manage (Kivaisi, 2001; Zhang et al., 2014; Milandri et al., 2012). South Africa provides an ideal opportunity to showcase the benefits of BGI, as challenges regarding access to public services, health impacts, over-exploitation and pollution of water resources, and leakage/wastage in some urban water distribution systems are widespread across the country, especially in catchments occupied by informal settlements (Carden et al., 2018; Armitage et al., 2009).

Previous studies have shown that surface water discharges from informal settlements are usually highly polluted and contain Chemical Oxygen Demand (COD) concentrations between

2

1500 and 8500 mg/L, oil and grease concentrations between 30 and 2000 mg/L, conductivity between 50 and 1500 mS/m and bacteriological counts that are often similar to that of raw sewage (Carden et al., 2007; Armitage et al., 2009). Therefore, without proper treatment, surface water discharges from informal settlements threaten the quality of available freshwater and can have negative impacts on both human and environmental health.

Biofiltration systems (which are referred to as biofilters throughout the thesis) represent the most promising NBS for removing environmental pollutants to date (Oral et al., 2020). Biofilters can effectively remove pollutants including organic and inorganic matter, nutrients and pathogens from contaminated surface water (Saeed and Sun, 2012). Reduction is generally achieved through various treatment modules which are similar to the processes found in natural wetlands (Roy-Poirier et al., 2010). However, the extent to which these treatment processes remove pollutants depends, among other factors, on the type of biofilter used, the quantity and quality of water and local climate conditions (Oral et al., 2020).

In general, biofilters have shown a consistent removal of heavy metals, Total Suspended Solids (TSS) and Total Phosphorus (TP) (Bratieres et al., 2008; Henderson et al., 2007; Davis et al., 2006; Davis, 2008), however, total nitrogen removal (TN) has ranged considerably due to nitrate (NO_3^-) leaching (Hathaway et al., 2011; Zinger et al., 2011). For example, Bratieres et al. (2008) emphasised the significance of designing a biofiltration treatment train, as the removal of each pollutant is determined by a combination of different factors. For example, if TN reduction is the main objective, then the layout and configuration of the treatment train, as well as the plant and soil type, must be designed to prevent NO_3^- leaching (Davis et al., 2006). However, Davis et al. (2001) showed that organic matter enhanced the removal of heavy metals in biofilters, but also resulted in nutrient leaching. Several papers have also indicated that biofilters consistently removed at least 80% of TP and TSS, regardless of the treatment train design (Bratieres et al., 2008; Henderson et al., 2007). Therefore, although biofiltration is a widely accepted treatment method, knowledge gaps regarding the effects of design and operation on the removal of pollutants by biofilters still exist. More research on underlying biofiltration processes is thus required to improve the performance of these systems.

The literature also highlights several other knowledge gaps in biofiltration research. Firstly, although research demonstrates that biofilters can successfully reduce runoff volumes and

improve runoff water quality, there is limited research on the extent to which these systems can meet the water quality targets in conditions likely to be found in informal settlements. Biofilters have been used to clean domestic sewage in developing countries (Mburu et al., 2013), however, they have also been used to clean other types of wastewaters, including agricultural wastewater (Lee et al., 2004), industrial wastewater (Chen et al., 2006; Maine et al., 2007), stormwater runoff (Sim et al., 2008) and landfill leachate (Nahlik and Mitsch, 2006), among other types (Zhang et al., 2014). This suggests that the application of biofilters could be extended to informal settlements, as surface water conditions in these areas are often comparable to that of wastewater (Carden et al., 2007; Armitage et al., 2009). However, more evidence is needed to confirm this.

Secondly, although studies have indicated that treated waters from biofilters may be suitable for some reuse applications, there is limited research on the extent to which treated waters can be reused, for example, to irrigate vegetables. Some emerging studies have shown that biofilters can be integrated with other engineered solutions, such as anaerobic processes, to meet strict water reuse regulations (Kisser et al., 2020). For example, the EU-funded project HYDROUSA incorporated biofilters with up-flow anaerobic sludge blankets (UASB) to treat domestic sewage and reuse the nutrients for agricultural purposes (Kisser et al., 2020). Similarly, the HOUSEFUL project used biofilters to treat domestic wastewater and reuses the nutrient-rich water to irrigate food crops in greenhouses (Bertino et al., 2018). However, there has been no attempt to recover and/or reuse the runoff from informal settlements, despite its high nutrient loadings. This is largely due to concerns regarding the elevated COD concentrations and presence of pathogens such as *Escherichia Coli* (*E. coli*), which are potentially harmful to human health (Carden et al., 2007; Armitage et al., 2009). Therefore, more evidence is needed to confirm the extent to which biofilters can be used to safely recover and/or reuse the runoff from informal settlements.

1.2. Research aim and objectives

This research aims to determine the extent to which biofilters can be used to clean and reuse contaminated surface water runoff from informal settlements. The objectives to achieve this aim were:

- To analyse the performance of two field-scale biofiltration cells (one vegetated and one non-vegetated) that are batch-fed with surface water runoff from an upstream informal settlement.
- To determine the effects of various operating conditions (hydraulic retention time), design parameters (presence of vegetation) and environmental factors (rainfall, temperature, evaporation, evapotranspiration and inflow water quality) on the performance of the cells.
- To develop a multiple linear regression model for predicting the outflow ammonia (NH_3) and Total Phosphate (TP) concentrations of the cells under varying conditions.

1.3. Study site

The biofiltration system is located at a research and demonstration site known as the Water Hub. The Water Hub was established on an abandoned wastewater treatment plant roughly 3 km west of the formal town of Franschhoek, and less than 800 m south of a low-cost housing area and informal settlement. Franschhoek is situated in a Mediterranean climate region with seasonal precipitation and warm, dry summers and cool, wet winters. The average annual rainfall is 863 mm, 80% of which falls between April and September (De Clerq et al., 2006).

The separation of the formal town of Franschhoek and lower-income settlements represents the spatial divide resulting from the Apartheid era in South Africa. La Motte (lower reaches), Groendal (middle reaches) and Langrug (upper reaches) developed because of Apartheid laws of separate development based on racial classification. These lower-income settlements, along with the Water Hub, are positioned in the Stiebeuel River catchment (Figure 1).
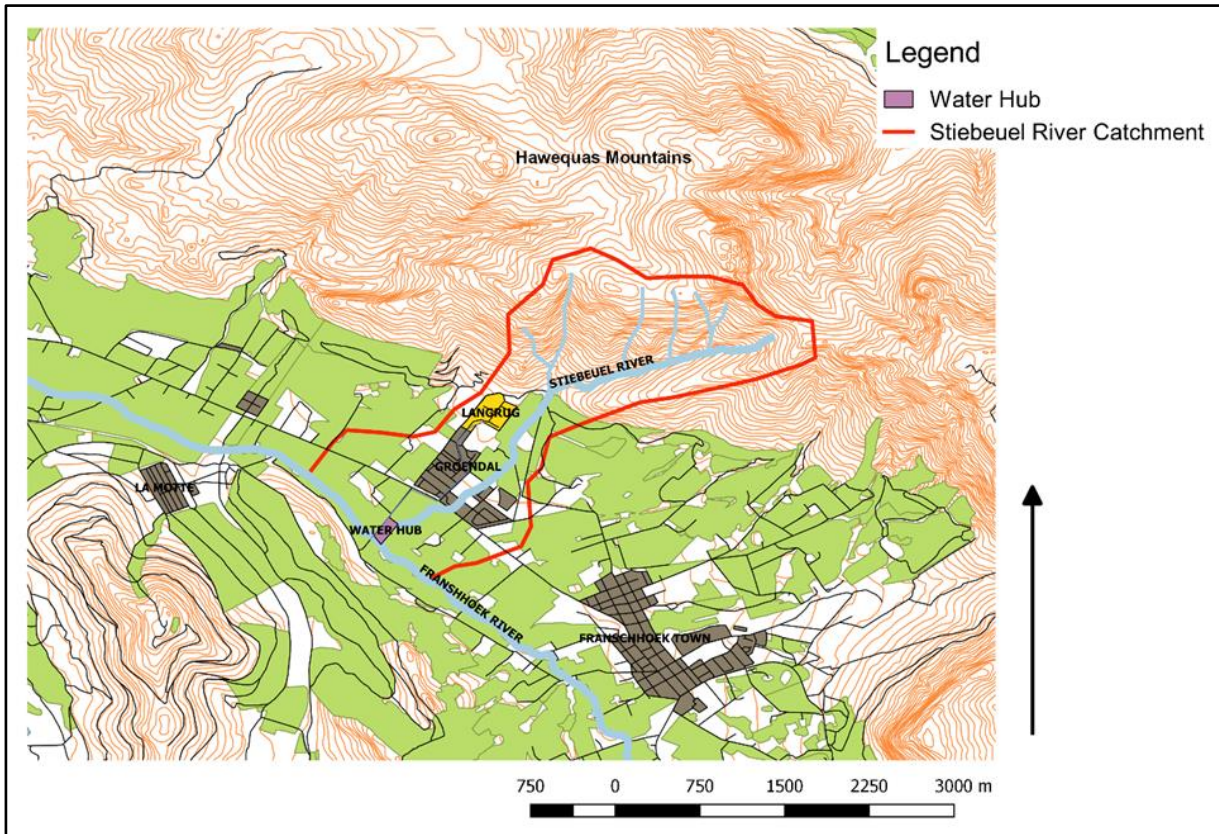
Figure 1: Map of the Stiebeuel River catchment, settlements and location of the Water Hub (National Geo-spatial Information, 2021).

The Stiebeuel River catchment drains an area of approximately 4.69 km². The Stiebeuel River flows through the Water Hub before its confluence with the larger Franschhoek River. The river originates in the Hawequas mountains and flows alongside the informal settlement of Langrug (Armitage et al., 2009). Langrug consists of densely packed shack dwellings constructed from various makeshift materials including iron, wood and plastic sheeting (Armitage et al., 2009). By comparison, the low-income settlement of Groendal is characterised by formal housing structures, tarmacadam roads and basic stormwater infrastructure.

According to the Stellenbosch municipality, the local authority for the area, the total population of Langrug informal settlement in 2011 was 4,864 people, with a total number of 1,807 informal dwellings that share 150 waterborne ablution toilets (Stellenbosch Municipality, 2011). Population numbers have rapidly increased over the years, however, there is no recent census data available.

Previous research has shown that limited or absent formal sewerage and stormwater infrastructure in the settlement often leaves residents with no option but to dispose of their unwanted waste and/or water close to their dwellings (Armitage et al., 2009). This results in the accumulation of organics at the surface, which causes soil clogging and reduces the potential for infiltration, leading to the continual discharge of contaminated runoff into the Stiebeuel River. This has negative consequences for the water quality of the river, particularly in the form of nutrient contamination (Fell, 2018).

This study focuses on the contaminated surface water runoff from Langrug informal settlement. Elevated concentrations of nutrients, microbiological and other emerging pollutants from dysfunctional limited and/or dysfunctional sewerage and stormwater infrastructure in the settlement are discharged into the Stiebeuel River. The downstream location of the Water Hub, therefore, provided an ideal opportunity to investigate the capabilities and limitations of biofilters for cleaning contaminated surface water runoff from informal settlements.

1.4.   The biofiltration system

The Water Hub research and demonstration site received initial funding from the Western Cape government in 2013 and was set up by the Future Water Institute (University of Cape Town) in partnership with the Stellenbosch municipality (the landowners of the site). Before 2013, the site was operated by the municipality as the Franschhoek Wastewater Treatment Works but was later converted into a centre for research in sustainable drainage systems (SuDs). The local government acquired the services of Isidima, a small consulting engineering company, and in partnership with the Future Water Institute, drafted a conceptual plan for converting the site into a research and demonstration centre. The plan included converting the old drying beds from the treatment plant into a biofiltration system, which would later be used to clean surface water runoff from Langrug informal settlement. The treated waters would then be reused to irrigate vegetables. This system has been in operation since 2017.

The biofiltration system includes 6 rectangular treatment cells, each measuring 16 m long, 3 m wide and 0.73 m deep, with a surface area of approximately 48 m^2 and a total volume of approximately 8811 L. A diagrammatic representation of the cell dimensions and layout is shown in Figure 2. The cells are lined with low-density polyethene (LDPE) sheets (i.e.,

waterproof material) to prevent the loss of any water from the cells and are filled with an assortment of natural media, including large stone aggregates (19–25 mm diameter), small stone aggregates (7–9 mm diameter) and peach pips. These media were selected for infiltration purposes and because they provide a suitable substrate for plant and microbial growth.
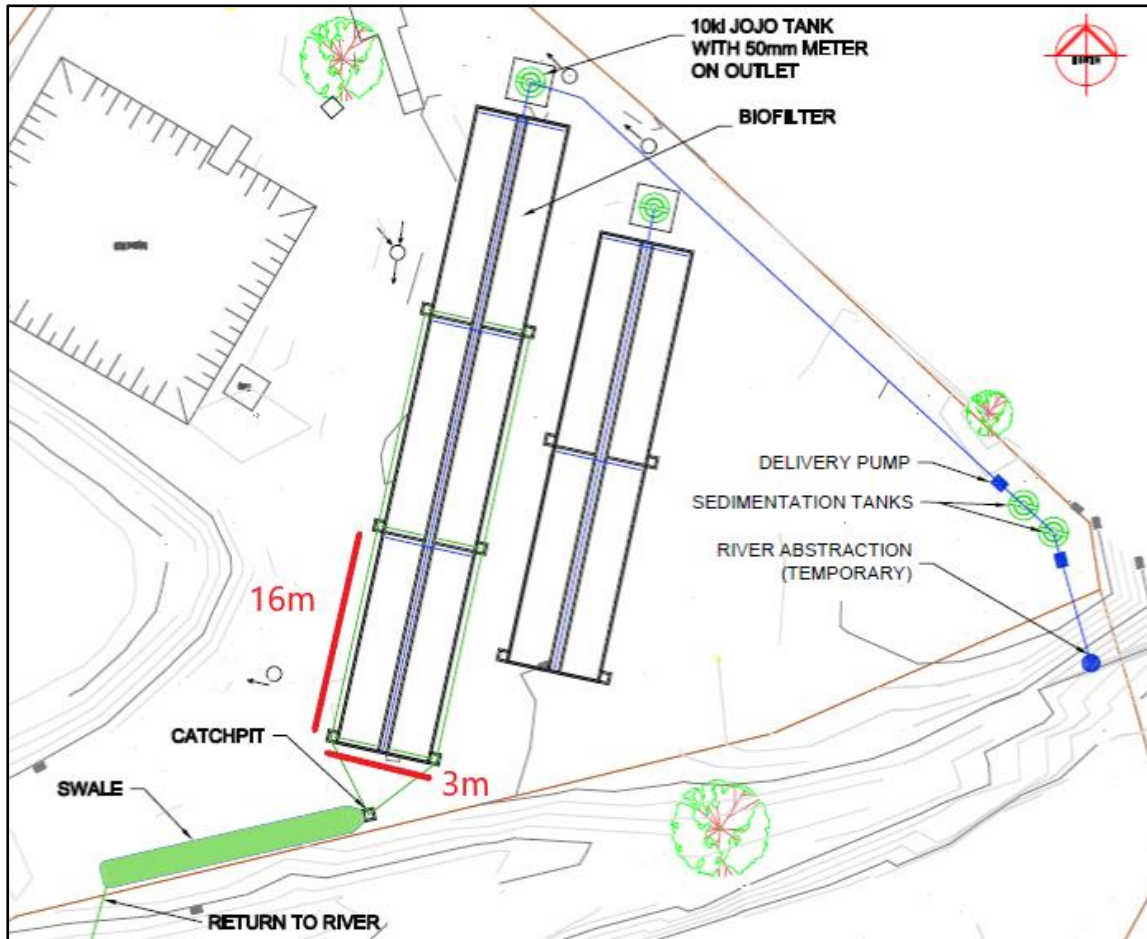
Figure 2: Cell dimensions and layout of the biofiltration system at the Water Hub (Isidima, 2017).

Two 10,000 L water tanks are connected to the inlet pipe of the cells. These tanks store water that has been abstracted and pumped from the Stiebeuel River, allowing coarser sediment particles to settle at the bottom of the tanks. This helps extend the design life and reduces replacement maintenance of the biofiltration system (Woods-Ballard et al., 2007). Water is pumped from these tanks directly into the cells. A rock trench consisting of large stones (35–50 cm diameter) is situated at the inlet and outlet ends of each cell. These rocks ensure that the water is evenly distributed at the inlet and outlets (Vymazal, 2005a).

The inflow to each cell is controlled by a network of pipes and valves (Figure 3). The U-bend in the outlet pipe was used to ensure that the volume of water in each cell remains approximately 3–5 cm from the surface of the cell medium (Figure 4). Water is released from the cell by removing the U-bend coupling.
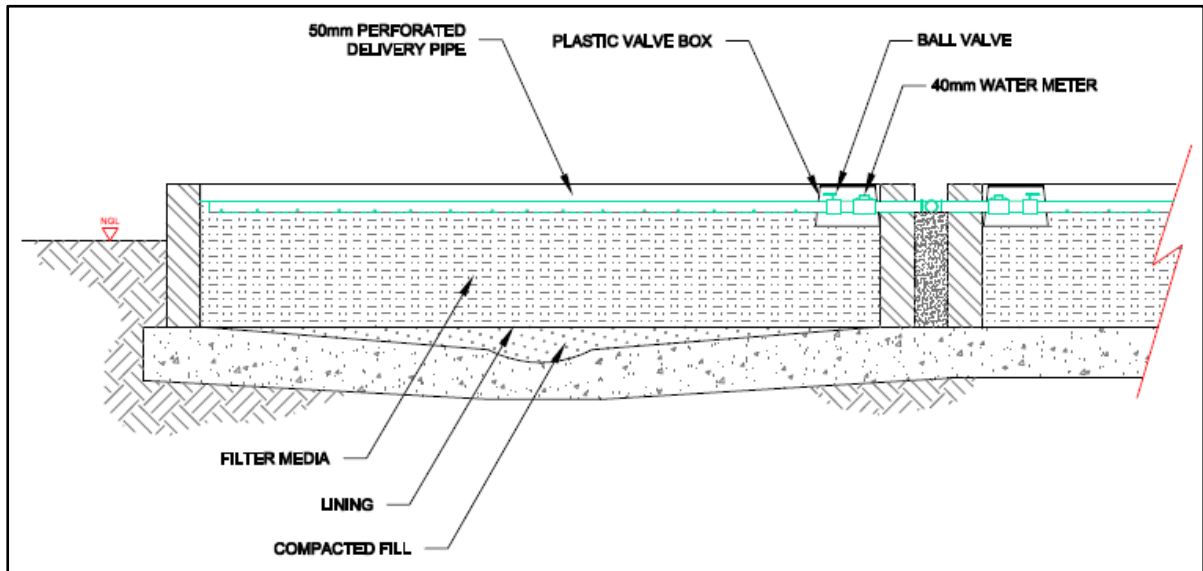
Figure 3: Inlet section detail of the cell (Isidima, 2017).
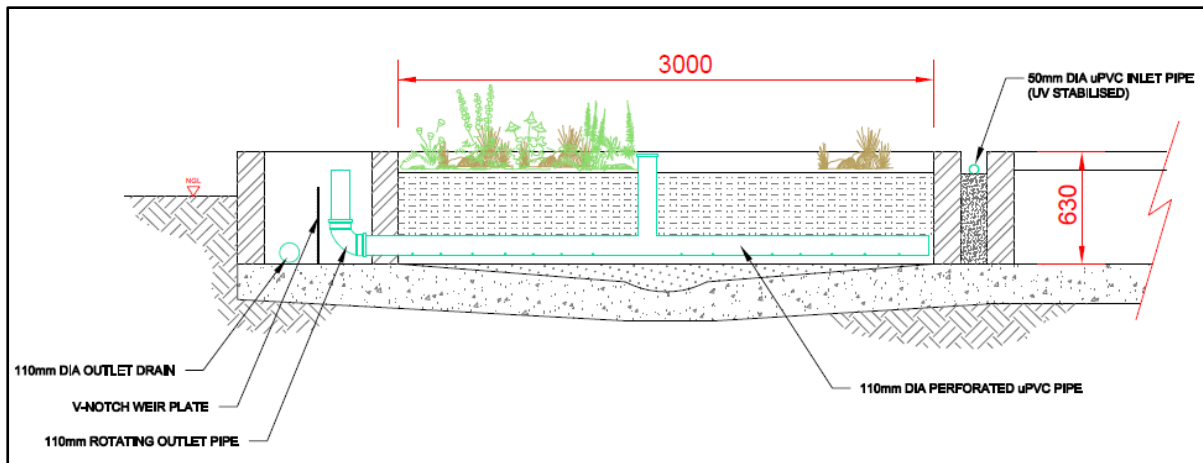
Figure 4: Outlet section detail of the cell (Isidima, 2017).

Most of the flow passes through the porous media of the cells and the predominant flow direction is horizontal (Figure 5). Hence, the system is classified as a horizontally-orientated, subsurface flow wetland (Fonder and Headley, 2013).
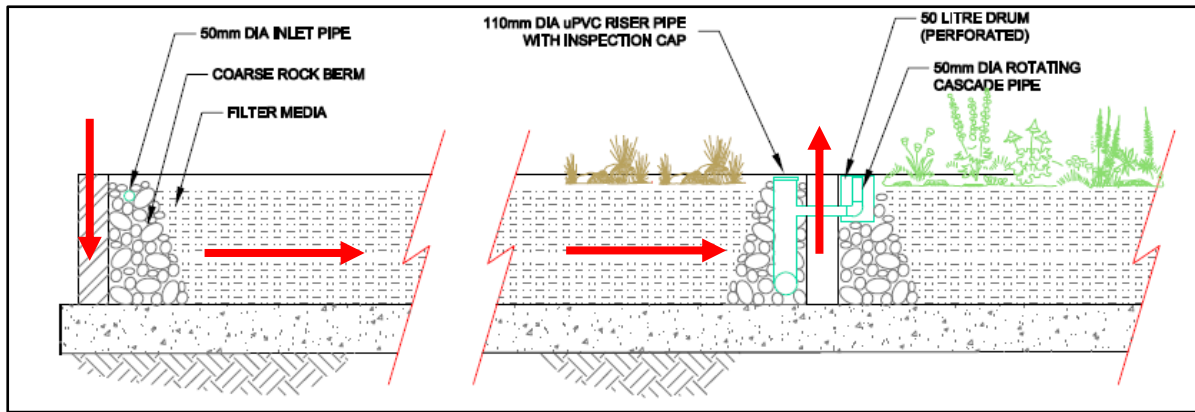
Figure 5: Longitudinal section detail with arrows indicating the predominant horizontal, subsurface flow (Isidima, 2017).

Three out of the six cells are planted with indigenous wetland species including *phragmites australis, typha capensis* and *cyperus textilis*. These plants were selected because they have the potential to readily absorb environmental pollutants such as heavy metals and nutrients and can survive a variety of environmental conditions (Milandri et al., 2012).

1.5. Overview of study design and methods

The study design incorporates two distinct research activities to analyse the performance of two field-scale biofiltration cells in the present – through water quantity and quality analyses – and the future – through multiple regression modelling. Data collection for both research activities was conducted between November 2020 and March 2021. An experiment was designed to determine the effects of three main treatment factors: (i) hydraulic retention time (HRT), (ii) vegetation and (iii) inflow water quality on the performance of the cells. The effects of multiple environmental variables (rainfall, evaporation, evapotranspiration and air temperature) were also determined using multiple linear regression analyses. These variables were then used to develop a multiple linear regression model which predicts the performance of the cells under varying conditions.

1.6.   Limitations

The study was limited by not continuously monitoring the water quality and quantity of the biofiltration cells over the 7-day retention period. Consequently, the results did not indicate the variability between sample intervals, during which interesting patterns may have emerged. In addition, the exclusion of water quality parameters such as contaminants of emerging concern (CEC), TSS and heavy metals meant that the study could not account for the accumulation of these pollutants in the cells. Therefore, the potential impacts of these pollutants on the performance of the cells were not considered. Furthermore, the study did not consider the effects of other potentially influential environmental parameters, such as dissolved oxygen (DO), which limited the assumptions about the performance of the cells under varying environmental conditions.

While a mass balance is regarded as the ideal performance metric, the main challenge in this study was the uncertainty around how much water and what quality of water would be introduced into the supply tank and then into each cell. This is largely due to the nature of the field site which receives variable runoff water quality depending on upstream activities in the informal settlement. Further, it is impossible to achieve an accurate mass balance at the field scale given the time it takes to fill the supply tanks and distribute the water to the cells. Mass balances need to be accurate for the water quality in the inflow, the same water quality to the cell and then release after treatment. This would allow an accurate measurement of the change in water quality.

The findings are limited to the summer dry period, as the weather conditions of the winter months were not considered by the study. Although rainfall was included in the regression analyses, very few rainfall days were captured during the monitoring period, which meant that the study could not fully account for the effects of rainfall on the performance of the cells. Therefore, the model predictions are only applicable during the summer dry period when minimal rainfall occurs.

The ET estimates were calculated using a reference ET model and therefore relied on local meteorological data. The closest weather station was in Franschhoek town centre, approximately 2 km away from the Water Hub and biofiltration cells, which may have reduced the accuracy of the ET estimates.

Another key limitation was the mode of operation. The cells could only be operated under a batch feeding mode due to site constraints (limited power supply), which limits our understanding of the cell performance under other operating modes (for example, continuous flow). Furthermore, the relationship between HRT and performance was analysed by retaining the water in the cells for a specified period and analysing the outflow water quality over this period. This meant that the study did not consider the effects of HRT with respect to hydraulic loading rate, an approach used by many biofiltration studies to analyse the relationship between HRT and cell performance. This made it difficult to directly compare the results from this study to the results of other studies. It also limits the findings to batch-fed systems, which are less common than continuous flow systems. Nevertheless, batch-fed systems are easier to operate in informal settlements where access to power is generally limited.

CHAPTER 2: LITERATURE REVIEW

2.1.   Biofiltration systems in the form of constructed wetlands

Researchers often refer to biofilters as 'Constructed Wetlands (CWs)', which Saeed and Sun (2012a) describe as "engineered wetlands that have a saturated or unsaturated substrate, floating/emergent/submergent vegetation and a wide variety of microbial communities that are purposely built for water pollution control" (Saeed and Sun, 2012). Although biofilters perform similar functions to natural wetlands, for example, runoff reduction and pollutant control, they are designed to maximise all available biological, physical and chemical processes in the system (Roy-Poirier et al., 2010). Therefore, biofilters have the unique advantage of reducing and improving the water quality of contaminated surface water runoff without the input of additional chemicals or energy (Sim et al., 2008).

A similar comparison is made by Fonder and Headley (2013), who describe planted surface systems (biofilters) as a type of CW. However, the authors extend the definition by classifying the systems into different types of CWs, depending on their flow characteristics. According to Fonder and Headley (2013), the two main types of CWs are surface flow (SF) and subsurface flow (SSF) wetlands. SF wetlands are most comparable to natural wetlands due to the shallow flow of water (<60 cm deep) over a saturated substrate, whereas SSF wetlands mostly utilise coarse material (e.g., gravel) as the main substrate to support the growth of plants, with water flowing in either a horizontal or vertical direction through the filter media. Therefore, SSF wetlands are further classified into vertical flow (VF) and horizontal flow (HF) wetlands (Fonder and Headley, 2013).

Previous research suggested that SSF wetlands, in comparison to SF wetlands, are more effective at removing pollutants (Vymazal, 2005b). However, more detailed studies indicated that a combination of both HF and VF wetlands are the most effective in terms of organics and nitrogen removal, largely because of the aerobic and anaerobic phases present in the system (Kadlec and Wallace, 2008). Nevertheless, pollutant removal efficiencies are strongly influenced by the quantity and quality of infiltrating runoff, as well as the local climate conditions (Oral et al., 2020). Therefore, empirical evidence grounded in the local context is imperative to establish the 'true' performance of a biofilter (Milandri et al., 2012).

This study focuses on biofilters in the form of HF wetlands, and thus the literature review largely draws on research conducted on HF wetlands. Although HF wetlands differ from other types of wetlands (both in terms of layout and configuration), the pollutant removal processes are largely the same across all wetland types (Kadlec and Wallace, 2008). The following section, therefore, provides a broad overview of these pollutant removal processes.

2.2. Pollutant removal processes in biofiltration systems

Unlike conventional water treatment technologies, biofilters typically utilise vegetation, natural filter media (soil, gravels, crushed rock, sand) and associated microbial assemblages to clean contaminated water (Jurries, 2003). Collectively, these components enhance pollutant removal in biofilters, however, their relative importance remains highly contested among researchers. For some, the filtration media is most important because it controls the biological removal (microbial decay), chemical removal (adsorption) and physical removal (filtration, sedimentation) of pollutants (Jurries, 2003; Davis et al., 2006; Hatt et al., 2007). Others argue that the vegetation is more important because it promotes pollutant removal through phytoremediation and evapotranspiration (Henderson et al., 2007; Chandrasena et al., 2014; Rycewicz-Borecki et al., 2017). However, Garcia et al. (2010) highlighted that the major removal process ultimately depends on the target pollutant in question. Therefore, the following paragraphs focus on phosphorus (P), nitrogen (N) and *E. coli* and their respective removal processes, as these were selected as the main target pollutants in the study.

N removal is a significant process in biofilters, with many full-scale biofilters being designed specifically for this purpose (Garcia et al., 2010). Vymazal (2007) noted that the processes involved in removing N may vary depending on the dominant N chemical species. Typically, organic N, ammonia N, nitrate (NO_3^-) and nitrite (NO_2^-) are the dominant forms of N involved in the N cycle of biofilters (Borin and Tocchetto, 2007; Mayo and Mutamba, 2004). Accordingly, the major removal mechanisms include nitrification, denitrification, ammonification, plant and microbial uptake, adsorption/desorption, NH_3 oxidation and leaching (Vymazal, 2007). Denitrification is often cited as the main N removal process in well-established biofilters, however, different microbial N removal processes, including NH_3 oxidation, could have a greater effect in biofilters designed to clean NH_4^+-rich runoff (Tanner, 2004). In general, NO_3^- reduction is the dominant removal process in SSF biofilters, largely

because of prevailing anaerobic conditions, however, a combination of multiple removal processes usually occurs (Kadlec et al., 2005).

P is largely removed via microbial removal, plant uptake and harvesting, as well as adsorption/desorption and chemical precipitation (Garcia et al., 2010). However, unlike denitrification, microbial P removal shows no similar sink, as bacteria can only provide temporary storage and/or removal. This process is partly reversible due to the continuous cycle of bacterial growth, die-off and/or decay, which releases most of the assimilated P. Plant uptake of P is also limited in biofilters, about 6% of the inflow load (Davies and Cottingham, 2020), while the degree of P adsorption by the filter media depends on its texture and grain size distribution, as well as the iron (Fe), aluminium (Al) and calcium (Ca) content (Garcia et al., 2010).

Past research suggests that adsorption/desorption and straining, adsorption play a fundamental role in removing faecal microorganisms in saturated biofilters, (Rusciano and Obropta, 2007; Zhang et al., 2012), whereas inactivation and die-off are more significant in non-saturated biofilters (Chandrasena et al., 2014). However, vastly different removal performances have been reported at both the field and laboratory scales (Li and Davis, 2009; Hathaway et al., 2011; Zhang et al., 2012), suggesting that knowledge gaps regarding bacterial removal still exist.

2.3. Hydrologic performance of biofiltration systems

2.3.1. Overview

Research on the hydrologic performance of biofilters generally focuses on the overall runoff reduction capabilities of biofilters under different storm events (EPA, 2000). The aim here is to demonstrate that biofilters can mimic greenfield runoff rates (defined by reduced runoff volumes and peak flows). Typically, biofilters reduce runoff volumes via infiltration, exfiltration, evapotranspiration (ET) and evaporation (Roy-Poirier et al., 2010). These processes are akin to those occurring in natural wetlands, and therefore enable biofilters to mimic the natural hydrologic cycle.

Several studies have shown that biofilters can improve watershed hydrology (Davis et al., 2001; Davis, 2008; Dietz and Clausen, 2005; Hunt et al., 2008). However, quantifying these

hydrologic benefits in field situations is often complicated by the variation in design and rainfall characteristics, resulting in a wide variation of reported performance values. Surface water runoff reductions usually range between 70–90% (Davis, 2008), 30–40% (Li et al., 2009) and 80% (Hatt et al., 2009), depending on seasonal conditions. However, these values are significantly reduced (13%, respectively) during winter months when ET and evaporation rates are lower (Hunt et al., 2008).

The quantification of hydrologic performance is not uniform across biofiltration research, making it difficult to compare individual studies. Many of the original studies on the hydrologic performance focused on the overall runoff reduction capabilities of biofilters, demonstrating that a majority of runoff produced by small rainfall events could be captured (EPA, 2000). However, the results did not capture the variability in performance between storm events. Subsequent research efforts were dedicated to capturing the existence of hydrologic performance, including its seasonal variability, and showed that design factors (e..g, layout and configuration, ponding depth, infiltration capacity, media composition) and environmental conditions (e.g., annual precipitation and potential ET) significantly influenced the hydrologic performance of biofilters (Hunt et al., 2008; Dietz and Clausen, 2005). Nevertheless, attempts to quantify these hydrologic processes had received limited research attention.

Initial attempts to quantify the hydrologic performance of biofilters involved the application of multiple hydrologic parameters, for example, Manning's roughness coefficient and the rational method's runoff coefficient, which were used to characterise pre-and post-development conditions (Davis et al., 2006; Davis, 2008). Although these parameters determined the hydrologic benefits of biofilters, they only broadly related to the impacts of vegetation on hydrologic performance, and therefore excluded ET from the overall water balances. By the mid-2000s, the significance of ET was being increasingly recognised, however, the relationship between biofiltration performance, ET and percolation processes were still poorly understood (Ahiablame et al., 2012). Conventional event-based approaches to modelling biofiltration water balances were also considered insufficient (Denich and Bradford, 2010), and thus a continuous modelling approach, along with advanced modelling tools, was introduced by Shi et al. (2011). The authors correlated mean actual precipitation, annual precipitation and potential ET using hydrologic data from 250 watersheds across the

world (Shi et al., 2011). This provided more detailed and accurate analyses of individual hydrologic processes. Similar approaches have since been utilised, however, performance values vary significantly depending on the biofilter used as well as local climate conditions.

Overall, there is considerable evidence to suggest that biofilters have the potential to shift the urban hydrologic condition towards a more natural state. However, more holistic modelling approaches to modelling biofiltration water balances, whereby individual processes (infiltration, exfiltration, ET and evaporation) are quantified, are recommended to adequately capture hydrologic performance. These approaches can improve our understanding of underlying biofiltration processes, and in turn, allow for design and/or operating enhancements. This study analyses lined biofilters, and thus exfiltration is not considered in the literature review. Instead, it focuses on infiltration, ET and evaporation as the main hydrologic processes influencing biofiltration performance. These processes are discussed in greater detail in the following sections of the literature review.

2.3.2. Runoff percolation in the biofilter

Biofilters divert the infiltrating runoff through vegetation and then allow the water to filter through the granular medium (Hatt et al., 2009). In doing so, biofilters are able to remove pollutants via several processes, including filtration, sorption, sedimentation, and plant and microbial uptake. Infiltration is therefore a key factor controlling both hydrologic and treatment performance (Brander et al., 2009). Accordingly, many studies have investigated how different media types improve infiltration and enhance the treatment performance of biofilters. However, performance values vary significantly depending on local conditions (Hunt et al., 2008). This has resulted in a wide variation of biofiltration designs, including vastly different media materials and compositions.

In general, the infiltration capacity of biofilters is a function of the void space, and thus can be designed by specifying media texture and structure (Skorobogatov et al., 2020). Some researchers recommend more mixed substrates (e.g., 20% compost, 50% sand and 30% topsoil) to reduce inflow volumes significantly (Carpenter and Hallam, 2010), while others argue that additional carbon sources (such as compost) impede drainage, and hence negatively impact infiltration and performance (Stander and Borst, 2010). Factors including solids loading, clay particle content and plant decay also impede drainage and contribute to

the operational clogging of biofilters (Le Coustumer et al., 2007). Clogging, following the long-term accumulation of sediment, is listed as a major concern to the hydrologic and treatment performance of biofilters (Kandra et al., 2014; Subramaniam et al., 2018). Some researchers claim that clogging increases maintenance costs and decreases the lifespan of biofiltration media (Jenkins et al., 2010). Therefore, the appropriate media texture and structure is considered essential to the construction and continued viability of biofilters (Jurries, 2003).

In general, media consisting of fine clay and soil are less suitable for promoting infiltration due to their low hydraulic conductivity and extended retention time (Vymazal, 2005b). By contrast, media consisting of coarser sediment (e.g., crushed rock or gravel) create more void space which allows water to percolate quickly. However, there are performance trade-offs associated with coarser filter media. For example, Hatt et al. (2009) investigated the performance of three field-scale biofilters with varying media types and concluded that media with higher infiltration rates (e.g., sand, gravel) are associated with higher concentrations of outflow particulates and their associated pollutants (Hatt et al., 2009). Therefore, although media with high hydraulic capacities can treat a higher percentage of mean annual runoff, the pollutant removal efficiencies are often reduced.

Many studies have also acknowledged the role that vegetation plays in influencing the infiltration capacity of biofilters (Gonzalez-Merchan et al., 2014; Virahsawmy et al., 2014). For example, Skorobogatov et al. (2020) suggested that plants impact the media through the development of macropores in the root zone (Skorobogatov et al., 2020). In addition, plants with thicker roots can maintain the infiltration capacity of biofilters and prevent clogging in the system (Le Coustumer et al., 2012; Hart, 2017). However, despite these benefits, some researchers have noted that plants may cause preferential flow pathways in the filter media, resulting in erratic infiltration and potentially the breakthrough of poor water quality (Skorobogatov et al., 2020). Therefore, improving the understanding of plant-media interactions is considered essential to determine the long-term performance of biofilters. Nevertheless, most studies have and continue to analyse the effect of vegetation independently of the media (Read et al., 2010). Furthermore, there have been few attempts to capture the interactive effects to date (Skorobogatov et al., 2020).

2.3.3. ET and evaporation

Although infiltration is a critical factor controlling the hydrologic performance of biofilters, Ebrahimian et al. (2019) argued that the significance of ET and evaporation cannot be overlooked when evaluating the hydrologic performance. This is reiterated by Beebe et al (2014) who report that changes in volumetric flow attributed to ET and evaporation can alter both the hydrologic and treatment performance of biofilters by removing water from the system, thereby increasing hydraulic retention time, as well as the concentrations of dissolved pollutants. Therefore, ET and evaporation are fundamental components of biofiltration water balances and can provide greater insight into the hydrologic functions of biofilters.

Despite the known benefits of ET and evaporation, there have been few attempts to quantify these processes in biofilters. This is largely due to the complexity of ET and evaporation calculations, which depend on multiple meteorological factors such as relative humidity, air temperature, solar radiation and wind speed, including design features such as plant species diversity and density (Allen et al., 1998). Furthermore, the individual contribution of ET and evaporation to overall runoff reduction is often difficult to differentiate (Sharkey, 2006). Therefore, performance studies usually combine ET and evaporation measurements into a single metric, often ET, to reflect the impacts of plants on overall water balances. However, this approach is only applicable to vegetated biofilters, and thus negates the impact of evaporation in non-vegetated biofilters. Moreover, it assumes that evaporation is negligible in biofilters, which undermines the accuracy of water balance analyses.

Due to the complexity of ET calculations, biofiltration ET estimates range widely across the literature (Table 1). These differences are largely attributed to biofilter size, climate region and plant selection, however, ET estimates also differ depending on the prediction tool and/or analysis used.

Table 1: A summary of ET estimations and associated water balances across biofiltration research.

% ET in water balance	Equation formula	Equation description	Reference
Up to 19%	$Q_i = ET + Q_u + EXF + \Delta S$,	where, Q_i = inflow, ET = evapotranspiration, Q_u = outflow from the underdrain, EXF = exfiltration to groundwater, and ΔS = change in storage	(Sharkey, 2006)
Up to 19% (even when the biofilter is only 4.5% of its catchment)	$Q_i = ET + Q_u + EXF + \Delta S +$ bypass	where Qi = inflow volume; ET = evapotranspiration volume; Qu = outflow volume from the underdrain; EXF = exfiltration volume to groundwater; ΔS = change in storage; and bypass is the difference between the inflow and infiltration/ surface water storage volumes.	(Li and Davis, 2009)
3% of the annual runoff	$$\frac{AET}{P} = \frac{1 + w\frac{PET}{P}}{1 + w\frac{PET}{P} + \frac{P}{PET}}$$	where AET = mean annual ET (mm); P = precipitation (mm); PET = potential ET (mm); w = plant-available water coefficient (0.5)	(Brown and Hunt, 2011)
Up to 82% for prairie vegetation and up to 52% for both turf grass and shrub mesocosms at 17% of the contributing impervious catchment	$SI + P = D + \Delta S + ET$	where SI = stormwater input (mm) collected roof runoff; P = precipitation (mm); D = cumulative drainage (mm) from each lysimeter; ΔS = change in soil water storage (mm); and ET = cumulative ET (evaporation for bare soil, mm)	(Nocco et al., 2016)
< 5%	$ET = \frac{W_{pre} - W_{dusk}}{W_{biomass[1:5]}} \times W_{final.biomass}$	where W_{pre} and W_{dusk} represent pot weights at pre-dawn and dusk; $W_{biomass[1:5]}$ = total dry biomass of replicates 1 to 5 on the same day (in g); and $W_{final.biomass}$ = mean total dry biomass for all 5 replicates as determined as the final harvest (in g)	(Szota et al., 2018)

Sharkey (2006) and Li and Davis (2009) were among the first researchers to quantify ET in biofilters. Both studies compared the water losses from two biofilters with the same media (one lined and the other unlined) and used a simple water balance to calculate the percentage exfiltration and ET from the biofilters. The water balance equation consisted of the inflow and outflow volumes, with the outflow defined as the volume of water lost to ET, outflow from the underdrain, exfiltration to groundwater and change in storage. Since exfiltration and

change in storage were assumed to be zero in the lined biofilter, the percentage ET was equated to the system's outflow water volume. Both studies reported an ET loss of up to 19% in the biofilters.

Other studies have used similar water balance equations to estimate ET, however, estimates vary considerably across the literature due to varying local climate conditions. Some studies showed that ET accounted for less than 5% of the overall water balance (Szota et al., 2018) while others reported percentage losses of up to 52–82% (Nocco et al., 2016). Typically, higher percentage losses are associated with potential or reference ET models, for example, the Hammon, Prietstley-Taylor and FAO Penman-Monteith models. This is because they rely on regional (as opposed to local) meteorological data (Allen et al., 1998). For example, the FAO Penman-Monteith model (the most complex model) requires data on solar radiation, vapour pressure deficit, temperature and windspeed to calculate reference ET (Allen et al., 1998), whereas the Hamon model (the least complex ET model) requires the daily temperature to calculate PET. Incorporating these broad meteorological parameters may lead to over predictions of ET at the biofiltration scale, and therefore provide misleading information on the water balance. Consequently, ET models may be more suitable for predicting ET at the catchment scale as opposed to predicting ET in an individual biofilter.

Studies have shown that ET can also vary depending on the type of vegetation (Szota et al., 2018). For example, plant characteristics (e.g., leaf area index, stomatal conductance, root density and architecture) can have significant impacts on ET (Moene and Van Dam, 2014). Furthermore, large, woody plants (e.g., trees and shrubs) generally contribute to higher ET rates, whereas herbaceous vegetation is expected to have lower ET rates (Szota et al., 2018). Therefore, the inclusion of crop-specific factors is arguably a more accurate approach to estimate ET, and in turn, can improve our understanding of biofiltration water balances.

2.4. Water quality performance of biofiltration systems

2.4.1. Overview

In general, biofilters are used to remove traditional runoff pollutants, including organic matter, TSS, heavy metals, faecal microorganisms (*E. coli*) and nutrients (Roy-Poirier et al., 2010). In addition, biofilters improve other water quality parameters, including pH, DO levels, turbidity, temperature and electrical conductivity (EC). The target pollutants selected for in this study included *E. coli* and nutrients (N and P), while the water quality parameters include pH, temperature and EC. Therefore, the literature review largely focuses on the performance of biofilters with respect to these target pollutants and water quality parameters.

There is substantial evidence to suggest that biofilters provide significant water quality improvements; however, performance efficiencies vary depending on biofiltration design, quantity and quality of infiltrating runoff and local climate conditions (Oral et al., 2020). In addition, metrics used to quantify the water quality performance of biofilters differ across studies and thus limits our ability to directly compare biofiltration performances. The following sections of the literature review address these challenges by discussing various design, operation and environmental parameters and their respective effects on biofiltration performance. In addition, the limitations of fixed performance metrics are discussed and the opportunities for flow and mass balances in the evaluation of biofiltration performance are considered.

2.4.2. Media selection and adsorption

The amount of P adsorbed by the media depends on its grain size distribution and texture, as well as the iron (Fe), aluminium (Al) and calcium (Ca) content (Garcia et al., 2010). Therefore, many studies have considered media selection as a tangible approach to improving the performance of biofilters (Li and Davis, 2016; Liu and Davis, 2014). Gravel is the most widely used media type in biofilters because it does not clog easily (Garcia et al., 2010). However, gravel can only absorb a limited amount of P due to its coarse texture and because it has a lower Fe and Al content. Furthermore, the binding sites of gravel become saturated within a relatively short space of time (i.e., several weeks or months), which reduces the sorption capacity of the media (García et al., 2005). Several attempts have therefore been made to improve the sorption of P (which is largely particle-bound) by amending the media with

different types of reactive materials, including iron-enriched sand (Erickson et al., 2012), fly ash (Kandel et al., 2017), lime and alum sludge water (Adhikari et al., 2016), and treatment residuals (Lucas and Greenway, 2011). Although these media amendments have improved P removal to some degree, the impact of the media on N removal is not as straightforward.

In contrast to P removal, the removal of N is primarily determined by a combination of plant-soil interactions and microorganisms in N speciation and removal (Skorobogatov et al., 2020). In addition, the dominant species of N in biofilters usually include NO_3^- and dissolved N, which are both poorly retained by the media (Liu and Davis, 2014). However, studies have indicated that N removal can be increased by improving the conditions for microbial denitrification (Wan et al., 2018). This is further discussed in section 2.4.4. of the literature review.

Similar to N, *E. coli* is largely removed via microbial processes (Chandrasena et al., 2014). However, few studies have examined the effects of different media types on faecal microorganism removal (Ferguson et al., 2003). In general, biofilters containing fine and/or coarse media have limited capacity to adsorb *E. coli*, resulting in lower *E. coli* removal rates (Bradford et al., 2006). By comparison, biofilters with loamy sand media and/or organic matter (Jiang et al., 2019) have higher sorption capacities and can lead to higher microbial removal rates (Ferguson et al., 2003).

2.4.3. Plants and phytoremediation

Plants remove, transfer, stabilise and/or transform pollutants, especially nutrients, through a process known as phytoremediation (Saeed and Sun, 2012). Consequently, several studies have examined the role and importance of plants in removing pollutants in biofilters, however, no consensus has been reached. Davis et al. (2006) were among the first researchers to confirm the role of vegetation in removing nutrients in biofilters. Subsequent research efforts demonstrated that vegetated biofilters could remove more nutrients than non-vegetated biofilters (Lucas and Greenway, 2008; Glaister et al., 2017). However, several studies have shown that vegetation can improve the removal of nutrients across several different media textures, which suggests that plant uptake is not the only mechanism responsible for removing nutrients (Bratieres et al., 2008; Henderson et al., 2007; Lucas and Greenway, 2008). Furthermore, improvements in nutrient removal exceeded plant nutrient requirements.

According to Read et al. (2008), the performance of vegetation in nutrient removal varies across plants species. The authors showed that only some species could improve the uptake of nutrients. Furthermore, Read et al. (2010) demonstrated that plants are closely linked to biofiltration performance and further concluded that plant characteristics, namely root length and mass, were among the most significant parameters when analysing nutrient uptake. However, there is an insufficient characterisation and understanding of the processes underlying the benefits of vegetation in biofilters (Muerdter et al., 2018). Therefore, although the role of vegetation was recognised a long time ago, its role in practice is still very limited.

Another influential factor is the availability of nutrients within the media itself, which further complicates the role of plants in nutrient removal (Skorobogatov et al., 2020). The degree of pollutant removal via plant uptake depends on the number of nutrients in the media, as well as the rate at which each nutrient can be delivered to the plant (Muerdter et al., 2018). In addition, plants play different roles under wet and dry conditions, as the degree of media saturation influences denitrification and the associated transformation of N species to N gas (Glaister et al., 2017). For example, Cho et al. (2011) demonstrated that biofiltration columns containing additional N and carbon sources contained less organic N when subject to longer dry periods. This indicated that organic N was broken down into NH_3 through the process of ammonification. Therefore, the presence of aerobic conditions is also vital to the transformation and removal of N in biofilters. However, some studies have indicated that ET (by plants) is critical for forming aerobic conditions as it causes fluctuations in the media saturation and oxygen availability. Therefore, plants are also important for facilitating the transformation and removal of N in biofilters through ET (Subramaniam et al., 2018). Consequently, the role of vegetation in N removal cannot be ignored when analysing the water quality performance of biofilters.

Overall, limited research efforts have been made to analyse the effects of vegetation on the microbial removal of *E. coli*. Many *E. coli* removal studies have examined a limited range of vegetation types (Rusciano and Obropta, 2007; Chandrasena et al., 2014) or have excluded the impacts of vegetation from their studies completely (Zhang et al., 2010). However, there is some evidence that vegetation may be important for removing *E. coli* (Le Coustumer et al., 2012; Read et al., 2010). For example, Stottmeister et al. (2003) showed that faecal microorganisms colonise the rhizosphere, with root exudates having either stimulating

and/or inhibiting effects on microorganisms. Plants can also impact the hydrologic performance of biofilters (Le Coustumer et al., 2012), which in turn affects the adsorption/desorption of faecal microorganisms by the filter media. However, different vegetation types have varying effects on *E. coli* removal. For example, biofilters planted with either *Melaleuca icana* or *Leptospermum continentale* reduced *E. coli* concentration by over 2 log reductions, while non-vegetated biofilters removed slightly fewer *E. coli* (1.7 log reductions) (Chandrasena et al., 2016; Chandrasena et al., 2014). Nevertheless, the processes underlying these changes in *E. coli* remain poorly studied.

2.4.4. Microorganisms and microbial degradation

Microorganisms are known to perform a major role in stabilising, removing and converting organic carbon and nutrients (Jurries, 2003). Consequently, many biofiltration studies have examined the potential benefits of microorganisms in nutrient retention (Stottmeister et al., 2003; Nocco et al., 2016). Microorganisms make substantial contributions to N removal in biofilters through processes such as ammonification, nitrification and denitrification (Saeed and Sun, 2012). In general, ammonification is the first step of N transformation in biofilters when the infiltrating runoff is rich with organic N. Ammonification tends to decrease with depth, which suggests that this removal process mostly occurs in the upper reaches of the media (where conditions are largely aerobic) and to a lesser degree in the lower reaches of the media (where conditions are largely anaerobic) (Reddy et al., 2009). Furthermore, ammonification is often the main process in pH ranges between 6.5 and 8.5 and is enhanced at higher temperatures, with doubling rates at temperature increases of 10°C (Vymazal, 2005b).

Ammonification is usually followed by nitrification, which occurs when the infiltrating runoff is primarily composed of NH_4^+ (Saeed and Sun, 2012). However, nitrification is an intermediary process that occurs between nitrification and denitrification and thus is considered a temporary process in the conversion of N. Therefore, denitrification is often considered the major mechanism behind the removal of TN in biofilters (Chung et al., 2014; Matheson and Sukias, 2010). It releases N in the form of N gas, nitrous oxide, or organic oxide from the system into the atmosphere (Craft et al., 1995). However, denitrification also produces alkalinity in the system and hence is usually observed in suspended or attached

bacteria growth environments with lower dissolved oxygen contents and anaerobic conditions (Cerezo et al., 2001).

Past research has shown that denitrification can be enhanced in biofilters if anaerobic conditions and/or carbon sources are present in the media. For example, Internal Water Storage (IWS) layers and saturated zones (SZ) have produced saturated conditions which enhance denitrification, and hence, N removal (Qiu et al., 2019; Wang et al., 2018; Xiong et al., 2019). However, denitrification can also occur without IWS layers and SZ. For example, Norton et al. (2017) found that anaerobic microsites and carbon in the media promoted denitrification (Norton et al., 2017). Similarly, Lynn et al. (2015) showed dissolved organic carbon accumulated in the media pore spaces during saturation, and in turn, increased denitrification (Lynn et al., 2015). These discrepancies have cast doubt on the significance of IWS layers and SZ for improving the microbial removal of N in biofilters. Therefore, more evidence is needed to determine the actual contribution of IWS layers and SZ to the overall N removal capabilities of biofilters.

E. coli removal, like N removal, relies on microorganisms in the media (Chandrasena et al., 2014). Therefore, anaerobic conditions and/or carbon sources may also be essential to the removal of *E. coli* in biofilters. For example, Chandrasena et al. (2012) showed that IWS layers may be able to mitigate the adverse impacts of extended dry periods on *E. coli* removal, and hence, can sustain the long-term performance of biofilters. However, the authors failed to fully explain the function of an IWS layer and its effects on faecal microbe removal. This issue was addressed by Chandrasena et al. (2014) who noted that IWS layers result in predation/competition and natural die-off of faecal microbes, and therefore have the potential to improve *E. coli* removal in biofilters. However, more evidence is needed to confirm this theory.

2.4.5. Hydraulic load and retention time

Hydraulic retention time (HRT), defined as "the average time the contaminated runoff spends in contact with the filtration medium" (Rahman et al., 2020), is one of the most significant operating parameters controlling the performance of biofilters. HRT is usually controlled by adjusting the hydraulic loading rate (HLR), which refers to the rate at which the infiltrating runoff enters the biofilter. Therefore, HRT and HLR are collectively responsible for influencing

the duration over which the infiltrating runoff remains in the biofilter and can have varying effects on the performance of the system.

In general, lower HLRs (and thus longer HRTs) enhance pollutant removal efficiencies in biofilters due to an extended contact time between the infiltrating runoff and filter media (Saeed and Sun, 2012). This increases sedimentation rates (due to lower flow velocities) and provides more time for adsorption and microbial removal to occur in the media (Reddy et al., 2009). Past research has indicated that nutrient removal is strongly influenced by HRT, with reported increases in nutrient removal over longer HRTs. For example, Wu et al. (2013) showed that the average TP removal efficiencies increased with increasing HRTs. The researchers explained that longer HRTs increased the number of contacts and interactions of phosphate with the media and plant roots, which enhanced the adsorption, transformation and uptake of TP by the media. Other studies have reported similar results (Lu et al., 2009; Konnerup et al., 2009; Bojcevska and Tonderski, 2007; Lin et al., 2002; Jing and Hu, 2010), however, the 'optimal' HRT varies across different biofilters, suggesting that other factors might also be responsible for influencing TP removal efficiency.

By comparison, there is no consistent pattern in the removal of N and HRT. For example, Bratieres et al. (2008) showed that longer HRTs improved organic N, TN, NH_4^+ and NO_3^- removal in biofilters. Similar findings were made by Huang et al. (2000) who determined that outflow NH_4^+ and TKN concentrations of biofiltration mesocosms decreased dramatically with longer HRTs. However, Jay et al. (2019) examined biofiltration columns and showed that no relationship between TN removal and HRT existed. Similarly, Lopez-Ponnada et al. (2020) conducted a field study on conventional biofiltration units with sand media and showed that HRT did not significantly influence NO_x removal. Some studies have also shown that increasing HLR (and thus, reducing HRT) decreases outflow NH_3 concentrations (Trang et al., 2010). These discrepancies indicate that N removal is influenced by additional factors (apart from microbial degradation), as increasing HLR typically decreases the contact time between the infiltrating runoff and attached biofilms and hence would be expected to diminish the removal efficiency. Therefore, there is still a limited understanding of the effects of HRT on N removal.

E. coli removal, like N removal, is primarily influenced by microorganisms, and hence *E. coli* removal is expected to increase with increasing HRTs. According to Rahman et al. (2020),

longer contact times between the infiltrating runoff and media favour the adsorption of *E. coli* to the media surface, which in turn will reduce the concentration of *E. coli* in the outflow. In addition, longer HRTs provide more opportunity for the attachment, filtering, predation and die-off of faecal microorganisms. However, the limited surface area of the filter media means the bacteria cannot be adsorbed indefinitely via the biofilter. Therefore, when the adsorption site cannot accommodate more bacterial individuals, the un-adsorbed *E. coli* will flow out of the system, resulting in the increasing outflow concentration of *E. coli*.

2.4.6. Inflow feeding mode

Another important operating parameter controlling the performance of biofilters is the inflow feeding mode. The inflow feeding mode is used to maximise the mixing of infiltrating runoff into the packed media, and therefore increase pollutant removal efficiencies (Saeed and Sun, 2012). In the literature, there are two main inflow feeding modes: continuous and intermittent loading. Intermittent loading involves separating the inflow into several individual flushes and has been used to enhance N removal in biofilters (Li et al., 2011; Sun et al., 1998a; Sun et al., 2006; Gervin and Brix, 2001). For example, Laber et al. (1997) found that intermittent loading significantly improved N biodegradation in biofilters fed with domestic outflow. According to the authors, the intermittently loaded cells were associated with higher denitrification rates and carbon levels (which promoted N removal), whereas the continuously loaded cells were associated with an uneven distribution of organic carbon (which limited NO_3^- reduction in the system). Similar findings were made by Caselles-Osorio and Garcia (2007) who showed that intermittently loaded biofilters achieved higher NH_4^+ removal performance (between 80–99% removal) compared to continuously loaded biofilters (between 71–85% removal). It was suggested that (i) increased turbulence in the media (as a consequence of the applied flushes during intermittent loadings) exposed the wastewater to both aerobic and anaerobic conditions, and (ii) the exposure of greater volume in the reactor to higher loadings resulted in the higher release of DO by plants. However, both studies were conducted at low media depths, which limits our understanding of these processes at shallower media depths.

Batch mode is a type of intermittent loading and has been used in several studies to determine the impacts of continuous compared to intermittent loading on the performance

of biofilters (Huett et al., 2005; Zhao et al., 2010; Babatunde et al., 2010). For example, Zhang et al. (2012) compared the performance of batch-fed and continuously-fed biofilters and reported similar COD removal performance for both loading methods. However, the removal of NH_4^+ increased in the batch mode (average removal was between 89.6 and 95.8%) compared to the continuous mode (average removal was between 87.7 and 95.9%). A more in-depth analysis revealed that a substantial contribution of oxygen was made by plants during the fill-and-dry method (under the batch mode), which facilitated the removal of NH_4^+ by the media.

2.4.7. Inflow loading strength

Previous studies have indicated that inflow loading strength can influence the performance of biofilters. According to Saeed and Sun (2012), the concentration of effluent N is strongly dependent on inflow loading. This is reiterated by several other authors who noted that increased N loading is associated with greater removal rates, within tolerable limits (Lee and Scholz, 2007; Tunçsiper, 2009; Dan et al., 2011). Past research has shown that biofilters can perform efficiently at NH_4^+ loading rates between 0.15 and 30 $g/m^2/d$ (Zachritz et al., 2008; Saeed and Sun, 2011), however, if inflow NH_3 concentrations are excessive, then it could negatively impact the growth of certain wetland plants and biomass. For example, Paredes et al. (2007) reported that plants were no longer a significant factor in biofiltration performance under high nitrate concentrations due to high NO_2^- toxicity levels. The authors speculated that other factors, namely microorganisms, played a more significant role in N removal under these high inflow NO_3^- loadings. However, more evidence is needed to confirm this theory.

The presence of organics in infiltrating runoff can also contribute to nitrification rates in biofilters (Saeed and Sun, 2012). For example, Sun et al. (1998b) reported that nitrification was inhibited in biofilters until BOD dropped below 200 mg/L. Similarly, O'Luanaigh et al. (2010) showed that nitrification was reduced by 6.3–18.5% at inflow COD concentrations between 193 and 514 mg/L. Wu et al. (2011) also observed lower levels of nitrification in tidal flow biofilters when the mean inflow BOD increased (193–366 mg/L). A possible explanation for this phenomenon could be that the higher specific growth rate of heterographic bacteria enhanced the rapid consumption of available oxygen and therefore limited nitrification in the system.

By contrast, outflow TP concentrations are largely independent of inflow TP concentration. McNett et al. (2011) showed that no relationship between inflow and outflow TP loading existed. However, outflow TN concentrations were moderately influenced by inflow TN loadings. The authors noted that TN removal is dependent on the contact time with the biofiltration media. Accordingly, the cells with shorter contact times may also explain why inflow TN concentrations were partially predictive of outflow TN concentrations. By comparison, higher inflow nutrient concentrations led to higher outflow nutrient concentrations but produced significantly higher removal efficiencies, particularly for TN. Outflow TP concentration, irrespective of inflow concentration, approached a baseline outflow concentration. Therefore, lower inflow TP concentrations increased, while higher inflow TP concentrations decreased (McNett et al., 2011).

There appears to be an overall positive relationship between outflow *E. coli* concentrations and inflow *E. coli* loadings. This was demonstrated by Søberg et al. (2019) and Liu et al. (2020) in biofiltration column and batch studies. According to the authors, *E. coli* removal is primarily achieved by adsorption in the media. However, the limited surface area of the media means the bacteria cannot be adsorbed indefinitely via the biofilter. Therefore, high inflow *E. coli* loadings have the potential to exhaust the adsorption capacity of the media faster than low inflow loadings, resulting in the release of *E. coli* from the system. However, more research is needed to confirm this theory.

2.4.8. Temperature

The effects of cooler temperatures on biofiltration performance are largely unknown, as many biofilters are designed without consideration for their operation in cold environments (Roseen et al., 2009). However, several factors contributing to nutrient removal may be affected by varying seasonal conditions (Saeed and Sun, 2012). For example, low temperatures might negatively impact N removal since denitrification is highly dependent on soil temperature (Roseen et al., 2009). The Arrhenius equation captures this temperature effect best, as nitrification occurs optimally at temperatures ranging between 20℃ and 35℃ (Russell et al., 2007). However, some studies have highlighted that the optimal temperature range for nitrification to occur lies between 16.5℃ and 32℃ (Demin and Dudeney, 2003) while other studies have shown that nitrification is extremely limited between 5℃ and 6℃

and over 40℃ (Katayon et al., 2008). Similarly, previous research has shown that denitrification occurs slowly at low temperatures (e.g., 5℃), with an exponential increase in the reaction rate under increasing temperatures. However, denitrification tends to stabilise between 20℃ and 25℃, holding all other environmental factors constant (EPA, 2000).

Temperature also influences NH_4^+ fixation and microbial N uptake in biofilters (Juang et al., 2001). For example, Tunçsiper (2009) showed a 9% increase in NH_4^+ removal and a 7% increase in NO_3^- removal during the summer (compared to winter) in biofilters fed with tertiary treated wastewater. Another paper published by Langergraber (2007) demonstrated a reduction in NH_4^+ removal when the temperature dropped below 12℃. Similarly, Nivala et al. (2007) attributed the higher NH_4^+ removal performances during summer (60–97%) compared to winter (44–88%) to the lower accumulation of NO_3^- in the outflow during warmer periods. By contrast, some studies have observed no difference in the removal rates in biofilters between summer and winter periods (Jenssen et al., 2005; Bulc, 2006). This observed lack of differences was attributed to (i) a greater supply of oxygen in colder water and (ii) the predominance of physical removal processes (e.g., filtration) compared to microbiological processes (e.g., denitrification/nitrification). However, given the dependency of N on temperature, it seems that the latter reason is more likely.

Like N removal, bacterial transport and destruction are also significantly influenced by temperature (Zhang et al., 2012). Temperature influences the growth, inactivation and/or die-off of bacterial microorganisms and hence is considered an important environmental factor controlling the removal of *E. coli* in biofilters. In general, bacteria survive better in lower temperatures due to a reduction in predation by bacterial predators and indigenous protozoa, as well as lower rates of decay (Jiang et al., 2017). Therefore, lower temperatures are often associated with increased bacterial survival.

By comparison, P removal remains consistently high (>90–95% at all temperatures) across biofiltration performance studies. This is due to the high percentage of particle-bound P, which is less dependent on biological removal processes (e.g., denitrification) and more dependent on physical removal processes (e.g., sedimentation) (Blecken et al., 2010). Consequently, P removal is less dependent on temperature than N removal (Kadlec and Reddy, 2001). Nevertheless, some studies have shown that lower temperatures are associated with lower P concentrations (Gardner and Jones, 2008). The authors attributed

these findings to increased sorption, whereby higher plant-available P was present at lower temperatures. However, decreased plant activity could also be associated with lower temperatures, which reduced the uptake and subsequent removal of P (Kadlec and Reddy, 2001). More field studies are thus needed to verify the role of temperature on P removal in biofilters.

2.4.9. pH

Studies have shown that pH is also a key factor influencing microbial removal in biofilters (Kadlec and Reddy, 2001). Nitrification reduces the total alkalinity of the biofilter due to a significant amount of bicarbonate that is consumed during the conversion of ammonia to nitrate (EPA, 2000). Therefore, significant nitrification can lead to a substantial drop in the alkalinity of the treated stormwater, which in turn minimises denitrification processes in the system. Research indicates that denitrification can be reduced at pHs below 6.0 and pH above 8.0, with the highest rate having been observed at a pH range between 7.0 and 7.5 (EPA, 2000). However, previous studies have shown that denitrification occurs at a slower rate under a pH of 5 (Vymazal, 2007). Furthermore, pH plays an important role in the anaerobic degradation of pollutants in biofilters. For example, the optimal pH range for methane-forming bacteria lies between 6.5 and 7.5, while any deviation could potentially inhibit the function of such bacteria (Vymazal, 1999).

In general, there is limited research on the effects of pH on pollutant removal efficiencies in biofilters. However, Davis et al. (2006) conducted biofiltration box experiments and showed that variations in runoff pH (i.e., increases or decreased from neutral pH) resulted in the leaching of P from the upper soil layer. Similarly, NO_3^- removal was significantly decreased under higher and lower pHs. Nevertheless, there is insufficient evidence to show that microbial denitrification rates and/or aqueous NO_3^- speciation is significantly impacted by pH changes (given the limited pH range tested) and more research is needed to confirm these findings.

2.4.10. Drying and wetting cycles

Alternate drying and wetting cycles are significantly influenced by variations in rainfall and evaporation, which in turn impact the plant and soil microbial communities, as well as the efficiency of the biochemical and physiological removal processes (Chen et al., 2021). In

general, drying and wetting increase the number of nutrients available to microbes, which helps build the microbial biomass of the system and provides energy through redox reactions.

Drying and wetting cycles are known to directly influence N removal through the transformation and migration of N in the filter media. For example, Guo et al. (2014) found that alternate drying and re-wetting shifts the moisture status of the soil moisture, which in turn affects the rate of nitrification. Although nitrification largely occurs during dry periods, any NO_3^- formed during these periods migrates during subsequent re-wetting, resulting in NO_3^- leaching in some extreme cases (Leitner et al., 2017). Subsequent research efforts investigated the role of saturated zones (SZ) in enhancing N removal during dry periods and preventing NO_3^- leaching upon re-wetting. For example, Hermawan et al. (2020) showed that the presence of SZ can maintain similar TN and TP removal rates for as long as three weeks. However, the study mostly focused on the effects of plants, and therefore only considered dissolved nutrients. It also lacked a detailed understanding of nutrient removal processes, for example, nitrification and denitrification, across different biofiltration zones.

More recent studies have examined NO_3^- removal in biofiltration soil and emphasised the importance of SZ for enhancing NO_3^- removal (Wang et al., 2018; Lopez-Ponnada et al., 2020). However, the studies used a maximum antecedent dry weather period (ADWP) of 14 days, which was previously noted as insignificant for N removal in biofilters. Therefore, any reduction in NO_3^- could have been attributed to the presence of anaerobic conditions at the bottom of the biofilter. Subsequent research efforts incorporated ADWPs of up to 30 days, however, they only considered fully submerged biofilters, which were deemed insignificant for capturing the trade-offs between denitrification and mineralisation in biofilters with SZ (Lynn et al., 2015).

Biological removal involving microorganisms and vegetation are also controlled by the drying and wetting cycles in biofilters (Navarro-García et al., 2012). According to Wan et al. (2018), moisture content is a major factor regulating enzymic activity in the system. Therefore, the enzyme activity, which plays a key role in the biotransformation and migration of N, has the potential to be significantly impacted by drying and re-wetting (Payne et al., 2014). However, the soil microbial community, plant roots and physicochemical properties are also impacted by drying and wetting cycles (Chen et al., 2021). Any variation in these factors can therefore affect and regulate N transformations. In addition, drying and wetting cycles are dependent

on weather conditions and are random to a certain degree (Cunqi et al., 2007; Wan et al., 2018). Random drying and wetting cycles, therefore, might produce completely different enzyme activity under different environmental conditions (Chen et al., 2021).

Rapid drying in biofilters also has the potential to enhance aerobic P removal processes (Bunce et al., 2018). However, an extended period of drying could also negatively impacts the mobility of P and N in the system, which in turn will reduce nutrient removal efficiencies (Brown et al., 2017). In addition, drying may cause the soil to crack, thereby forming preferential pathways with large amounts of bio-available P and N being released upon re-wetting, however, more evidence is needed to confirm this theory.

Overall, few research efforts have been made to measure soil moisture and the exchange of water between biofiltration zones. This limits the understanding of water dynamics in biofilters (Chen et al., 2021). Similarly, no studies have examined the nutrient removal recovery after re-wetting, which suggests that there is a limited understanding of what happens after extended drying periods. Lastly, few studies have determined the moisture level at which biofilters will start leaching pollutants. This is mostly analysed in agricultural studies for optimising the growth of crops (Pathan et al., 2007), however, different pollutant and soil factors have not been examined in biofilters.

2.4.11. Performance metrics

The metrics used for quantifying treatment performance vary considerably across the biofiltration literature, making direct comparisons between datasets difficult. The most common metric, however, is a fixed performance metric, typically a percent removal or removal efficiency (McNett et al., 2011). Removal efficiencies compare the movement of pollutants in and out of the biofilter and thus provide an overview of the net removal in the system. Although easy to interpret, removal efficiencies have been widely criticised for being overly simplistic when they are used as a standalone metric. For instance, Davis et al. (2010) noted that removal efficiencies do not capture the large variation in biofiltration design and expected performance. This often results in inaccurate and misleading performance measurements and analyses. Other researchers have highlighted that percent removals are not useful for characterising water quality performance (Strecker et al., 2001). The main concern here is that source controls can be discouraged if requirements specify that biofilters

must remove some percentage of pollutants. Therefore, removal efficiencies cannot account for baseline water quality, inter-region variability or background pollutant concentrations (Smith et al., 2001).

According to Davis et al. (2010), a more holistic evaluation of treatment performance encompasses flow and mass balance analyses, in addition to fixed performance metrics (i.e., percent removals). Flow and mass balance analyses can provide further insight not the underlying removal mechanisms in biofilters, which in turn can lead to design and/or operational enhancements. This notion is reiterated by Smith et al. (2001) who noted that flow and mass balance analyses are essential to determine the number of pollutants entering the biofilter due to runoff, the number of pollutants that are transported to receiving rivers and the number of pollutants that are retained by the biofilter. Furthermore, information from the mass and flow balance analyses can be used in models to predict the water quality performance of a biofilter based on selected input variables. As such, design and/or operational improvements can be made to enhance the overall removal performance of biofilters.

Although currently limited, some studies have used mass balance analyses to determine the main pollutant removal pathways in biofilters. For example, Muthanna et al. (2007) and Sun and Davis (2006) showed that the most important mechanisms for removing metal from biofilters were filtration of suspended solids and adsorption onto the top media layer. However, these findings were limited because the mass balances were largely incomplete. Other studies have adopted a similar approach to investigate the primary removal mechanisms for nutrients such as P and N. For example, Chung et al. (2007) demonstrated that less than 5% of N and P accumulated in plants, as denitrification and substrate were the main removal mechanisms in a biofilter fed with primary treated municipal water. Similarly, García et al. (2005) found that denitrification was the most significant biochemical reaction in removing dissolved organic matter in biofilters at depths of 0.27 m, whereas sulphate reduction played the most important role in biofilters with 0.5 m depths.

Some researchers have used mass balance analyses to quantify denitrification in plants. For example, Borin and Salvato (2012) showed that data from the N mass balance, expressed in relative terms with respect to TN load, provided useful information for understanding the primary removal processes with different plant species. These findings enabled managers to

make better decisions about the appropriate vegetation and/or plant harvesting time in order to enhance nutrient removal. However, the accuracy of these results is limited because the study provides no formal evidence of the total percent recovery of the constituent mass. This issue was later addressed by Rycewicz-Borecki et al. (2016) who used a similar approach to examine the retention and uptake of nutrients by stormwater biofiltration microcosms, but calculated the percent recovery to account for nutrient mass at the beginning and towards the end of the study. These findings were significant because they showed that the choice of plant species can be used to improve nutrient retention from runoff and decrease pollutant loadings to receiving water bodies.

Lastly, flow and mass balance analyses can be used to determine the effects of various environmental parameters on the treatment performance of biofilters. For example, Maniquiz et al. (2012) analysed the impacts of monitored storm events on the pollutant removal efficiency of biofilter mesocosms and showed that rainfall significantly influenced the flow balances of the system, but had little effect on the pollutant mass balances.

Overall, fixed performance metrics, namely removal efficiencies, offer limited insight into biofiltration performance. Instead, flow and mass balance analyses are recommended to understand the underlying biofiltration processes, and therefore determine the optimal design and/or operation of biofilters.

CHAPTER 3: RESEARCH METHODS

3.1. Study design

Biofiltration performance is influenced by various design, operating and environmental parameters, however, the impacts of these parameters on the performance of the biofiltration cells at the Water Hub was previously unknown. These unknowns extended to future changes, both environmental and climatological, which presented more uncertainty about the performance and continued viability of the cells at the Water Hub.

The study design addresses these unknowns through two main research activities. First, the study analysed the performance of the two field-scale biofiltration cells in the present through water quantity and quality analyses. Second, the study examined the performance of the cells in the future through multiple regression modelling. The cells were operated under a batch mode (regular fill and draw cycles) and samples were collected during the summer period (between November 2020 and March 2021). A batch operation mode was selected due to various site constraints, namely a limited power supply, and because operating conditions (HRT) were easier to control. The summer period was selected due to the high pollutant concentrations associated with the low flow conditions of the Stiebeuel River during this period (Fell, 2018). This showcased the performance of the cells under high pollutant loadings (the 'worst-case' scenario), and therefore provided more insight into the full pollutant removal capabilities of the cells.

The batch study was designed to incorporate three main treatment factors: (i) HRT (to determine the effects of varying HRTs on the performance of the cells), (ii) vegetation (to determine the role and importance of plants in removing pollutants and reducing flow) and (iii) inflow water quality (to determine the effects of varying inflow water quality conditions on the performance of the cells) (Table 2). These treatment factors were selected because they provided insights on the treatment capabilities (and limitations) of the cells, which in turn allowed for quantitative design and predictable performance characterisation of the biofilter.

Table 2: Treatment factors and associated levels used in the batch study.

Treatment Factor	Levels
HRT	1, 3, 5 and 7 days
Vegetation	Present or absent
Inflow water quality	Water pH, water temperature and inflow pollutant concentrations

Previous research showed that an HRT of approximately 7 days produced the best water quality outcomes in the cells, while longer HRTs resulted in a decline in the water quality performance (Ghanashyam, 2018). However, the effects of HRT on the flow and mass balances of the cells were largely unknown, which limited the understanding of underlying the biofiltration processes. A two-day sampling interval (of 1, 3, 5 and 7 days) was used to examine whether any statistically meaningful relationship existed between HRT and the outflow water quality of both cells.

Previous research showed that plant uptake played a significant role in removing pollutants, as the vegetated cell packed with large stones (19–35 mm aggregates) (LSV) had the most improved water quality overall, with percentage reductions of up to 97%, 90% and 100% for NH_3, PO_4^{3-} and *E. coli* (Ghanashyam, 2018). Therefore, vegetation was selected as a treatment factor to confirm the role and importance of plants in removing pollutants. This was demonstrated through the vegetated (LSV) and unvegetated large stone (LS) cells, which were the best-performing cells to date (Ghanashyam, 2018).

Inflow water quality was used as a treatment factor to control for the large fluctuation in weekly runoff water quality. This minimised the unexplained variance in the experiment and isolated the effects of the selected treatment factors. Multiple environmental parameters, including rainfall, evaporation, ET and temperature were also analysed to reduce any unexplained variance.

To establish the relationship between HRT and cell performance, correlation analyses were performed using R statistical software. Similar analyses were also conducted between inflow water quality and cell performance, as well as the selected environmental parameters and cell performance. Multiple regression modelling was then used to develop equations for

predicting the outflow water quality of the cells under varying HRTs, inflow water quality conditions and environmental parameters.

3.2.   Water quality methods

3.2.1. Sampling procedure

Both cells were operated using a fill-and-draw batch process, similar to that of a sequencing batch reactor (SBR). During the 7-day batch cycle, the cells were filled in the 'fill' phase (± 2 hours) and remained saturated in the 'react' phase (± 7 days) until they were emptied in the 'draw' phase (± 2 hours).

Grab samples of the inflow water quality were collected from the influent during the 'fill' phase of each batch cycle, while grab samples of the outflow water quality were collected from the effluent during the 'react' phase of the batch cycle. The inflow water quality samples were therefore collected before each batch cycle (at the end of day 7 on the previous batch cycle), while the outflow water quality samples were collected during each batch cycle on days 1, 3, 5 and 7 (Table 3). Hence, a total of 5 samples were collected from each cell per batch (1 from the cell inlet and 4 from the cell outlet). The cells were then drained during the 'draw' phase and re-filled during the 'fill' phase at the end of day 7 of each batch cycle.

Table 3: Water sampling procedure over the 7-day batch cycle.

Water quality parameter	Collection point	Day 7 (previous batch cycle)	Day 1	Day 3	Day 5	Day 7
Inflow COD, TP, TKN, NH_3, NO_3^-, NO_2^-, EC, temperature, pH	Cell inlet	✗				✗
Outflow COD, TP, TKN, NH_3, NO_3^-, NO_2^-, EC, temperature, pH	Cell outlet		✗	✗	✗	✗
Inflow and outflow *E. Coli*	Cell inlet and outlet	✗				✗

✗ indicates when a water sample was taken.

Both inflow and outflow water quality samples were refrigerated upon collection and transferred to a laboratory where they were analysed for COD, TKN, NH_3, NO_3^-, NO_2^-, TP and *E. coli*. Pen meters were used to take in situ measurements of the inflow pH, temperature and EC.

3.2.2. Laboratory procedures

The samples were analysed for NH_3, NO_3^- and NO_2^- in the water analysis laboratory at the University of Cape Town. The remaining water quality parameters, namely TP, TKN, COD and *E. coli* were analysed at A.L. Abbotts commercial laboratory. Table 4 describes the laboratory procedures that were used to analyse these water quality parameters.

Table 4: Description of laboratory procedures used to analyse water quality.

Water quality parameter	Laboratory procedure
COD	SANS 6048:2005 (A.L. Abbotts & Associates (Pty) Ltd)
TKN	HACH Method 8075 (A.L. Abbotts & Associates (Pty) Ltd).
TP	STD Method 4500-PB & HACH Method 8114 (A.L. Abbotts & Associates (Pty) Ltd)
E. coli	Colilert-18/Quanti-Tray method (A.L. Abbotts & Associates (Pty) Ltd)
NH_3	Salicylate method for powder pillows (HACH DR 2700 spectrometer)
NO_3^-	Cadmium reduction method for powder pillows (HACH DR 2700 spectrometer)
NO_2^-	Diazotization method for powder pillows (HACH DR 2700 used a stored program in place to test for NO_2^-)

3.2.3. Pollutant removal efficiency calculations

The pollutant removal efficiencies were determined by calculating the percentage reduction of TKN, NH$_3$, NO$_3^-$, NO$_2^-$, TP and *E. coli* by each cell:

$$RE = \frac{C_{Final} - C_{Initial}}{C_{Initial}} \times 100\%$$

where RE is the percentage reduction of each pollutant; C_{Final} is the final concentration of each pollutant (in mg/L); and $C_{Initial}$ is the initial concentration of each pollutant (in mg/L).

3.3. Water quantity methods

3.3.1. Water level measurements

The water level of the cells was determined to quantify the contribution of evaporation/ET to the overall volume reduction. These measurements were taken alongside water quality measurements to determine whether evaporation/ET influenced the outflow water quality of the cells. The initial water level was determined by measuring the height of the water level after each cell was filled during the 'fill' phase of the batch cycle. The water level was subsequently measured on days 1, 3 and 5 during the 'react' phase until the final water level was measured on day 7 before the water was released during the 'draw' phase of the batch cycle.

The water level in the cells was measured by inserting a measuring tape into the middle inspection pipe and measuring the distance (in meters) between the water level in the cell and the top of the inspection pipe (Figure 6). This value was converted into the 'actual' water level by subtracting the length of the inspection pipe above the surface of the cell from the measured distance, and then by subtracting this amount from the height of the cell.
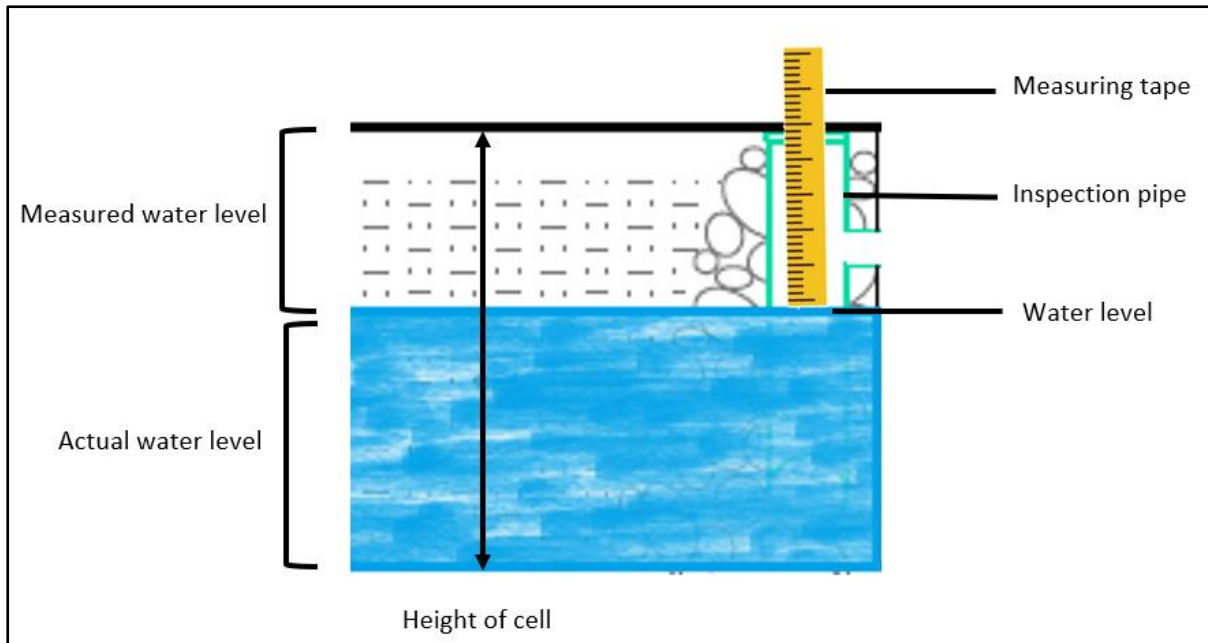
Figure 6: Method used to measure the water level in the cells.

3.3.2. Water volume calculations

The water level measurements were inserted into the following equation to determine the water volume of each cell:

$$Vol = l \times w \times h \times p \times 1000$$

where Vol is the volume of water (in litres); l is the length of the cell (16 metres); w is the width of the cell (3 metres); h is the height of the water level in the cell (in metres); p is the cell porosity (0.353), and 1000 is the m^3 to volume converter. The cell porosity (p) was calculated as a percentage of the large stones' total volume by measuring the amount of water it takes to fill all the pores between the stones.

3.3.3. Evaporation and ET estimates

The volume of water lost to evaporation in the LS cell was determined by subtracting the final volume from the initial volume. This calculation draws on the assumption that minimal leakage occurs in the cell, which is justified because the cell is lined with waterproof LPDE sheeting to prevent water from leaving the cell via exfiltration into the surrounding soil.

For the LSV cell, both evaporation and ET were considered flow reduction pathways due to the presence of vegetation. To separate the effects of evaporation and ET, a pan evaporation

experiment was set up adjacent to the cells to determine the percentage contribution of ET to the overall flow reduction. The pan included a 240 L container with the same filter media (19– 25 mm stone aggregates) and depth (0.7 m) as the life-sized biofiltration cells. Hence, it was assumed that the total percentage of water lost via evaporation in the pan experiment was equivalent to the total percentage of water lost via evaporation in the life-sized cell. The water quantity of the pan was therefore measured following the same method as the one described above, with measurements being taken on the same days as the life-sized cells to ensure that environmental conditions remained relatively constant. The pan evaporation values were then plugged into a formula developed by Allen et al. (1998) to calculate the reference ET:

$$ET_0 = K_p \times E_{pan}$$

where ET_0 is the reference evapotranspiration (L/day); K_p is the pan coefficient; and E_{pan} is the pan evaporation (L/day).

The pan coefficient (K_p) was calculated using an equation developed by Snyder (1992), which required information on the upwind fetch (distance to the nearest obstruction), relative humidity and windspeed:

$$K_p = 0.482 + 0.024 \ln(F) - 0.000375U + 0.0045H$$

where K_p is the pan coefficient; F is the upwind fetch (in m); U is the mean daily wind speed (in km/day); and H is the mean daily relative humidity in percentage.

The actual ET was calculated by multiplying the reference ET estimates by the pan evaporation values. These absolute values were then converted into percentages (% ET), which were used to determine the percentage of water lost to ET in the LSV cell.

3.3.4. Water balance analyses

The water balance analyses were determined by incorporating the water quantity data collected from both cells for every batch cycle. Figure 7 provides a visual representation of the water balance in the cells:
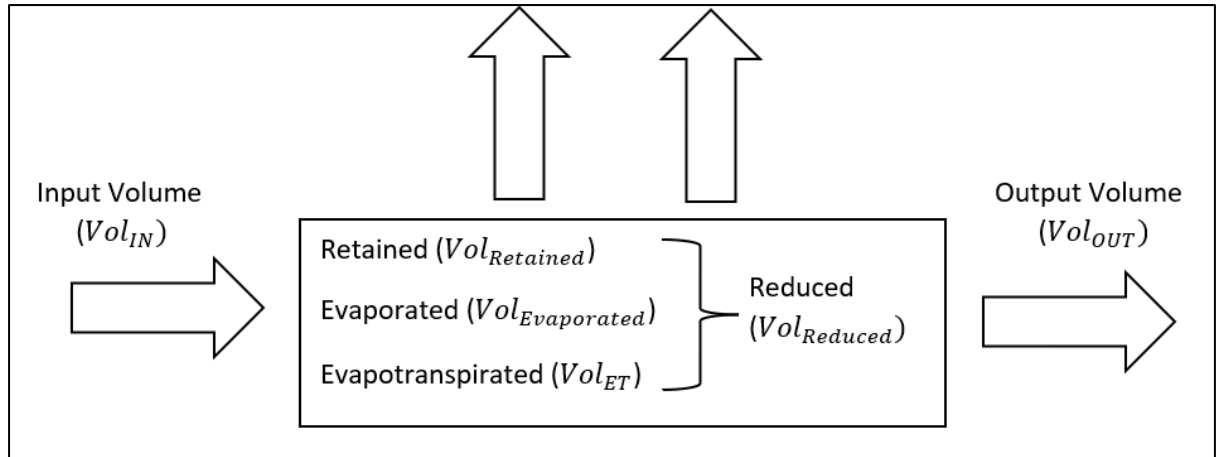
Figure 7: Conceptual water balance for the cells.

The reduced volume was assumed to consist of the combined retained, evaporated and evapotranspirated volume occurring in the system and roughly estimated as the difference between the initial and final water volumes:

$$Vol_{inital} - Vol_{final}$$

$$= Vol_{retained} + Vol_{evaporated} + Vol_{ET}$$

$$= Vol_{reduced}$$

where $Vol_{initial}$ is the initial volume; Vol_{final} is the final volume; $Vol_{retained}$ is the volume retained by the cell; $Vol_{evaporated}$ is the volume lost via evaporation; Vol_{ET} is the volume lost via ET; and $Vol_{reduced}$ is the volume reduced by the cell.

3.4. Statistical analyses

The statistical analyses for the water quantity and quality data comprised the following subsections:

i. Standard descriptive statistics including graphs, tables, box-and-whisker diagrams and five-number summaries of the inflow and outflow water quality and quantity data. These analyses were employed to clearly demonstrate the differences in the mean inflow and outflow water quality and quantity of the cells. The graphs were selected based on their ability to graphically display the hydrologic and treatment efficiencies of the cells over the 13 batch cycles. The box-and-whisker diagrams are equivalent to a nonparametric analysis of variance and were selected because the data did not

follow a normal distribution. A five-number summary was included to highlight the important information from the box-and-whisker diagrams and therefore provide more information about the spread of the data.

ii. Correlation analyses were conducted between HRT and output water quality, inflow water quality and cell performance, and the selected environmental parameters and cell performance. Pearson corelation coefficients were used to determine the strength of the linear relationship between the variables. The p-values were also included in the analysis to determine the significance of the relationships.

iii. Multiple linear regression models were used to explore the effects of varying environmental parameters (rainfall, air temperature and evaporation/ET), operating conditions (HRT) and inflow water quality conditions (water temperature, pH and pollutant concentration) on the output NH_3 and TP concentrations in the cells. Non-linear relationships were detected for both output NH_3 and TP when they were plotted against the explanatory variables (i.e., the environmental, operating and inflow water quality parameters). Therefore, the data was transformed into a polynomial regression model by adding polynomial terms to the explanatory variables in the model. The model assumptions were checked by testing for linearity, constant error variance, independence and normality.

CHAPTER 4: RESULTS AND DISCUSSION

4.1. Water quality performance

4.1.1. Comparison of inflow and outflow water quality

4.1.1.1. Box-and-whisker diagrams and five-number summaries

Nitrogen

Total Kjeldahl Nitrogen (TKN) was calculated as the sum of NH_3, NO_3^- and NO_2^- and was analysed using a box-and-whisker diagram (Figure 9). This included a five-number summary of the inflow and outflow TKN concentrations over 13 batch cycles. The five-number summary consisted of the mean ($\hat{x}$), median (Q2), maximum value (Max), minimum value (Min) and interquartile range (IQR). A total of 65 samples (n = 65) were collected

Figure 8: Box-and-whisker diagrams for TKN concentration in the inflow (INF) and outflow (LS and LSV) of the cells (n = 65).

The median values for the LS (Q2= 3.8) and LSV (Q2= 3.2) boxplots are lower than the median value for the INF (Q2= 14.3) boxplot, showing that there is a difference in TKN concentration between the inflow and outflow of both cells (Figure 8). In addition, the INF boxplot (Max= 16.8, Min= 13.8) is much higher than the LS (Max= 16.7, Min= 2.1) and LSV (Max= 8.0, Min= 2.0) boxplots, indicating that the overall TKN concentrations were greater in the inflow compared to the outflow of both cells (Figure 8). However, the LSV (IQR= 2.8) and INF (IQR=

2.8) boxplots are short in comparison to the LS boxplot (IQR= 6.1) (Figure 8). This suggests that the overall TKN concentrations were less variable in the LSV cell and inflow than in the LS cell. The LS and INF boxplots have asymmetrical distributions with positive skewness, suggesting that most TKN concentrations were higher than the group median in the inflow and LS cell (Figure 8). Both boxplots also have several outliers which are higher than the group medians (Figure 8). By comparison, the LSV boxplot has a more symmetrical distribution and no outliers, indicating that TKN concentrations were more evenly spread across the group (Figure 8). Neither cell has a maximum TKN concentration exceeding 30 mg/L, while the mean outflow TKN concentration of both cells is below 5 mg/L. This meets the minimum water quality requirements for irrigational reuse (Table 5).

Table 5: Effects of nitrogen on crop yield (DWAF, 1996).

Concentration range (mg/L)	Crop quality
Target water quality range · 5	**The unintended nitrogen application should, at normal irrigation applications, be low enough not to affect even sensitive crops such as grapes and most fruit trees.**
5–30	Sensitive crops are increasingly likely to be affected (depending on the magnitude of irrigation application). Other crops remain largely unaffected in the lower concentration range but are increasingly affected as concentration increases.
> 30	Most crops are affected. A limited range of crops can utilise the nitrogen applied. Severe restrictions are placed on the utilisation of these waters.

Nitrogen, as used in the DWAF (1996) guideline, refers to all inorganic nitrogen forms present in water, including NH_3, ammonium (NH_4^+), NO_3^- and NO_2^-. Hence, Table 5 also applies to the following.

Inflow and outflow TKN were broken down into NH_3, NO_3^- and NO_2^- and box-and-whisker diagrams and five-number summaries were used to analyse these N species over 13 batch cycles (Figures 9, 10 & 11).

Figure 9: Box-and-whisker diagrams for NH_3 concentration in the inflow (INF) and outflow (LS and LSV) of the cells (n = 65).

The median values for the LS (Q2= 2.0) and LSV (Q2= 1.9) boxplots are lower than the median value for the INF boxplot (Q2= 13.4), showing that there was a difference in NH_3 concentration between the inflow and outflow of both cells (Figure 9). In addition, the INF boxplot (Max= 22.7, Min= 1.8) is much higher than the LS (Max= 14.8, Min= 0.1) and LSV (Max= 7.5, Min= 0.01) boxplots, indicating that the overall NH_3 concentrations were higher in the inflow than in the LS and LSV cells (Figure 9). However, the LSV boxplot (IQR= 2.5) is short in comparison to the LS (IQR= 6.2) and INF (IQR= 7.3) boxplots (Figure 9). This suggests that the overall NH_3 concentration was less variable in the LSV cell than in the LS cell and inflow. The LS boxplot has an asymmetrical distribution with positive skewness, suggesting that most of the NH_3 concentrations were higher than the group median (Figure 9). Comparatively, the LSV boxplot has a more symmetrical distribution, which indicates that NH_3 concentrations were more evenly spread across the group (Figure 9). The INF boxplot is slightly positively skewed, suggesting that most of the NH_3 concentrations were higher than the group median (Figure 9). The INF boxplot has two outliers that are higher than the group median, while the LS boxplot has only one outlier above the group median (Figure 9). Neither cell has a maximum NH_3 concentration exceeding 30 mg/L, which meets the minimum water quality requirements for irrigational reuse (Table 5).

Figure 10: Box-and-whisker diagrams for NO_3^- concentration in the inflow (INF) and outflow (LS and LSV) of the cells (n = 65).

The median values for the LSV (Q2= 0.6) and INF (Q2= 0.8) boxplots are lower than the median value for the LS boxplot (Q2= 1.3), showing that there was a difference in NO_3^- concentration between the inflow and the outflow of both cells (Figure 10). In addition, the INF boxplot (Max = 6, Min = 0.45) is higher than the LS (Max= 4, Min= 0.3) and LSV (Max= 1.6, Min= 0.5) boxplots, indicating that the overall NO_3^- concentrations were higher in the inflow than in the outflow of both cells (Figure 10). However, the LSV boxplot (IQR= 2.9) is short in comparison to the LS (IQR= 1.5) and INF (IQR= 0.5) boxplots (Figure 10). This suggests that the overall NO_3^- concentration was less variable in the LSV cell than in the LS cell and inflow (Figure 10). All three boxplots have an asymmetrical distribution with positive skewness, indicating that most of the NO_3^- concentrations were higher than the group medians (Figure 10). The LSV boxplot also has three outliers above the group median, while the LSV and INF boxplots have no outliers (Figure 10). Neither cell has a maximum NO_3 concentration exceeding 30 mg/L, which meets the minimum water quality requirements for irrigational reuse (Table 5).
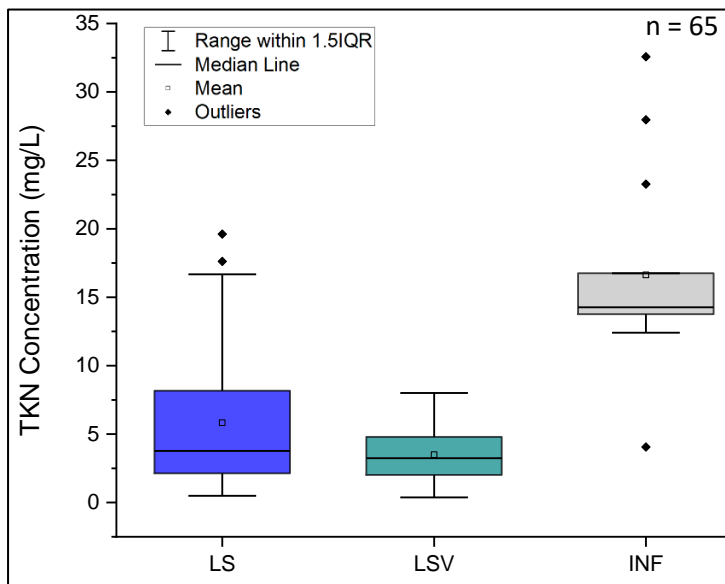
Figure 11: Box-and-whisker diagrams for NO_2^- concentration in the inflow (INF) and outflow (LS and LSV) of the cells (n = 65).

The median values are at similar levels across all the INF (Q2= 0.01), LS (Q2= 0.07), and LSV (Q2= 0.03) boxplots, showing that there was no significant difference in NO_2^- concentration between the inflow and outflow of both cells (Figure 11). However, the INF boxplot (Max= 0.23, Min= 0.004) is slightly higher than the LS (Max= 0.21, Min= 0.002) and LSV (Max= 0.14, Min = 0.004) boxplots, indicating that the overall NO_2^- concentrations were slightly higher in the inflow than in the outflow of both cells (Figure 11). The LSV boxplot (IQR= 0.05) is short in comparison to the LS (IQR= 0.1) and INF (IQR= 0.1) boxplots (Figure 11). This suggests that the overall NO_2^- concentration was less variable in the LSV cell than in the inflow and LS cell. All three boxplots have an asymmetrical distribution with positive skewness, indicating that most NO_2^- concentrations are higher than the group median (Figure 11). Several outliers are above the group medians in all three boxplots (Figure 11). Neither cell has a maximum NO_2 concentration exceeding 30 mg/L, which meets the minimum water quality requirements for irrigational reuse (Table 5).

Phosphorus

Box-and-whisker diagrams and five-number summaries were used to analyse the Total Phosphate (TP) concentrations in the inflow and outflow of both cells over 13 batch cycles (Figure 12).

Figure 12: Box-and-whisker diagrams for TP concentration in the inflow (INF) and outflow (LS and LSV) of the cells (n = 65).

The median values for the LS (Q2= 0.45) and LSV (Q2= 0.2) boxplots are at lower levels than the median value for the INF boxplot (Q2= 1.1), showing that there was a difference in TP concentration between the inflow and the outflow of both cells (Figure 12). In addition, the INF boxplot (Max= 1.2, Min= 0.6) is much higher than the LS (Max= 0.7, Min= 0.2) and LSV (Max= 0.4, Min= 0) boxplots, indicating that the overall TP concentrations were much lower in the outflow of both cells than in the inflow (Figure 12). However, the LS (IQR= 0.2), LSV (IQR= 0.1), and INF (IQR= 0.4) boxplots are all comparatively short (Figure 12). This suggests that there was a narrow distribution in TP concentration across the inflow and the outflow of both cells. All three boxplots have an asymmetrical distribution, with the LS and LSV boxplots being negatively skewed, and the INF boxplot being positively skewed (Figure 12). This indicates that most TP concentrations were lower than the group median in the LS and LSV boxplots, while most TP concentrations were higher than the group median in the INF boxplot. There are also several outliers in the LS and INF boxplots (Figure 12). The LS outliers are both higher and lower than the group median, while the INF outliers are much higher than the group median (Figure 12). The LSV boxplot has no outliers (Figure 12). While there are no DWAF water quality standards for COD, Rodda et al. (2010) suggest that a concentration below 10 mg/L is ideal for the use of greywater for small-scale irrigation in South Africa. Therefore, since the maximum outflow TP concentration is below 1 mg/L for both cells, the

treated water is suitable for unrestricted use with minimal risk to human health, plants or soil.

Chemical Oxygen Demand (COD)

Box-and-whisker diagrams and five-number summaries were used to analyse Chemical Oxygen Demand (COD) concentration in the inflow and outflow of both cells over 13 batch cycles (Figures 13).
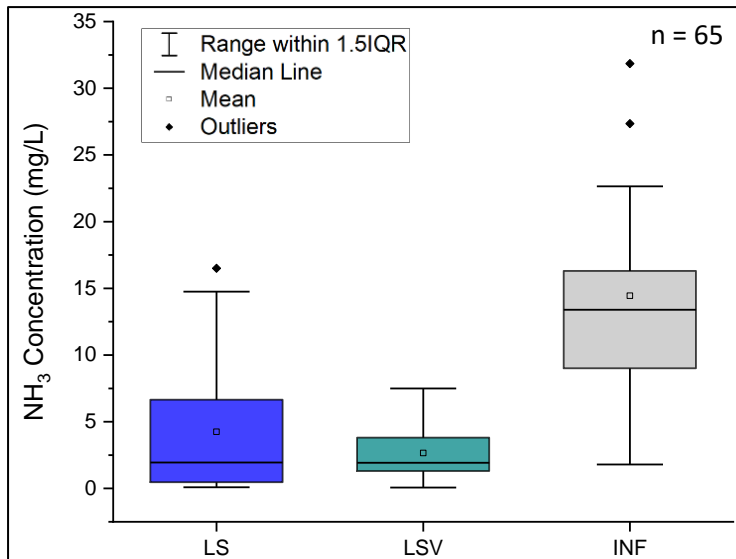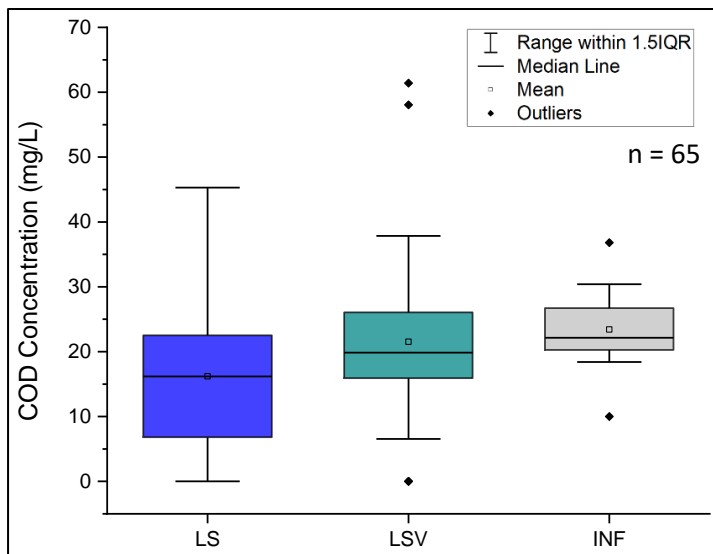

Figure 13: Box-and-whisker diagrams for COD concentration in the inflow (INF) and outflow (LS and LSV) of the cells (n = 65).

The median values for the LS (Q2= 16.2) and LSV (Q2= 19.9) boxplots are lower than the median value for the INF boxplot (Q2= 22.2), showing that there was a difference in COD concentrations between the inflow and the outflow of both cells (Figure 13). In addition, the INF boxplot (Max= 30.4, Min= 18.4) is higher than the LS (Max= 45.3, Min= 0) and LSV (Max= 37.9, Min= 6.6) boxplots, indicating that the overall COD concentrations were higher in the inflow than in the outflow of both cells (Figure 13). However, the LS (IQR= 15.6) and LSV (IQR= 10.1) boxplots are taller than the INF boxplot (IQR= 6.4) (Figure 13). This suggests that there was a wider distribution in COD concentration in the outflow of both cells compared to the inflow. All three boxplots have asymmetrical distributions with positive skewness, indicating that most COD concentrations were higher than the group medians (Figure 13). The LSV and INF boxplots also have a few outliers, which are both above and below the group medians (Figure 13). The LS boxplot has no outliers (Figure 13). While there are no DWAF water quality

standards for COD, Rodda et al. (2010) suggest that a concentration below 400 mg/L is ideal for the use of greywater for small-scale irrigation in South Africa. Therefore, since the outflow COD concentration of both cells falls within the target range, the treated water is suitable for irrigational reuse purposes.

pH

Box-and-whisker diagrams and five-number summaries were used to analyse pH in the inflow and outflow of both cells over 13 batch cycles (Figures 14).
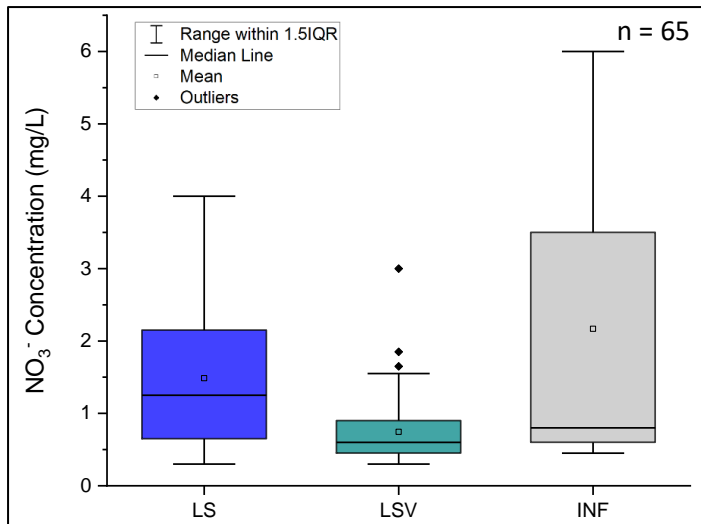

Figure 14: Box-and-whisker diagram for pH in the inflow (INF) and outflow (LS and LSV) of the cells (n = 65).

The median value is higher in the INF boxplot (Q2= 7.3) compared to the median values of the LS (Q2= 7) and LSV (Q2= 6.8) boxplots, showing that there was a difference in pH between the inflow and the outflow of both cells (Figure 14). In addition, the INF boxplot (Max= 7.5, Min= 6.7) is slightly higher than the LS (Max= 7.3, Min= 6.5) and LSV (Max= 7.4, Min= 6.3) boxplots, indicating that the overall pH was slightly higher in the inflow than in the outflow of both cells (Figure 14). However, the INF (IQR= 0.4), LS (IQR= 0.3), and LSV (IQR= 0.4) boxplots are all relatively short (Figure 14). This suggests that there was a narrow distribution in pH across the inflow and outflow of both cells. The LS and INF boxplots have asymmetrical distributions with positive skewness, indicating that most pHs were higher than the group medians (Figure 14). The LS boxplot also has a few outliers that are above and below the group median,

whereas the INF boxplot has no outliers (Figure 14). The LSV boxplot has one major outlier that is below the group median (Figure 14). The average pH for the outflow of the LS and LSV cells is 6.9 and 6.8 (Figure 14), which meets the minimum water quality requirements for irrigational reuse purposes (Table 6).

Table 6: Effects of pH on crop yield and quality and sustainability of soil (DWAF, 1996).

Concentration range (mg/L)	Crop yield and quality	Sustainability
< 6.5	Increasing problems with foliar damage when crop foliage is wet. This could give rise to yield reduction or a decrease in the quality of marketable materials.	Increasing problems with the availability of several micro-nutrients and macro-nutrients in toxic concentrations are experienced in this range over the long term.
Target water quality range 6.5–8.4	**Even when crop foliage is wetted, this should not cause foliar damage in plants which will result in a yield reduction or a decrease in the quality of marketable products.**	**Soil pH within this range does not present major problems with either unavailability of plant nutrients or toxic levels of elements.**
> 8.4	Increasing problems with foliar damage affecting yield or decrease in the visual quality of visual marketable products are experienced in this range.	Increasing problems with the unavailability of several micro- and macro-nutrients are experienced within this range over the long term.

Electrical conductivity (EC)

Box-and-whisker diagrams and five-number summaries were used to analyse Electrical Conductivity (EC) in the inflow and outflow of both cells over 13 batch cycles (Figures 15).
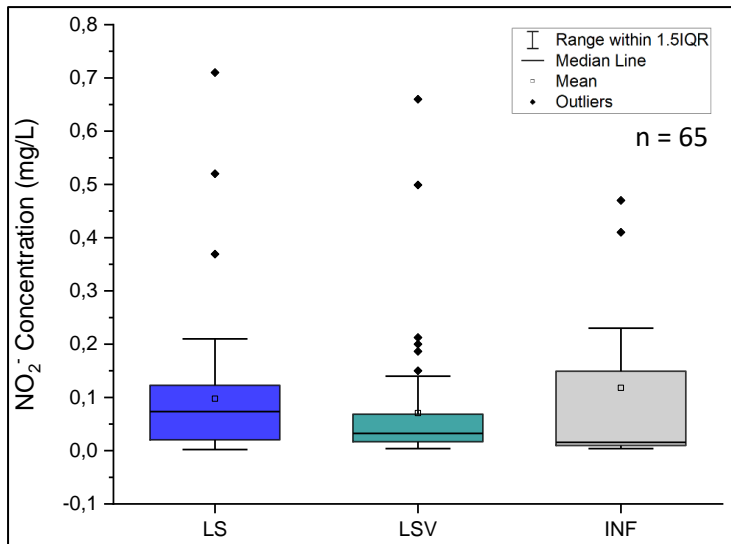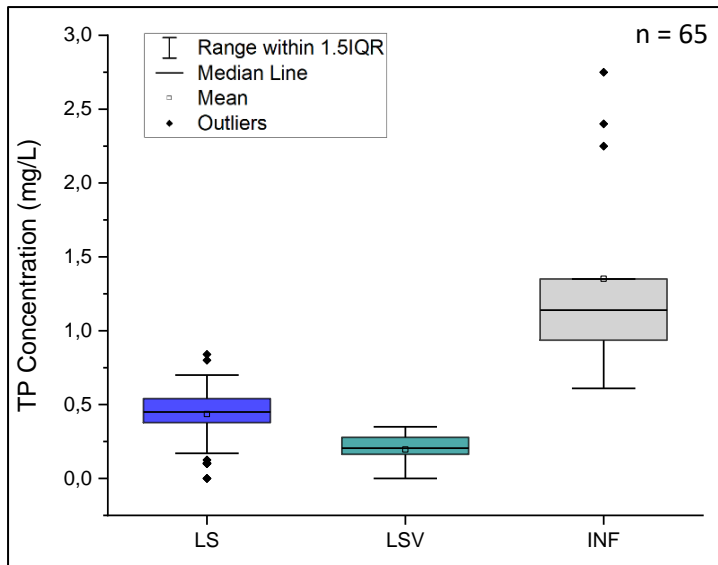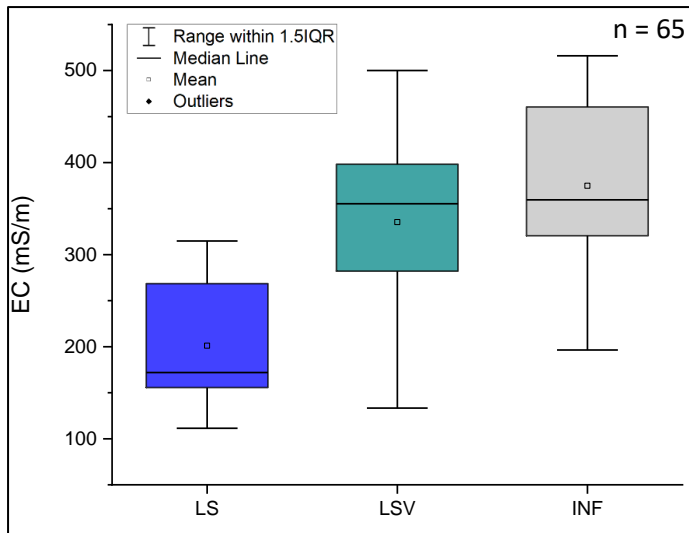
Figure 15: Box-and-whisker diagram for EC concentration in the inflow (INF) and outflow (LS and LSV) of the cells (n = 65).

The median value is at a slightly higher level in the INF boxplot (Q2= 359.5) than in the median values for the LS (Q2= 172) and LSV (Q2= 355.5) boxplots, showing that there was a difference in EC concentration between the inflow and the outflow of both cells (Figure 15). In addition, the INF boxplot (Max= 516, Min= 196.5) is slightly higher than the LS (Max= 314.9, Min= 111.4) and LSV (Max= 500, Min= 133.2) boxplots, indicating that the overall EC concentrations were slightly greater in the inflow than in the outflow of both cells (Figure 15). However, the INF (IQR= 140), LS (IQR= 113), and LSV (IQR= 116) boxplots are all relatively tall (Figure 15). This suggests that there was a wide distribution in EC concentration in the inflow and the outflow of both cells. The LS and INF boxplots have asymmetrical distributions with positive skewness, indicating that most EC concentrations were higher than the group median (Figure 15). Neither boxplot has any outliers (Figure 15). By contrast, the LSV boxplot has a more symmetrical distribution, suggesting that there is an even distribution in EC concentration across the group (Figure 15). The LSV boxplot has one outlier that is significantly lower than the group median (Figure 15).

The average EC concentration for the LS cell is 201.1 mg/L, while the average EC concentration for the LSV cell is 335.3 mg/L (Figure 15). This shows that both cells meet the requirements for the irrigation of most non-sensitive crops (Table 7). However, a leaching fraction of up to 0.15 may be required when using the outflow from the LS cell to irrigate vegetables, while a leaching fraction of up to 0.2 may be required when using the outflow from the LSV cell (Table

7). Therefore, if soils are adequately drained, then soil salinity can be controlled by providing for additional leaching (DWAF, 1996).

Table 7: Effects of TDS/EC on crop yield (DWAF, 1996).

EC range (mS/m)	Crop yield
Target water quality range · 40	**Should ensure that salt-sensitive crops can be grown without yield decreases when using low-frequency irrigation systems. A leaching fraction of up to 0.1 may be required and wetting of the foliage of sensitive crops should be avoided.**
40–90	Sensitive crops are increasingly likely to be affected (depending on the magnitude of irrigation application). Other crops remain largely unaffected in the lower concentration range but are increasingly affected as concentration increases.
90–270	A 90% relative yield of moderately salt-sensitive crops can be maintained by using a low-frequency application system. A leaching fraction of up to 0.15 may be required and wetting of the foliage of sensitive crops should be avoided.
270–540	An 80% relative yield of moderately salt-tolerant crops can be maintained provided that a high-frequency irrigation system is used. A leaching fraction of up to 0.2 may be required and wetting of the foliage of sensitive crops should be avoided.
>540	These waters can still be used for irrigation of selected crops provided sound irrigation management is practised and yield decreases are acceptable. However, the management and soil requirements become increasingly restrictive, and the likelihood of sustainable irrigation decreases rapidly.

Temperature

Box-and-whisker diagrams and five-number summaries were used to analyse the temperature in the inflow and outflow of both cells over 13 batch cycles (Figures 16).

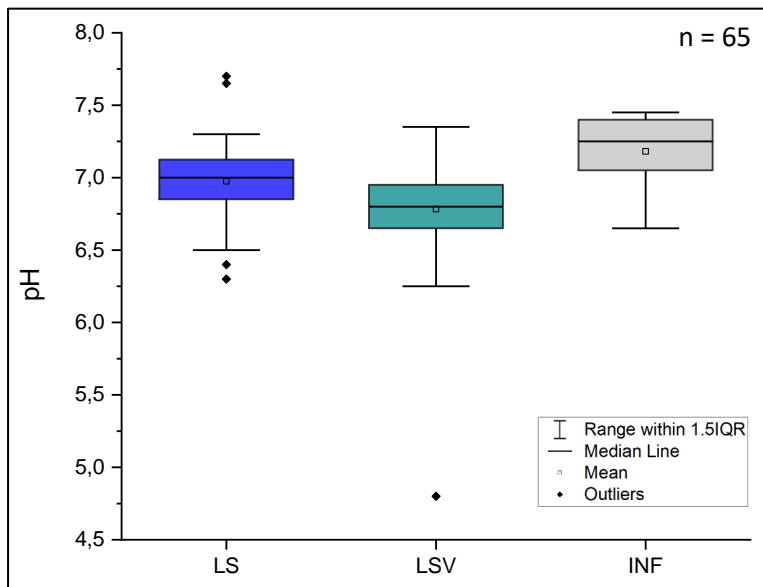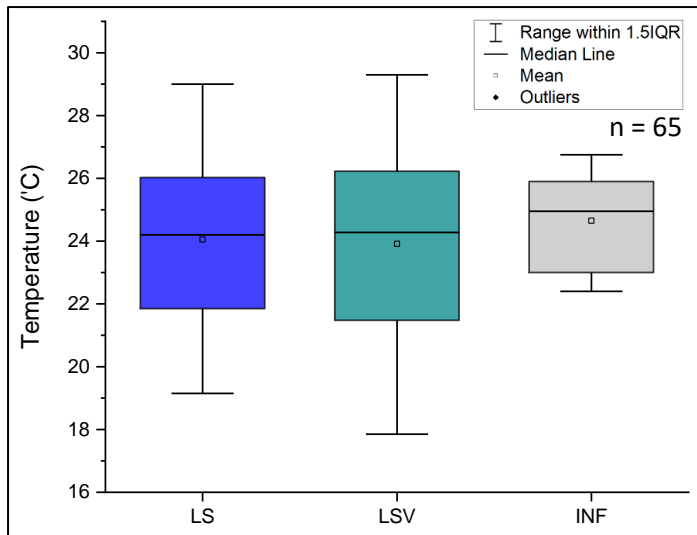Figure 16: Box-and-whisker diagram for temperature in the inflow (INF) and outflow (LS and LSV) of the cells (n = 65).

The INF (Q2= 25), LS (Q2= 24.2), and LSV (Q2= 24.3) boxplots have similar median values, showing that there was no significant difference in temperature between the inflow and the outflow of both cells (Figure 16). In addition, the LS (Max= 29, Min= 19.2) and LSV (Max= 29.3, Min= 17.9) boxplots are slightly higher than the INF boxplot (Max= 26.8, Min= 22.4), indicating that the overall temperature was slightly higher in the inflow than in the outflow of both cells (Figure 16). However, the LS (IQR= 4.2) and LSV (IQR= 4.8) boxplots are slightly taller than the INF boxplot (IQR = 2.9) (Figure 16). This suggests that there was a wider distribution in temperature in the outflow of both cells than in the inflow. The INF boxplot has an asymmetrical distribution with a negative skewness, indicating that most temperature values were lower than the group median (Figure 16). The LS and LSV boxplots have a more symmetrical distribution, suggesting that temperature is more evenly spread across the groups (Figure 16). There are no outliers in any of the boxplots (Figure 16).

4.1.1.2. Moving average values over time

Two-day moving average values were calculated for the inflow and outflow water quality of the LS and LSV cells over 13 batch cycles. Graphs were then used to illustrate these moving averages over time.
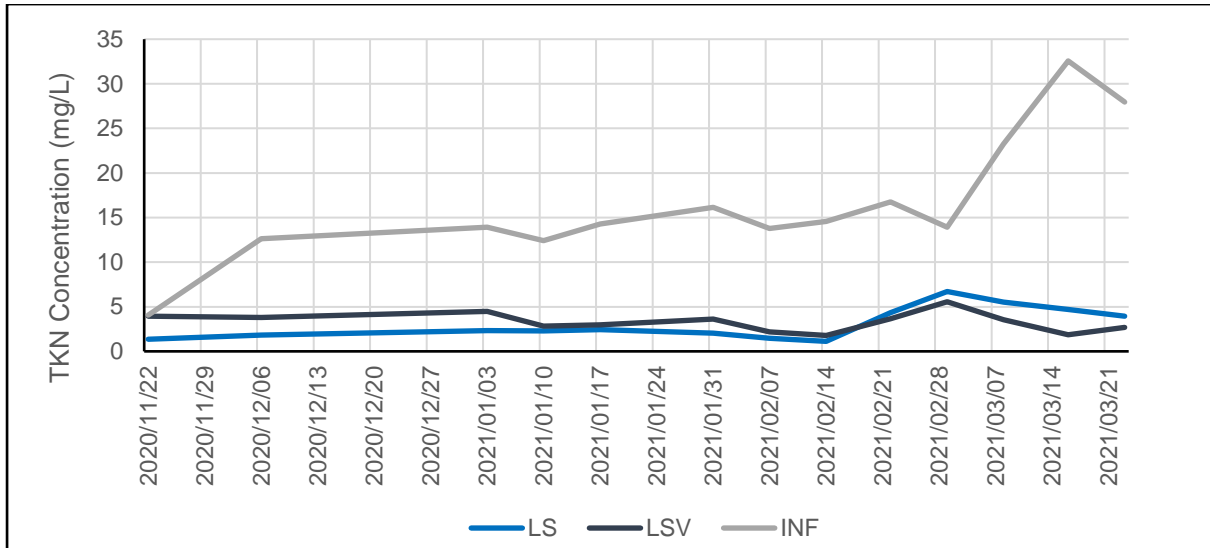
Figure 17: Moving average values for TKN concentration in the inflow (INF) and outflow (LS and LSV) of the cells over time.

TKN was consistently higher in the inflow compared to the outflow of both cells over time. After an initial increase from 5 mg/L to 12.6 mg/L, inflow TKN remained relatively constant (ranging between 12.4 mg/L and 16.8 mg/L) until the beginning of March when it elevated to a maximum of 32.6 mg/L by mid-March (Figure 17). LS and LSV TKN remained relatively constant over time, ranging between 1.1–6.7 mg/L and 1.8–5.6 mg/L (Figure 17). However, a slight increase in outflow TKN was observed towards the end of March (Figure 17). This increase coincided with the second elevated peak in inflow TKN (Figure 17).

Figure 18: Moving average values for NH_3 concentration in the inflow (INF) and outflow (LS and LSV) of the cells over time.

Inflow NH_3 was consistently higher than outflow NH_3 in both cells over time. Inflow NH_3 increased steadily (from 1.8 mg/L to 16.3 mg/L) between November and March (Figure 18). It then reached a maximum of 31.9 mg/L in mid-March (Figure 18). LSV NH_3 (0.9–3.9 mg/L) was higher than LSV NH_3 (0.1–0.5 mg/L) until mid-February when LSV NH_3 decreased to an average of 1.3 mg/L and LS NH_3 increased to an average of 1.9 mg/L (Figure 18). This shift coincided with the rise in inflow NH_3 (Figure 18).
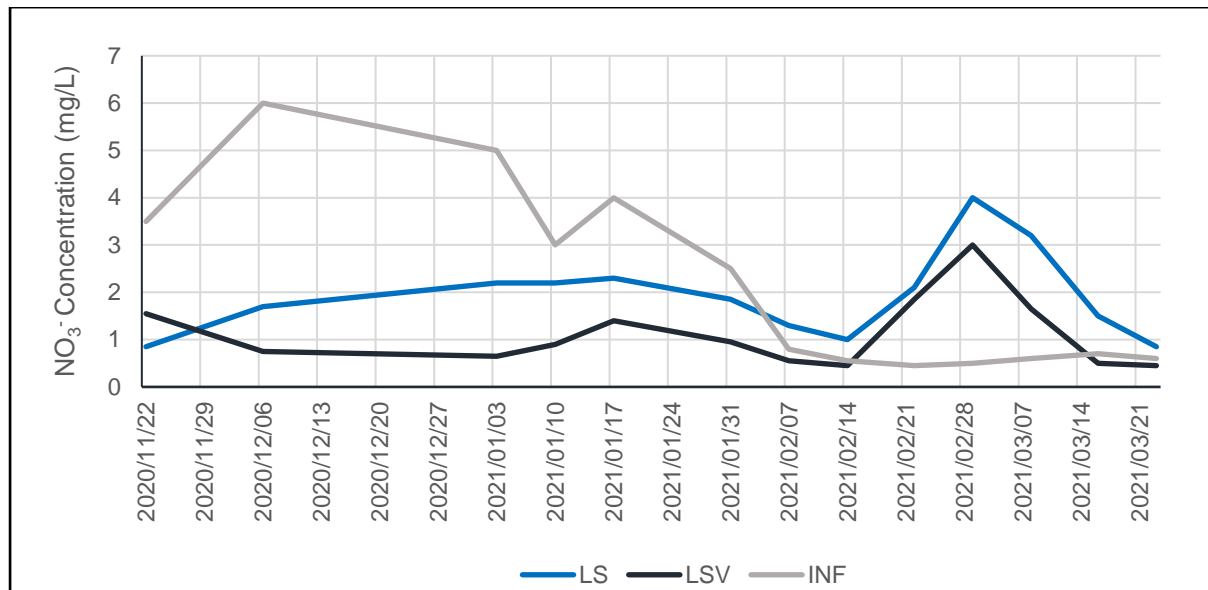
Figure 19: Moving average values for NO_3^- concentration in the inflow (INF) and outflow (LS and LSV) of the cells over time.

An increase in inflow NO_3^- (from 3.5 mg/L to 6 mg/L) was observed at the start of the study period, followed by a rapid decline (from 6 mg/L to 0.6 mg/L) over time (Figure 19). Initially, the inflow NO_3^- was much higher than the outflow NO_3^- of both cells, however, a sharp increase in LS (from 1 mg/L to 4 mg/L) and LSV (from 0.5 mg/L to 3 mg/L) NO_3^- was observed between mid-March and mid-February (Figure 19). This increase in outflow NO_3^- coincided with consistently low inflow NO_3^-, which ranged between 0.5 mg/L and 0.7 mg/L (Figure 19). LS NO_3^- was consistently higher than LSV NO_3^- over time (Figure 19).
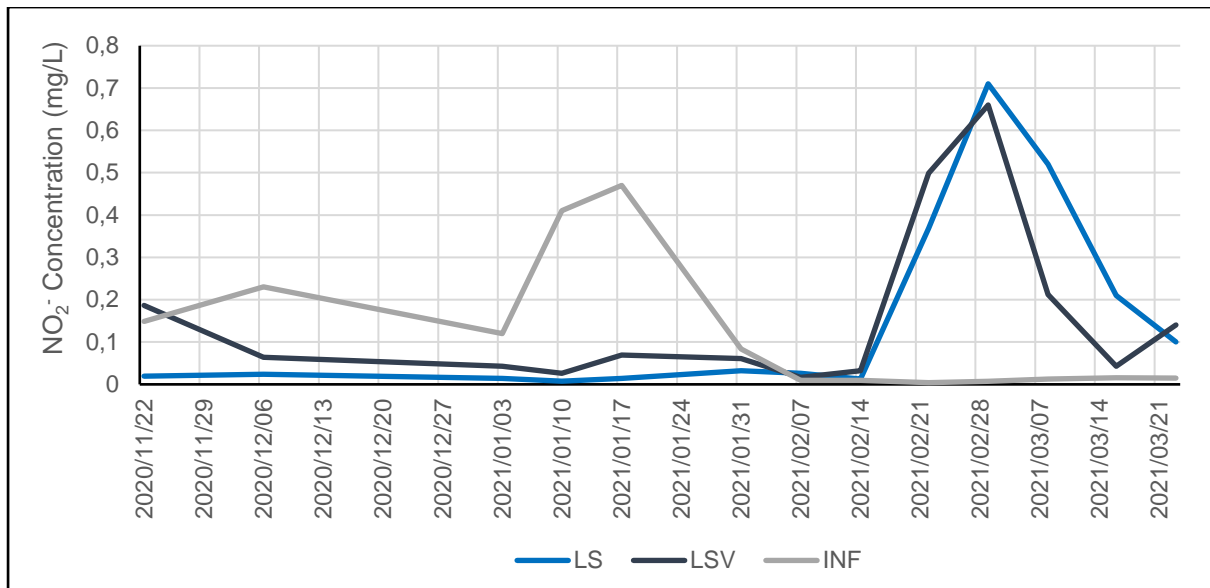
Figure 20: Moving average values for NO_2^- concentration in the inflow (INF) and outflow (LS and LSV) of the cells over time.

Two sharp increases in inflow NO_2^- were observed during the first half of the study period (Figure 20). Maximum values of 0.23 mg/L and 0.47 mg/L were reached during these increases (Figure 20). However, a sharp decrease in NO_2^- (from 0.47 mg/L to 0.005 mg/L) was observed in the inflow between mid and late January (Figure 20). It then stabilised (with a concentration range between 0.004 mg/L and 0.02 mg/L) until the end of the study (Figure 20). Initially, inflow NO_2^- was much higher than outflow NO_2^- (Figure 20). However, a sharp increase in LS and LSV NO_2^- was observed in mid-February, with LS reaching a maximum of 0.7 mg/L and LSV reaching a maximum of 0.5 mg/L (Figure 20). LSV NO_2^- was consistently higher than LS NO_2^- until the inflow NO_2^- stabilised (Figure 20). A significant drop in LS (from 0.7 mg/L to 0.1 mg/L) and LSV (from 0.7 mg/L to 0.04 mg/L) NO_2^- was observed following the initial increase in outflow NO_2^- (Figure 20). This decrease coincided with the stabilisation of inflow NO_2^- (Figure 20).
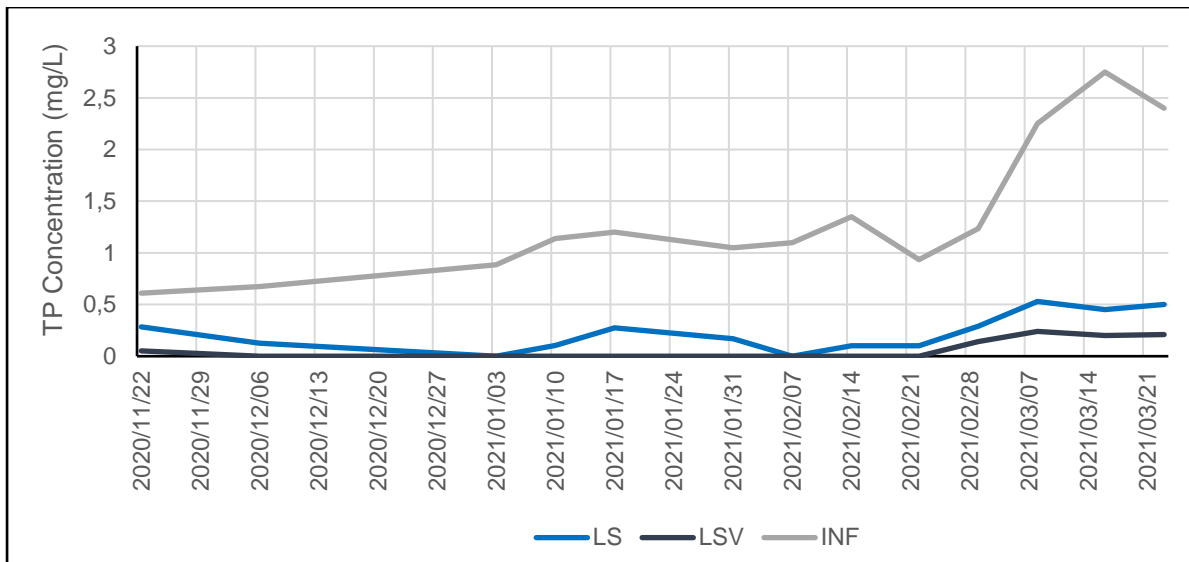
Figure 21: Moving average values for TP concentration in the inflow (INF) and outflow (LS and LSV) of the cells over time.

Inflow TP was consistently higher than outflow TP over time (Figure 21). Inflow TP increased steadily over time (from 0.6 mg/L to 1.35 mg/L) until the end of February when inflow TP increased rapidly from 0.9 mg/L to 2.8 mg/L (Figure 21). LS TP ranged between 0 mg/L and 0.5 mg/L, respectively, and remained consistently higher than LSV TP which ranged between 0 mg/L and 0.2 mg/L (Figure 21). An increase in outflow TP from the outflow of both cells coincided with the rapid increase in inflow TP towards the end of February (Figure 21). However, TP stabilised in the outflow of both cells following an initial increase (Figure 21).
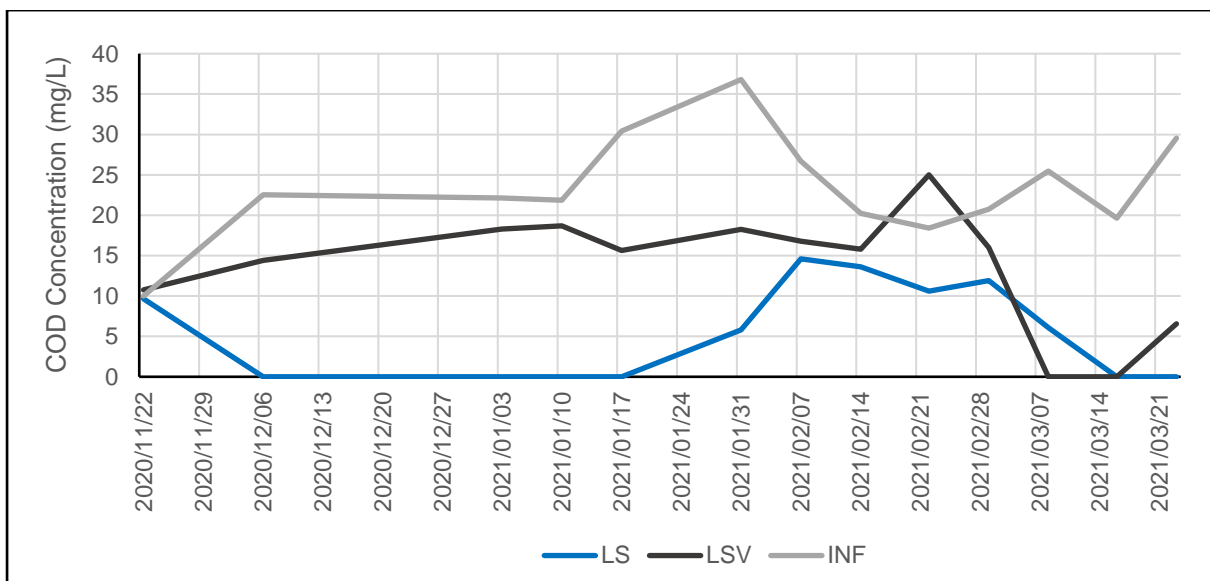
Figure 22: Moving average values for COD concentration in the inflow (INF) and outflow (LS and LSV) of the cells over time.

Inflow COD was consistently higher than the outflow COD over time, except for the sharp increase in LSV COD (from 15.8 mg/L to 25 mg/L) that was observed towards the end of February (Figure 22). This increase in LSV COD was observed following a sharp increase in inflow COD (from 21.9 mg/L to 36.8 mg/L) (Figure 22). A sharp increase in LS COD (from 0 mg/L to 14.6 mg/L) was also observed during this period (Figure 22). However, LS COD remained consistently lower than LSV COD over time (Figure 22). A decrease in both LS and LSV COD was also observed following a drop in inflow COD in February (Figure 22).
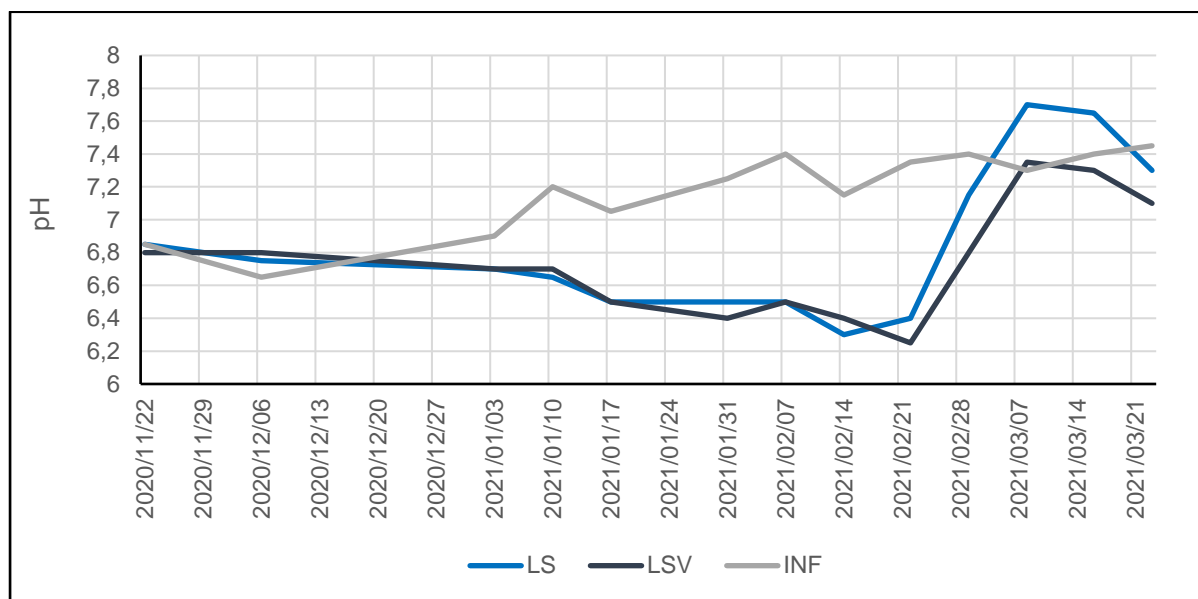
Figure 23: Moving average values for pH in the inflow (INF) and outflow (LS and LSV) of the cells over time.

The inflow and outflow pH remained relatively stable over time (Figure 23). The inflow pH increased steadily (from 6.9 to 7.4) between January and February until it eventually stabilised at 7.4 towards the end of February (Figure 23). The outflow pH of both cells was very similar, however, a sharp increase in pH was observed in both cells towards the end of February (Figure 23). This increase coincided with the stabilisation of inflow pH at 7.4 (Figure 23).
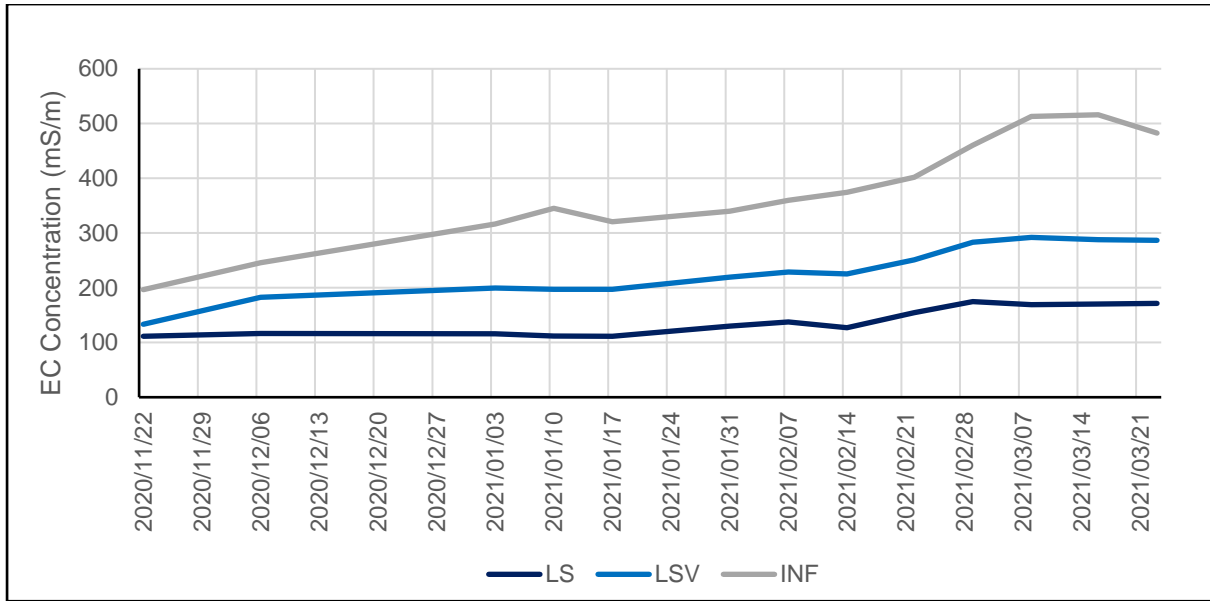
Figure 24: Moving average values for EC concentration in the inflow (INF) and outflow (LS and LSV) of the cells over time.

Inflow EC remained higher than the outflow EC over time (Figure 24). Inflow EC increased steadily from a low of 196.5 mS/m in November to a peak of 516 mS/m in March (Figure 24). LS and LSV EC followed a similar pattern to the inflow EC, with LS increasing from a low of 111.4 mS/m in November to a peak of 174.7 mS/m in March and LSV increasing from a low of 133.3 mS/m in November to a peak of 292 mS/m in March (Figure 24). Apart from January, the outflow COD of the LS cell remained consistently higher than the outflow COD of the LS cell over time (Figure 24). However, this difference is almost negligible.
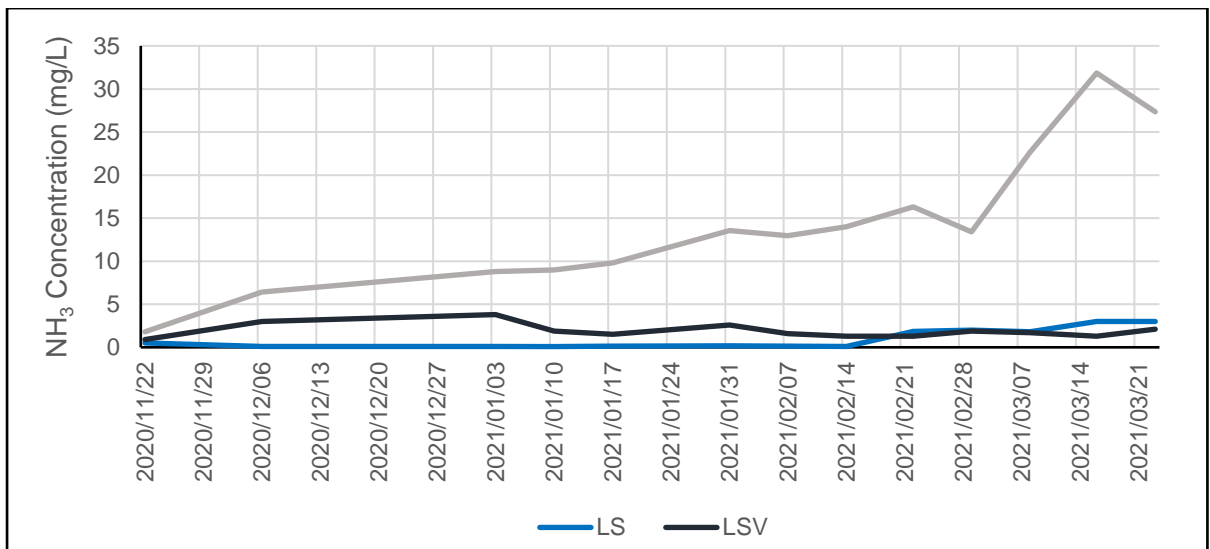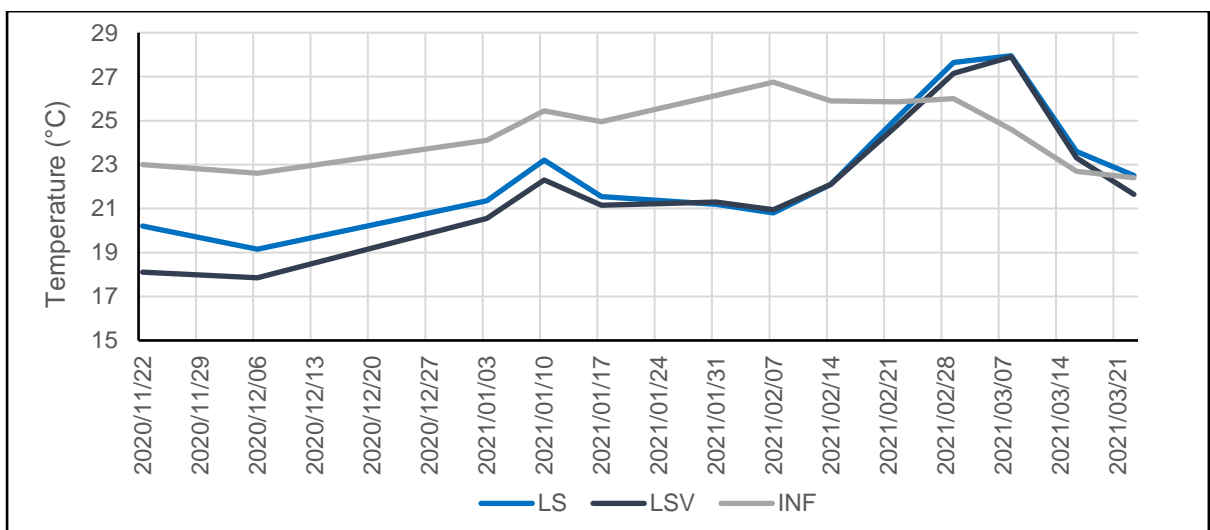

Figure 25: Moving average values for temperature in the inflow (INF) and outflow (LS and LSV) of the cells over time.

Inflow and outflow temperatures increased steadily over time (Figure 25). For most of the study period, inflow temperature ranged between 22.6°C and 26.8°C and was consistently higher than the outflow temperatures (Figure 25). However, the inflow temperature dropped towards the end of February (from 26°C to 22.4°C) (Figure 25). An increase in outflow temperature coincided with the drop in inflow temperature (Figure 25). The outflow of both cells reached a maximum temperature of 27.9°C during this period, which exceeded the inflow temperatures (Figure 25). For most of the study period, however, the outflow temperatures of the LS cell remained consistently higher than the outflow temperatures of the LSV cell over time (Figure 25).

4.1.1.3. Discussion

The results from this study show that the overall TKN concentrations were lower in the outflow of both cells than in the inflow. In addition, inflow TKN concentrations gradually increased over time, however, outflow TKN concentrations remained relatively consistent. This suggests that N was effectively removed by both cells. The net removal of N could be attributed to (a) sorption of organic N onto the media (Davis et al., 2006), (b) degradation of captured organic N by microbial populations (Kadlec and Reddy, 2001), or (c) uptake of organic N by plants (Bratieres et al., 2008). Given the small difference in outflow TKN between the cells, it seems unlikely that plant uptake was a major contributor to N removal. Therefore, the performance disparity could be attributed to differences in N sorption capacities and/or microbial degradation rates in the cells (Saeed and Sun, 2011).

By examining the individual N species, the overall NH_3 concentrations were lower in the outflow of both cells than in the inflow. In addition, inflow NH_3 concentrations increased gradually over time, however, outflow NH_3 concentrations remained relatively consistent. This indicates that NH_3 was effectively removed by the cells, which suggests that nitrification may have been enhanced in both cells (Bratieres et al., 2008). In addition, there was little difference in outflow NH_3 between both cells, which suggests that the microbial activity responsible for nitrification in the cell was not strongly dependent on symbioses with plants (Gerardi, 2003). Any variation in nitrification (and hence, NH_3) could therefore be attributed to changes in the availability of oxygen in the cells (Skorobogatov et al., 2020; Garcia et al., 2010).

The overall NO_3^- concentrations were higher in the outflow of the LS cell than in the inflow, which suggests that NO_3^- was produced from OM and leached from the LS cell during the study. Poor NO_3^- removal and/or leaching was also observed in several other biofiltration studies (Davis et al., 2006; Bratieres et al., 2008; Davis et al., 2001). The researchers showed that a breakdown of organic matter (OM) (resulting in the poor uptake of OM by the microbial community) caused an overall production of NO_3^- (and hence, poor TN removal) and a deteriorating performance over time. Davis et al. (2001) observed the same phenomenon and suggested that N leaching could be linked to the biological transformation of captured NH_3 and organic N to NO_3^- or NO_2^- between runoff events. The anionic form of oxidised N only shows minimal adsorption or physical interaction with soil (Henderson et al., 2007). Therefore, only limited amounts are removed, with minimal denitrification occurring in the soil columns (Kim et al., 2003). The high concentrations of NO_3^- in the LS cell could therefore suggest that denitrification was limited in the cell. This may be due to the breakdown of OM in the cell, or other environmental parameters including the pH value, temperature, absence of oxygen, presence of denitrifying bacteria, redox potential and moisture content of the cell (Garcia et al., 2010). The sharp increase in pH in both cells between mid-February and mid-March can be attributed to a shift in microbial activity. In particular, a rise in pH suggests that denitrification is may be the predominant process (Saeed & Sun, 2011).

The moving average graph (Figure 19) shows that outflow NO_3 concentrations increased gradually in both cells over time, which suggests that NO_3^- may have accumulated in the cells during the study period. These results are not surprising, as minimal adsorption or physical interaction between NO_3^- and the filtration medium can be expected (Davis et al., 2006). According to Davis et al. (2006), NO_3^- does not readily sorb onto the media, so biofilters are not expected to provide any NO_3^- removal. Therefore, any reduction in NO_3^- is considered an additional bonus (Davis et al., 2006). Similarly, Kim et al. (2003) reported that NO_3^- leaching is increased after extended drying periods as a result of long-dormant periods where nitrification proceeds without adequate denitrification to remove N completely from the system. These results could also explain the high concentrations of NO_2^- observed in this study. Several cases of NO_2^- leaching were found, whereby the outflow NO_2^- concentrations exceeded the inflow concentrations. This further supports the theory that minimal

denitrification occurred in the cells, and that nitrification was the predominant N removal process.

The overall TP concentrations were lower in the outflow of both cells than in the inflow. This suggests that phosphate was effectively removed by the cells during the study, despite the gradual increase in inflow TP over time. In general, the LSV cell performed slightly better than the LS cell, which suggests that the vegetation in the LSV cell may have contributed to greater reductions of TP in the infiltrating runoff. These results compare to several other studies which have shown that vegetated biofilters remove more nutrients than non-vegetated biofilters (Lucas and Greenway, 2008; Glaister et al., 2017; Davis et al., 2006; Bratieres et al., 2008). Accordingly, vegetation can enhance the pollutant removal efficiencies of biofilters directly through plant uptake and by maintaining the soil porosity, and indirectly by influencing the soil microbial communities (Read et al., 2008). However, considering the non-vegetated cell could also reduce nutrient concentrations, there is reason to believe that biofilters do not need to be vegetated to be effective. Hence, it is assumed that a significant amount of phosphate may have been removed by filtration and sorption onto aluminium, iron and clay mineral in the media (Davis et al., 2001). This observation is further explained in the paragraph on EC.

The outflow and inflow COD concentrations were extremely variable over time; however, the overall COD concentrations were lower in the outflow of both cells than in the inflow. In addition, the COD concentrations were slightly higher in the LSV cell than in the LS cell, which suggests that vegetation made very little difference to carbon removal. Similar findings were made by Henderson et al. (2007) who suggested that the type of media exerted more influence on carbon treatment than vegetation. Accordingly, smaller particle sizes and greater clay/silt fraction removed more carbon. This suggests that the LS cell may have had greater availability of clay and/or silt, resulting in the higher removal of carbon by the cell.

The overall EC (and hence, total dissolved solids or TDS) concentrations were lower in the outflow of both cells than in the inflow, which suggests that the cells were effective at removing TDS. However, the outflow EC concentration seemed to be positively correlated with the inflow EC (i.e., outflow TDS increased with inflow TDS). This could also explain the increase in outflow TP over time, which suggests that dissolved phosphate accumulated in the cells (LeFevre et al., 2015). According to previous research, phosphate sorbs onto Fe (II)

and Al oxides, however, if the system becomes anaerobic, then it might be reducing the Fe (II) oxides (Garcia et al., 2010). This mobilises Fe (II) in the system, which in turn mobilises phosphate. Therefore, the gradual increase in outflow TP could thus be attributed to the desorption of dissolved phosphate in the system over time. Similar findings were made by Hunt et al. (2006) who showed that soils with high availability of P that are near saturation released P due to desorption.

The outflow pH level of both cells was lower than the inflow pH level, which suggests that both cells increased the acidity of the inflow. These results further support the theory that nitrification was the predominant N removal process in the cells, as a drop of inflow pH and alkalinity consumption in outflow is usually associated with high levels of nitrification (Saeed and Sun, 2011). However, these results contrast with those noted for similar studies, in which variations in pH were buffered by the soil and produced little variation in removal efficiencies (Davis et al., 2006; Kim et al., 2003). Accordingly, biofilter soil media can significantly buffer pHs within the range of 6.0–8.0. The results from this study, therefore, suggest that the large stone media was not an effective pH buffer, which could explain the high levels of nitrification observed in the cells. The rise in pH in the outflow of both cells between mid-February and mid-March could indicate a shift in microbial activity, with denitrification becoming the predominant process (Saeed & Sun, 2011).

The outflow temperature of both cells was lower than the inflow temperature, which suggests that there are possible local temperature cycle linkages. By comparison, Dietz and Clausen (2005) showed that an average increase in water temperature was observed in the outflow of two field-scale biofilters in Haddam, Connecticut, over a year. However, it was determined that the temperature differences between the inflow and outflow were not statistically significant and fluctuations in outflow temperatures could be attributed to seasonal temperature variations. Jones and Hunt (2009) also showed the maximum inflow temperatures of four biofilters in North Carolina decreased substantially after the water travelled through the biofiltration media. Therefore, the filter media of the cells in this study possibly had cooling effects on the infiltrating runoff due to the increase in depth (below the surface level). The increase in temperature observed in the outflow of both cells between mid-February and mid-March can be attributed to warmer external temperatures experienced during the time of sampling.

4.1.2. Pollutant percentage reductions

4.1.2.1. Percentage nutrient reductions over varying HRTs and inflow water quality conditions

NH_3, TKN and TP removal efficiencies were quantified as percentage reductions in both cells over varying HRTs and inflow water quality conditions (Table 5). Batches 1–5 were grouped and were classified as having 'low' NH_3 and TP concentrations, which ranged between 1.8–9.8 mg/L and 0.6–1.2 mg/L. Batches 6-10 were grouped and were classified as having 'medium' NH_3 and TP concentrations, which ranged between 13–16.3 mg/L and 0.9–1.4 mg/L. Batches 11–13 were grouped and were classified as having 'high' NH_3 and TP concentrations, which ranged between 22.7–31.9 mg/L and 2.3–2.8 mg/L. These classifications were based on baseline data collected from the Stiebeuel River (i.e., the inflow) in a previous study (Fell, 2018).

Table 8: Percentage reduction of NH_3, TKN and TP in both cells under varying HRTs and inflow water quality conditions.

		HRT (days)	Batch 1	Batch 2	Batch 3	Batch 4	Batch 5	Batch 6	Batch 7	Batch 8	Batch 9	Batch 10	Batch 11	Batch 12	Batch 13
INF	NH_3 (mg/L)	0	1.8	6.4	8.8	9.0	9.8	13.6	13.0	14.0	16.3	13.4	22.7	31.9	27.4
	TP (mg/L)	0	0.6	0.7	0.9	1.1	1.2	1.1	1.1	1.4	0.9	1.2	2.3	2.8	2.4
LS CELL	% NH_3 Removal	1	72	98	79	67	83	92	85	89	68	52	62	54	88
		3	94	98	77	69	89	85	92	79	48	19	36	54	99
		5	94	98	80	77	96	87	99	89	60	19	27	67	87
		7	95	98	66	81	97	87	99	98	67	19	40	79	73
	% TP Removal	1	53	59	89	56	71	61	54	59	41	65	82	69	73
		3	80	75	67	57	68	57	59	69	30	54	81	80	71
		5	100	100	40	67	67	52	65	72	45	57	78	77	71
		7	83	85	49	70	67	52	53	72	58	60	64	78	74
LSV CELL	% NH_3 Removal	1	50	77	85	77	89	86	92	79	80	66	84	87	77
		3	0	59	78	80	89	80	97	85	72	59	81	81	79
		5	0	75	81	80	97	93	91	93	83	72	79	76	90
		7	0	80	85	87	99	93	85	89	88	72	83	79	94
	% TP Removal	1	91	100	100	82	87	80	68	84	79	81	89	91	87
		3	100	100	84	83	86	74	75	84	80	79	88	88	86
		5	100	100	73	85	85	70	83	86	84	75	89	88	87
		7	100	100	77	86	85	69	82	86	84	76	91	89	88

*Indicates low, medium and high inflow NH_3 and TP concentrations.

Table 9: Average NH$_3$, TKN and TP percentage reductions in both cells under varying HRTs and inflow water quality conditions.

	Batches 1-5		Batches 6-10		Batches 11-13	
	LS	**LSV**	**LS**	**LSV**	**LS**	**LSV**
NH$_3$	88%	69%	74%	85%	64%	85%
TP	71%	90%	59%	79%	72%	89%

*Indicates low, medium and high inflow NH$_3$ and TP concentrations.

NH$_3$ removal efficiencies in the LS cell were highest in batches 1, 2, 5, 7 and 8, with percentage reductions reaching and/or exceeding 95%, and lowest in batches 5, 6 and 7, with percentage reductions below 40% (Table 8). NH$_3$ removal efficiencies generally increased with HRT in these batches; however, the same pattern was not always observed for batches with lower NH$_3$ removal efficiencies (<75%) (Table 8). In general, the batches with low inflow NH$_3$ concentrations (i.e., batches 1-5) performed best, with an average percentage reduction of 88% (Table 9). However, the LS percentage reductions decreased under higher inflow NH$_3$ concentrations to 74% and 64% in batches 6–13 (Table 9).

NH$_3$ percentage reductions in the LSV cell were highest in batches 5,6 and 13, with percentage reductions reaching and/or exceeding 90%, and lowest in batch 1, with a percentage reduction of 0% (Table 8). NH$_3$ percentage reductions increased with HRT in these batches; however, the same pattern was not always observed for batches with lower NH$_3$ percentage reductions (<85%) (Table 8). In general, batches with medium to high inflow NH$_3$ concentrations (i.e., batches 6-13) performed best, with average percentage reductions of 85% (Table 9). The batches with low inflow NH$_3$ concentrations (i.e., batches 1–5) performed substantially worse than those with medium and high inflow NH$_3$ concentrations, with an average percentage reduction of 69% (Table 9).

The percentage reductions for TP in the LS cell were highest in batches 1 and 2, with percentage reductions exceeding 80%, and lowest in batches 3 and 7, with percentage reductions below 55% (Table 8). There was no distinct pattern in the relationship between TP percentage reduction and HRT. Some batches showed an increase in TP removal between days 1 and 5 followed by a decrease in TP removal (batches 1, 2 and 7), while others showed that TP removal either increased with HRT (batches 4, 8 and 13) or decreased with HRT (batch

6) (Table 8). In general, the batches with low and high inflow TP concentrations performed better than the batches with medium inflow TP concentrations. Average percentage reductions of 71% and 72% were reported for low and high inflow TP concentrations, while an average percentage reduction of 59% was reported for medium inflow TP concentrations (Table 9).

TP removal efficiencies in the LSV cell were highest in batches 1 and 2, with percentage reductions of up to 100%, and lowest in batch 6, with a percentage reduction of 69% (Table 8). In general, TP percentage reductions increased with HRT, except for batches 6 and 7 (Table 8). Batches with low inflow TP concentrations performed better than batches with medium and high TP concentrations, as the average percentage reduction for batches 1–5 was 90%, whereas the average percentage reductions for batches 6–10 and 11–13 were 70% and 89% (Table 9).

4.1.2.2. Nitrogen degradation over varying HRTs and inflow water quality conditions

Average values were calculated for NH_3, NO_3^- and NO_2^- in the LS and LSV cells over varying HRTs and inflow water quality conditions (Figure 27). Batches 1–5 were grouped and were classified as having 'low' NH_3 and TP concentrations, which ranged between 1.8–9.8 mg/L and 0.6–1.2 mg/L. Batches 6–10 were grouped and were classified as having 'medium' NH_3 and TP concentrations, which ranged between 13–16.3 mg/L and 0.9–1.4 mg/L. Batches 11–13 were grouped and were classified as having 'high' NH_3 and TP concentrations, which ranged between 22.7–31.9 mg/L and 2.3–2.8 mg/L.
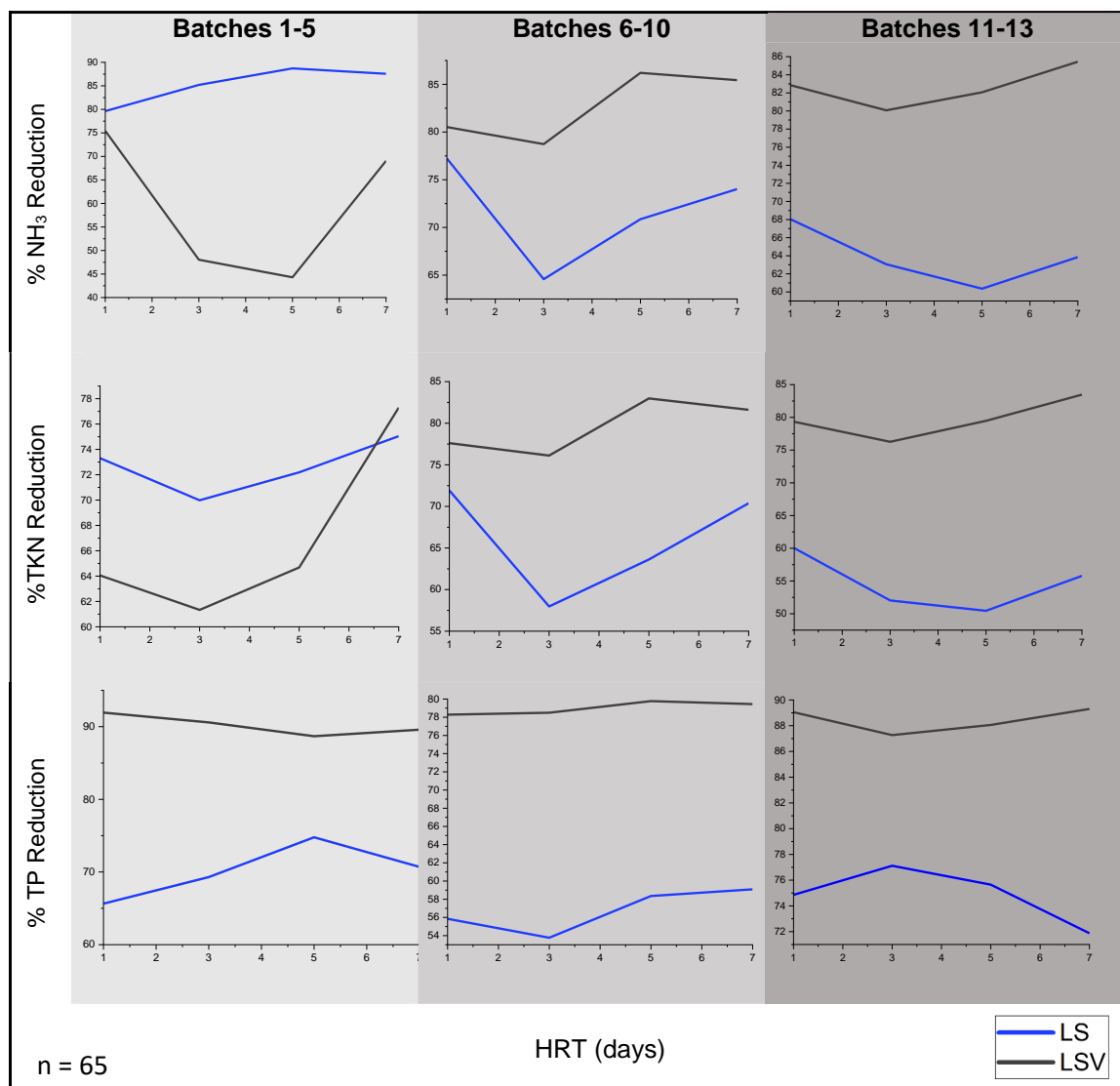
Figure 26: Average NH_3, NO_3^- and NO_2^- concentrations in the LS and LSV cells under varying HRTs and inflow water quality conditions. Batches classified according to inflow NH_3 concentrations: low (1.8–9.8 mg/L), medium (13–16.3 mg/L) and high (22.7–27.4 mg/L).

In batches 1-5, the average NH_3 concentration decreased from 1.4 to 0.9 mg/L between days 1 and 5 in the LS cell (Figure 26). This coincided with an increase in average NO_3^- and NO_2^- concentrations from 1.4 to 1.7 mg/L and 0.1 to 0.2 mg/L between days 1 and 3 (Figure 26). The average NH_3 concentration then increased from 0.9 to 1.0 mg/L between days 5 and 7, which coincided with a decrease in average NO_3^- and NO_2^- concentrations from 1.6 to 1.1 mg/L and 0.14 to 0.07 mg/L (Figure 26). In the LSV cell, the average NH_3 concentration increased from 1.4 to 2.1 mg/L between days 1 and 3 and subsequently decreased from 1.8 to 1.2 mg/L

between days 3 and 7 (Figure 26). The same pattern was observed for the average NO_3^- and NO_2^- concentrations (Figure 26).

In batches 6-10, the average NH_3 concentrations increased from 3.2 to 5.1 mg/L between days 1 and 3 in the LS cell and subsequently decreased from 5.1 to 3.7 mg/L between days 3 and 7 (Figure 26). The same pattern was observed for average NO_3^- and NO_2^- concentrations, which increased from 0.9 to 1.1 mg/L and 0.07 to 0.09 mg/L between days 1 and 3 and then decreased from 1.1 to 0.7 mg/L and 0.09 to 0.05 mg/L between days 3 and 7 (Figure 26). In the LSV cell, the average NH_3 concentrations increased from 2.7 to 3.0 mg/L between days 1 and 3 and then decreased from 3.0 to 2.0 mg/L between days 3 and 7, and thus followed a similar pattern to the LS cell (Figure 26). However, the average NO_3^- and NO_2^- concentrations increased gradually from 0.5 to 0.6 mg/L and 0.02 to 0.05 mg/L between days 1 to 7, which coincided with the decrease in average NH_3 concentration (Figure 26).

In batches 11-13, the average NH_3 concentrations increased from 8.8 to 10.2 mg/L between days 1 and 5 in the LS cell and subsequently decreased from 10.2 to 9.3 mg/L between days 5 and 7 (Figure 26). The average NO_3^- and NO_2^- decreased from 3.0 to 2.2 mg/L and 1.1 to 0.09 mg/L between days 1 and 7 (Figure 26). In the LSV cell, the average NH_3 concentrations increased from 4.6 to 5.4 mg/L between days 1 and 3 and subsequently decreased from 5.4 to 4.0 mg/L between days 3 and 7 (Figure 26). However, the average NO_2^- and NO_3^- concentrations decreased from 1.1 to 0.6 mg/L and 0.04 to 0.01 mg/L between days 1 and 7 (Figure 26).

4.1.2.3. Discussion

In batches 1–5, the average NH_3 percentage reductions were higher in the LS cell than in the LSV cell, which suggests that the LS cell performed better than the LSV cell under low inflow NH_3 concentrations. However, the average NH_3 percentage reductions in the LSV cell exceeded those in the LS cell in batches 6–13, which suggests that the LSV cell performed better than the LS cell under higher inflow NH_3 concentrations. The performance disparity between the two cells for handing variable inflow N loads can be attributed to the following reasons: (a) increments of N loading might have enhanced short-circuiting of the flow and created a deficiency of atmospheric oxygen for nitrification, or (b) a lower hydraulic gradient and smaller oxygen flux may have inhibited nitrification (Saeed and Sun, 2011). Therefore, the

reduced percentage reductions observed in the LS cell during batches 6–13 could suggest that nitrification was limited under higher inflow loadings. This could be attributed to reasons (a) and/or (b).

By comparison, the higher NH_3 percentage reductions in the LSV cell in batches 6–13 could suggest that the vegetation maintained and/or enhanced nitrification under higher inflow loadings. Previous research has shown that ET was primarily responsible for the soil moisture content in the biofilter between rainfall events and would impact the speciation of N by influencing the availability of oxygen and degree of saturation (Subramaniam et al., 2016). This suggests that ET in the LSV cell may have increased the availability of oxygen in the LSV cell, which in turn increased and/or maintained nitrification in the cell during higher inflow loadings. However, studies have also demonstrated that roots play a fundamental role in enhancing the infiltration capacity of biofilters and reducing clogging (Le Coustumer et al., 2012). This further supports the theory that vegetation increases the availability of oxygen in the cell, as higher infiltration rates are usually associated with higher levels of oxygenation. Therefore, the vegetation may have also maintained and/or enhanced the infiltration capacity of the LSV cell in batches 6–13, which in turn maintained and/or enhanced the availability of oxygen and subsequent nitrification in the cell under higher inflow loadings.

In general, the average NH_3 concentrations in the LSV cell reached a peak after 3 days before the concentrations started to decline. This suggests that a minimum HRT of 3 days would be required to reduce NH_3 in the LSV cell. Although no consistent pattern in the removal of NH_3 and HRT currently exists, there is a general recommendation that longer HRTs result in higher TN and NH_3 removal rates (Bratieres et al., 2008; Huang et al., 2000). HRT typically increases the contact time between the infiltrating runoff and attached biofilms, and hence would be expected to enhance the removal efficiency. By comparison, no distinct pattern was observed for outflow NH_3 and HRT in the LS cell. However, similar findings were made by Jay et al. (2017) who showed that no relationship between TN removal and HRT existed.

The overall TP percentage reductions remained high in the LSV cell, irrespective of the inflow P loadings. Similar findings were made by McNett et al. (2011) who determined that outflow TP concentrations were largely independent of inflow loading. However, TP percentage reductions were generally lower in the LS cell under higher inflow loadings. This suggests that the maximum P sorption capacity of the LS cell was lower under higher inflow loadings

(Skorobogatov et al., 2020). In addition, it shows that the vegetation played an important role in removing excess phosphate under higher inflow loadings.

There was no distinct pattern in the average TP concentrations in the cells over time. This contrasts with previous research which showed that TP percentage reductions generally increased with HRT (Wu et al., 2013; Lu et al., 2009; Konnerup et al., 2009). The authors explained that longer HRTs led to more contacts and interactions of P with the media and plant roots, resulting in higher levels of adsorption, transformation, and TP uptake by the media. However, this was not the case in this study as TP percentage reductions varied significantly across varying HRTs. This suggests that phosphate was highly mobile, which could be attributed to the varying levels of saturation in the media (Skorobogatov et al., 2020). Accordingly, higher levels of saturation would have caused the desorption of phosphate (and vice versa).

4.1.2.4. Percentage *E. coli* reduction

E. coli removal efficiencies in the LS and LSV cells were quantified as percentage reductions over 13 batch cycles (Table 10). These percentage reductions were analysed under varying inflow *E. coli* concentrations (Table 10).

Table 10: Percentage reduction of outflow *E. coli* concentration by both cells under different inflow *E. coli* concentrations over 13 batch cycles.

	HRT (days)	Batch 1	Batch 2	Batch 3	Batch 4	Batch 5	Batch 6	Batch 7	Batch 8	Batch 9	Batch 10	Batch 11	Batch 12	Batch 13
Inflow *E. coli* concentration (count per 100ml)	0	2419	1600	1553	1046	1553	5720	1390	2419	2419	2419	2419	14140	7220
Outflow *E. coli* concentration in LS cell (count per 100ml)	7	12	12	0	0	5	2	0	0	10	96	1330	179	1
% *E. coli* removal	7	99	99	100	100	100	100	100	100	100	96	45	99	100
Outflow *E. coli* concentration in LSV cell (count per 100ml)	7	326	4	76	378	91	89	461	4	39	41	125	86	47
% *E. coli* removal	7	87	100	95	64	94	98	67	100	98	98	95	94	99

Most batches in the LS cell had higher *E. coli* percentage reductions than the LSV cell, with 9 out of the 13 batches having achieved a percentage reduction of 100% (Table 10). In addition, the *E. coli* percentage reductions were more variable in the LSV cell, as percentage reductions ranged between 64% and 100% (Table 10). However, 10 out of the 13 batches in the LSV cell achieved a percentage reduction above 90% (Table 10). Batch 12 experienced the highest

inflow *E. coli* concentration (14,140 per 100 ml), while batch 4 experienced the lowest inflow *E. coli* concentration (1,046 per 100 ml) (Table 10). The LS cell performed slightly better than the LSV cell in both cases, as percentage reductions of 100% and 99% were achieved compared to 64% and 94% in the LSV cell (Table 10).

According to the water quality guidelines, it is likely that the vegetables are contaminated (DWAF, 1996). Most concentrations range between 1–1000 counts per 100 ml, however, some batches achieved 100% reduction, which suggests that there is a small likelihood of contamination (Table 11). These reductions are largely achieved by the LS cell, indicating that outflow from the LS cell could be reused to safely irrigate vegetables (in most cases).

Table 11: Effect of faecal coliforms (*E. coli*) on crop quality (DWAF, 1996).

Concentration range (*E. coli* count per 100ml)	Crop quality
Target water quality range · 1	**Irrigation water can be applied with any irrigation method to any crop with little likelihood that this will lead to the spread of human pathogens**
1–1000	The likelihood of contamination from vegetables and other crops are eaten raw and of milk from cows grazing on pastures will result in the transmission of human pathogens.
> 1000	Provided water treatment quality is equivalent to or better than primary and secondary treated wastewater, and that no contact is allowed to take place with humans, water can be used in irrigation for the production of fodder, tree plantations, nurseries, parks, etc.

4.1.2.5. Discussion

The results show that both cells effectively reduced the *E. coli* concentrations in the inflow (96–100% for LS, 64–100% for LSV). In general, faecal microorganisms are removed by biofilters through adsorption, straining, die-off/inactivation (due to temperature and moisture), and competition and predation (Chandrasena et al., 2014). However, the presence of aerobic conditions is usually the primary factor influencing *E. coli* removal in biofilters (Chandrasena et al., 2016). Aerobic conditions can influence faecal removal in the following ways: (i) by enhancing the growth of heterotrophic protozoa organisms that play a key role in removing *E. coli* via predation (Wand et al., 2007), and (ii) by *E. coli* oxidation, which enhances the mortality of faecal coliforms (Decamp and Warren, 2001). Consequently, the LS cell may

have had higher levels of *E. coli* oxidation and/or higher growths of heterotrophic protozoa organisms than the LSV cell.

The *E. coli* removal efficiencies seemed to be unaffected by the varying inflow *E. coli* concentrations, as both cells demonstrated similar removal efficiencies under high and low inflow *E. coli* concentrations. This contrasts with previous research which showed that *E. coli* removal is negatively correlated with inflow loadings (Liu et al., 2020; Søberg et al., 2019). According to the authors, higher inflow loadings reduced the adsorption capacity of the media, resulting in higher outflow *E. coli* concentrations. However, this did not seem to be the case in this study, suggesting that the media's adsorption capacity was not exceeded.

4.2. Water quantity performance

4.2.1. Comparison of inflow and outflow water quantity

4.2.1.1. Box-and-whisker diagram and five-number summaries

Box-and-whisker diagrams and five-number summaries were used to compare the inflow and outflow water quantity of both cells over 13 batch cycles. Water quantity was quantified using volumetric calculations of the inflow and outflow. A total of 65 samples (n = 65) were collected.
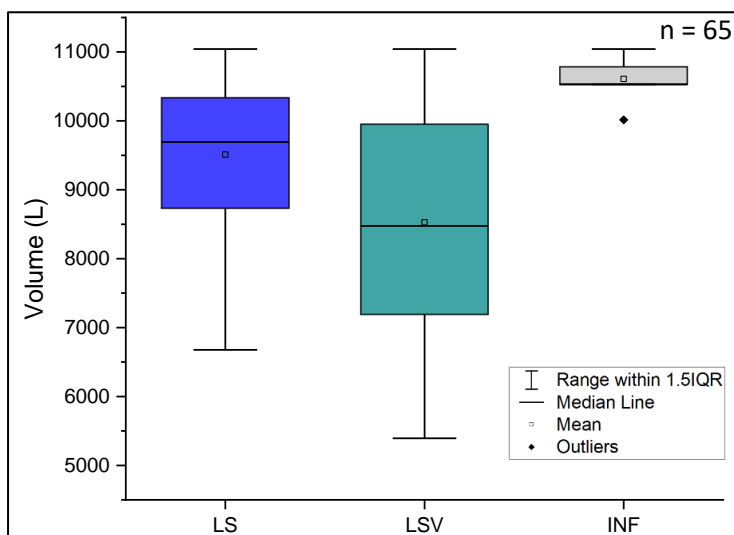
Figure 27: Box-and-whisker diagrams for the water quantity of the inflow (INF) and outflow (LS and LSV) of the cells (n = 65).

The median values for the LS (Q2= 9694) and LSV (Q2= 8474) boxplots are lower than the median value for the INF boxplot (Q2 = 1052), showing that there was a difference in inflow and outflow water volumes (Figure 27). In addition, the INF boxplot (Max= 1104, Min= 1052) is much higher than the LS (Max= 11042.4, Min= 6677) and LSV (Max= 9951, Min= 7190) boxplots, indicating that the overall inflow volumes were greater than the inflow volumes (Figure 27). However, the INF boxplot (IQR= 26) is short in comparison to the LS (IQR= 1605) and LSV (IQR= 2761) boxplots (Figure 27). This suggests that there was less variability in the inflow volumes than in the outflow water volumes. The LSV boxplot is taller than the LS boxplot, suggesting that there was more variability in the LS volume than in the LSV volume (Figure 27). The LS and INF boxplots have an asymmetrical distribution, with the LS boxplot being negatively skewed and the INF boxplot being positively skewed (Figure 27). This indicates that most outflow volumes are lower than the group median in the LSV boxplot, while most of the outflow volumes are higher than the group median in the INF boxplot. The LSV boxplot has a more symmetrical distribution, suggesting that outflow volumes from the LSV cell are more evenly spread around the group (Figure 27). The INF boxplot has one outlier, while the LS and LSV boxplots have no outliers (Figure 27).

4.2.1.2. Moving average values over time

Two-day moving average values were calculated for the inflow and outflow water volume of the cells over 13 batch cycles. Graphs were then used to illustrate these moving averages over time (Figure 28).
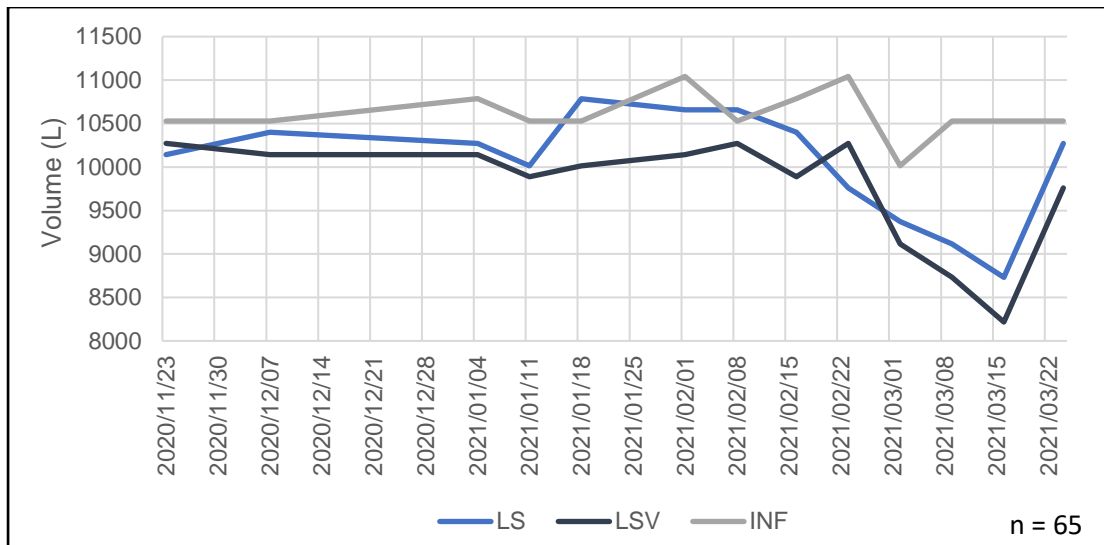
Figure 28: Moving average values for the water quantity of the inflow (INF) and outflow (LS and LSV) of the cells over time.

Inflow volume ranged between 10,015–11,042 litres and remained relatively stable over the study period (Figure 28). A slight drop in inflow volume was observed at the beginning of March, but it stabilised at 10,529 litres thereafter (Figure 28). The inflow volume was consistently higher than the outflow volumes over the study period (Figure 28). However, the outflow volume from the LS cell exceeded the inflow volume at one point, peaking at 10,786 litres following a major rainfall event (6 mm) in mid-January (Figure 28). The LSV volume also increased during this period, but not to the same degree as in the LS cell (Figure 28). The LS volume was consistently higher than the LSV volume over the study period, except for one spike which coincided with the sharp increase in inflow volume (Figure 28). Both LS and LSV cells dropped to minimum volumes of 8,731 and 8,218 L following a drop in inflow volume at the beginning of March (Figure 28). The outflow volumes subsequently increased to 10,272 and 9,758 L in both cells (Figure 28).

4.2.2. Water balance analysis

The water balance of both cells was analysed over 13 batch cycles (Figures 29 & 30). The LS water balance comprised of the percentage of water retained by the cell and the percentage of water lost via evaporation, while the LSV water balance comprised of the percentage of water retained by the cell and the percentage of water lost via evaporation and ET.
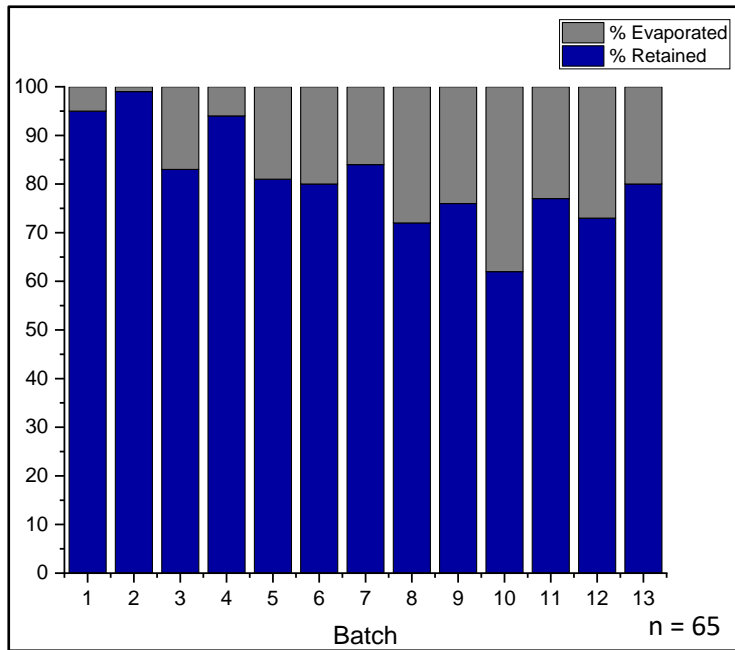
Figure 29: Percentage of the total inflow water volume retained and lost (via evaporation) in the LS cell.
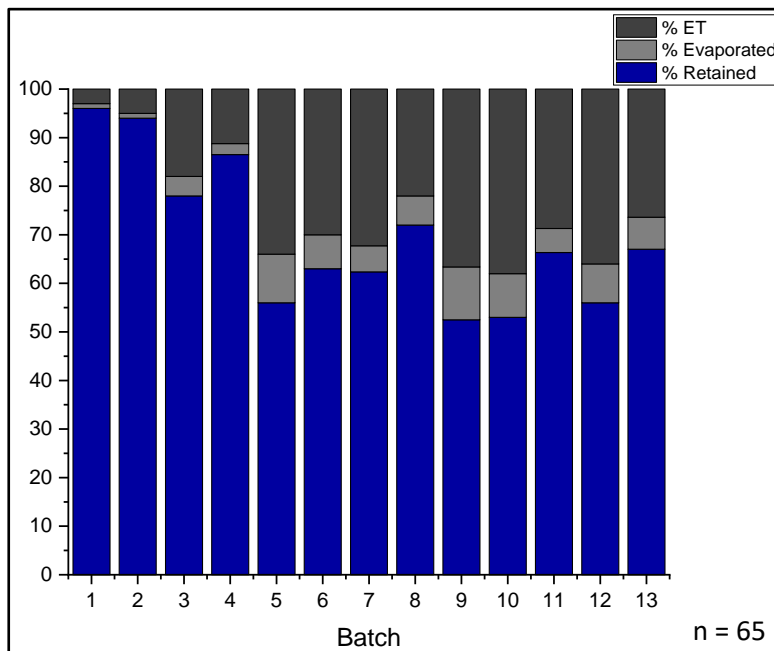
Figure 30: Percentage of the total inflow water volume retained and lost (via evaporation and ET) in the LSV cell.

On average, the LS cell ($\hat{x}$ = 81%) retained a larger percentage of the inflow water volume than the LSV cell ($\hat{x}$ = 68) (Figures 29 & 30). The average water loss via evaporation in the LS cell was 19%, while the LSV cell lost an average of 6% via evaporation and 24% via ET (Figures 29 & 30). The highest percentage of volume retained by the LS cell was in batch

2 (99%), while the lowest percentage of volume retained was in batch 10 (62%) (Figure 29). The highest percentage of volume retained by the LSV cell was in batch 1 (96%) (Figure 30). However, the lowest percentage of volume retained by the LSV cell was during batches 9 and 10 (53%) (Figure 30). ET accounted for approximately 37% of the overall volume reduction in the cell during these batches, while evaporation accounted for only 10% (Figure 30). A similar pattern was observed in the other batches, whereby ET contributed to a significantly higher proportion of the overall volume reduction than evaporation.

4.2.3. Discussion

The overall outflow water quantity was less than the overall inflow water quantity, which suggests that both cells effectively reduced the inflow water quantity. However, there are two points at which the water quantity in the LS cell exceeded the inflow water quantity. These points coincided with high rainfall events, which can be contributed to the increase in outflow water quantity (Passeport et al., 2009). Similar results were reported by Maniquiz et al. (2012) who showed that the outflow water volume was positively corrected with rainfall. By comparison, the LSV cell seemed to be largely unaffected by these rainfall events, as the outflow water quantity remained consistently lower than the inflow water quantity over the same period. This could suggest that excess water was removed by the vegetation.

The overall volumetric loss was greater in the LSV cell than in the LS cell, which suggests that ET played a significant role in reducing the volume of the inflow. In general, the average ET percentage reductions ($\hat{x}$= 24%) are higher than the values reported by other studies. Sharkey (2006) and Li and Davis (2009) reported percentage reductions up to 19%, while other studies reported values lower than 5% (Brown and Hunt, 2011; Szota et al., 2018). However, ET estimates from these studies were not cumulative (unlike in this study) and were therefore expected to be lower. Furthermore, a reference ET model was used to calculate ET in this study (Allen et al., 1998). These models are known to yield higher ET estimates as they rely on regional (as opposed to local) meteorological data. Therefore, the results from this study were more comparable to those of Nocco et al. (2016) who used a similar approach to estimate ET. The authors reported percentage reductions up to 82% for prairie vegetation

and up to 52% for both turf grass and shrub mesocosms, which are comparatively high to the percentage reductions observed in this study (Nocco et al., 2016).

ET and evaporation varied significantly across in both cells across the batches, which was expected since ET and evaporation are highly subjected to weather conditions. Warmer temperatures, higher wind speeds, and decreased levels of humidity are expected to increase ET, while cooler temperatures, lower wind speeds, and increased levels of humidity are expected to decrease ET (Allen et al., 1998). This was demonstrated by Hickman et al. (2011) who found that climatic parameters strongly correlate to actual ET and evaporation from biofilters. Therefore, the higher ET and evaporation rates observed during this study could be associated with higher temperatures and wind speeds and lower levels of relative humidity, while the lower ET and evaporation rates could be associated with lower temperatures and wind speeds and higher levels of relative humidity (Allen et al., 1998) (see Table 1A in Appendix A for relevant weather data).

Although the inflow water quantity was kept relatively constant throughout the study, a slight variation in the inflow water quantity was observed between the batches. This is because the volume of inflow water depended on the availability of solar power to pump water from the Stiebeuel River, and hence, less water was available when there was insufficient solar power to pump water into the cells. Therefore, batches with lower inflow water volumes indicate which weeks had insufficient solar power to fill the cells up completely. However, the variation in the inflow water quantity between the batches was largely negligible and therefore would not have had a significant impact on the results.

4.3. Relationships between outflow nutrient concentration and environmental parameters

4.3.1. Regression analysis for outflow NH$_3$

4.3.1.1. Correlations

A Pearson's r correlation analysis was used to determine the statistical relationships between outflow NH$_3$ concentration and several parameters, including HRT, air temperature, rainfall, evaporation, ET, inflow water pH, inflow water temperature and inflow NH$_3$ concentration (Table 12).

Table 12: Pearson correlations between output NH$_3$ concentration and selected parameters in LS and LSV cells.

		HRT	Air Temp	Rainfall	Evaporation	ET	Inflow pH	Inflow Temp	Inflow NH$_3$ Conc.
Outflow NH$_3$ Conc. (LS)	Pearson Correlation	0.004	-0.19	0.21	0.45	-	0.53	-0.04	0.64
	Sig. (2-tailed)	0.98	0.18	0.13	<0.001	-	<0.001	0.8	<0.001
Outflow NH$_3$ Conc. (LSV)	Pearson Correlation	-0.14	-0.29	0.1	-	0.24	0.43	-0.33	0.67
	Sig. (2-tailed)	0.34	<0.05	0.48	-	<0.1	<0.001	<0.05	<0.001

*Indicates significant parameters ($p < 0.05$)

The Pearson's r correlation analysis showed that there was a moderate positive correlation between evaporation and outflow NH$_3$ concentration (r= 0.45, p-value< 0.001) and between inflow water pH and outflow NH$_3$ concentration (r= 0.53, p-value< 0.001) in the LS cell (Table 12). A strong positive correlation was determined between inflow NH$_3$ concentration and outflow NH$_3$ concentration (r = 0.64, p-value<0.001) (Table 12). However, no significant correlations were found between outflow NH$_3$ concentration and HRT, air temperature, rainfall and inflow water temperature (Table 12).

There was a weak negative correlation between air temperature and outflow NH$_3$ concentration (r= -0.29, p-value< 0.05) and between inflow water temperature and outflow NH$_3$ concentration (r= 0.33, p-value< 0.05) in the LSV cell (Table 12). A weak positive correlation was determined between ET and outflow NH$_3$ concentration (r= 0.24, p-value< 0.1) and a moderate positive correlation was determined between inflow water pH and outflow NH$_3$ concentration (r= 0.43, p-value< 0.001) and between inflow NH$_3$ concentration and outflow NH$_3$ concentration (r= 0.67, p-value< 0.001) (Table 12). However, no significant correlations were found between outflow NH$_3$ concentration and HRT and rainfall (Table 12).

4.3.1.2. Predictor variables

The variables listed in Table 13 were selected to predict the outflow NH$_3$ concentration in both cells. HRT was included as a categorical variable with levels 1, 3, 5 and 7 days, while air temperature, rainfall, evaporation, ET, inflow water pH, inflow water temperature and inflow

NH$_3$ concentrations were included as continuous variables. Evaporation was selected as a predictor variable for outflow NH$_3$ concentration in the LS cell, whereas ET was selected as a predictor variable for outflow NH$_3$ concentration in the LSV cell. This is because evaporation was the primary flow reduction pathway in the LS cell, whereas ET was the primary flow reduction pathway in the LSV cell.

Table 13: Predictor variables for outflow NH$_3$ in LS and LSV cells.

Predictor Variable	Type
HRT (day)	Categorical (levels = HRT 1, HRT 3, HRT 5, HRT 7)
Air Temperature (°C)	Continuous
Rainfall (mm)	Continuous
Evaporation (mm)/ ET (mm)	Continuous
Inflow Water pH	Continuous
Inflow Water Temperature (°C)	Continuous
Inflow NH$_3$ Concentration (mg/L)	Continuous

Outcome variable: outflow NH$_3$ concentration

4.3.1.3. Model summaries and goodness-of-fit

Multiple linear regression models were used to predict the outflow NH$_3$ concentration in the LS and LSV cells based on seven predictor variables, namely HRT, air temperature, rainfall, evaporation/ET, inflow water pH, inflow water temperature and inflow NH$_3$ concentration. Before developing the models, the outflow NH$_3$ concentrations were plotted against the predictor variables to detect any non-linear relationships. Several non-linear relationships were detected, and thus polynomial terms of the predictor variables were added to give curvature to the models. This resulted in two polynomial regression models: NH$_3$LS (which predicted outflow NH$_3$ concentration in the LS cell) and NH$_3$LSV (which predicted outflow NH$_3$ concentration in the LSV cell).

A goodness-of-fit test was used to determine the discrepancy between the observed values and those that would be expected of the model in a normal distribution case. This included a summary of the model outcomes (R, R^2 and adjusted R^2 values and Residual Sum of Error or RSE) (Table 14), an Analysis of Variance (ANOVA) test (Table 15), and graphs to illustrate the fitted relationship (i.e., the fitted vs observed values) (Figures 31 & 32). The appropriateness of the fitted models was confirmed by testing the assumptions of linearity, constant error variance, independence and normality (see Figures B1 & 2 in Appendix B).

Table 14: Summary of the NH$_3$LS and NH$_3$LSV model outcomes.

Model	R	R^2	Adj R	RSE
NH$_3$LS	0.94	0.89	0.84	1.92
NH$_3$LSV	0.88	0.78	0.68	1.01

Table 15: ANOVA results for the NH$_3$LS and NH$_3$LSV models.

Model		SS	df	MS	F	p
NH$_3$LS	Regression	1078.7	15	71.9	18.9	<0.001
	Residual	133.3	36	3.7		
	Total	1212	41			
NH$_3$LSV	Regression	113.8	15	7.6	8.32	<0.001
	Residual	36.4	36	1.01		
	Total	150.2	41			
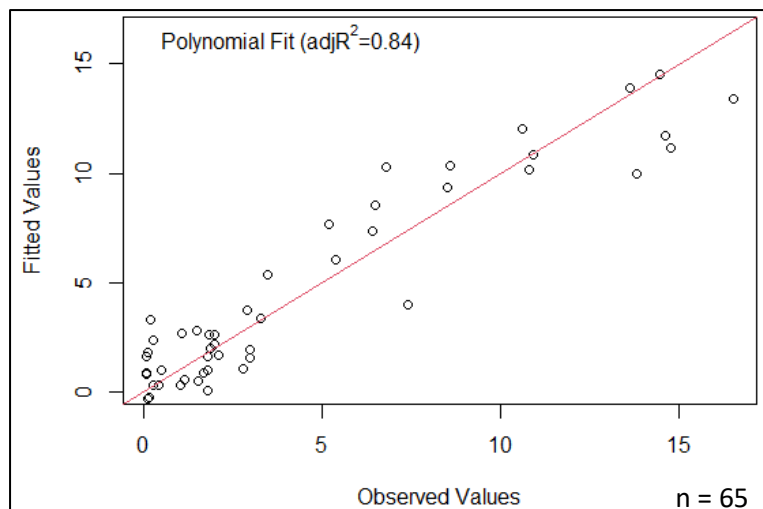
Figure 31: Fitted relationship (fitted vs observed values) of the NH$_3$LS model with adjusted R^2 value (n = 65).
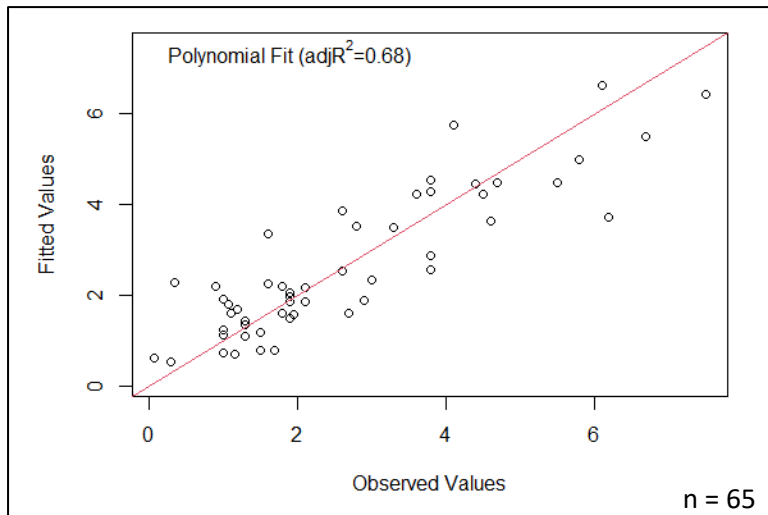
Figure 32: Fitted relationship (fitted vs observed values) of the NH$_3$LSV model with adjusted R^2 value (n = 65).

The results indicate that 84% of the variance in outflow NH$_3$ concentration can be accounted for by the NH$_3$LS model, F $(2,36)$ = 18.9, p< 0.001 (Tables 10 & 11, Figure 31), whereas 68% of the variance in outflow NH$_3$-N concentration can be accounted for by the NH$_3$LSV model, F $(1,36)$ = 18.9, p< 0.001 (Tables 10 & 11, Figure 32). Therefore, both models are relatively good predictors of outflow NH$_3$ concentration.

4.3.1.4. Model equations and coefficients

The model coefficients along with the summary statistics were calculated for each model (Table 16). These coefficients were incorporated into an equation that predicted outflow NH$_3$ concentrations in both cells (Equations 1 & 2).

Table 16: Coefficients for NH_3LS and NH_3LSV models.

Model		β	SE	t	p
NH_3LS	(Intercept)	2366.431	416.149	5.686	<0.001
	HRT3	-0.003	0.839	-0.004	0.997
	HRT5	-0.018	0.854	-0.021	0.983
	HRT7	-0.688	0.801	-0.858	0.396
	AIRTEMP	2.572	1.496	1.719	0.094
	$I(AIRTEMP^2)$	-0.063	0.036	-1.765	0.086
	EP_LS	0.001	0.002	0.429	0.671
	$I(EP\_LS^2)$	0.0000009	0.002	0.520	0.607
	RAIN	-0.054	0.199	-0.270	0.789
	$I(RAIN^2)$	0.004	0.006	0.677	0.503
	PH_IN	-1208.427	160.098	-7.548	<0.001
	$I(PH\_IN^2)$	85.235	11.231	7.589	<0.001
	TEMP_IN	151.345	16.579	9.129	<0.001
	$I(TEMP\_IN^2)$	-3.026	0.333	-9.090	<0.001
	NH_3_IN	-0.301	0.259	-1.161	0.253
	$I(NH_3\_IN^2)$	0.026	0.008	3.368	<0.001
NH_3LSV	(Intercept)	710.929	227.179	3.129	<0.05
	HRT3	0.915	0.440	2.079	<0.05
	HRT5	0.080	0.492	0.163	0.871
	HRT7	-0.351	0.449	-0.781	0.440
	AIRTEMP	1.291	0.782	1.652	0.107
	$I(AIRTEMP^2)$	-0.033	0.019	-1.755	0.084
	ET_LSV	-0.003	0.002	-1.748	0.089
	$I(ET\_LSV^2)$	0.000002	0.000001	1.721	0.094
	RAIN	-0.005	0.103	-0.047	0.963
	$I(RAIN^2)$	-0.001	0.003	-0.279	0.782
	PH_IN	-323.206	88.058	-3.670	<0.001
	$I(PH\_IN^2)$	22.888	6.177	3.705	<0.001
	TEMP_IN	33.596	8.983	3.740	<0.001
	$I(TEMP\_IN^2)$	-0.672	0.180	-3.732	<0.001
	NH_3_IN	-0.098	0.144	-0.682	0.500
	$I(NH_3\_IN^2)$	0.008	0.004	2.109	<0.05

*Indicates significant parameters ($p < 0.05$)

The following equation was used to predict outflow NH_3 concentration in the LS cell:

$NH_3\_OUT = 2366.431 - (0.003*HRT3) - (0.018*HRT5) - (0.688*HRT7) + (2.572*AIRTEMP) - (0.06*AIRTEMP^2) + (0.001*EP\_LS) + (0.0000009*EP\_LS^2) - (0.054*RAIN) + (0.004*RAIN^2) - (1208.427*PH\_IN) + (85.235*PH\_IN^2) + (151.345*TEMP\_IN) - (3.026*TEMP\_IN^2) - (0.301*NH_3\_IN) - (0.026*NH_3\_IN^2)$

Equation 1

where NH_3_OUT is outflow NH_3 concentration (in mg/L) in the LS cell; HRT is

hydraulic retention time (with four levels: 1, 3, 5, and 7 days); AIRTEMP is the air

temperature (in °C), AIRTEMP^2 is the polynomial term of AIRTEMP, RAIN is rainfall (in mm), RAIN^2 is the polynomial term of RAIN; EP_LS is evaporation in LS cell (in mm); EP_LS^2 is the polynomial term of EP_LS; PH_IN is the inflow water pH; PH_IN^2 is the polynomial term of PH_IN; TEMP_IN is the inflow water temperature (in °C); TEMP_IN^2 is the polynomial term of TEMP_IN; NH$_3$_IN is the inflow NH$_3$ concentration (in mg/L); NH$_3$_IN^2 is the polynomial term of NH$_3$_IN.

The following equation was used to predict outflow NH$_3$ concentration in the LSV cell:

NH$_3$_OUT = 710.929 − (0.915*HRT3) − (0.080*HRT5) − (0.351*HRT7) + | Equation 2 |
(1.291*AIRTEMP) − (0.033*AIRTEMP^2) − (0.003*ET_LS) + (0.000002*ET_LSV^2) − (0.005*RAIN) − (0.001*RAIN^2) − (323.206*PH_IN) + (22.888*PH_IN^2) − (33.596*TEMP_IN) − (0.098*TEMP_IN^2) − (0.098*NH$_3$_IN) + (0.008*NH$_3$_IN^2)

where NH$_3$_OUT is outflow NH$_3$ concentration (in mg/L) in the LSV cell; HRT is hydraulic retention time (with four levels: 1, 3, 5, and 7 days); AIRTEMP is the air temperature (in °C), AIRTEMP^2 is the polynomial term of AIRTEMP, RAIN is rainfall (in mm), RAIN^2 is the polynomial term of RAIN; EP_LS is evaporation in LS cell (in mm); EP_LS^2 is the polynomial term of EP_LS; PH_IN is the inflow water pH; PH_IN^2 is the polynomial term of PH_IN; TEMP_IN is the inflow water temperature (in °C); TEMP_IN^2 is the polynomial term of TEMP_IN; NH$_3$_IN is the inflow NH$_3$ concentration (in mg/L); NH$_3$_IN^2 is the polynomial term of NH$_3$_IN.

Table 16 shows that inflow water pH, temperature and NH$_3$ concentration significantly contributed to both NH$_3$LS and NH$_3$LSV models ($p < 0.05$), while HRT, air temperature, evaporation, ET and rainfall did not ($p > 0.05$). Therefore, the influence of inflow water pH, temperature and NH$_3$ concentration (i.e., the significant predictors) on outflow NH$_3$ concentrations were determined by plotting the partial relationships (i.e., holding the effects of the other variables constant) (Figure 33).
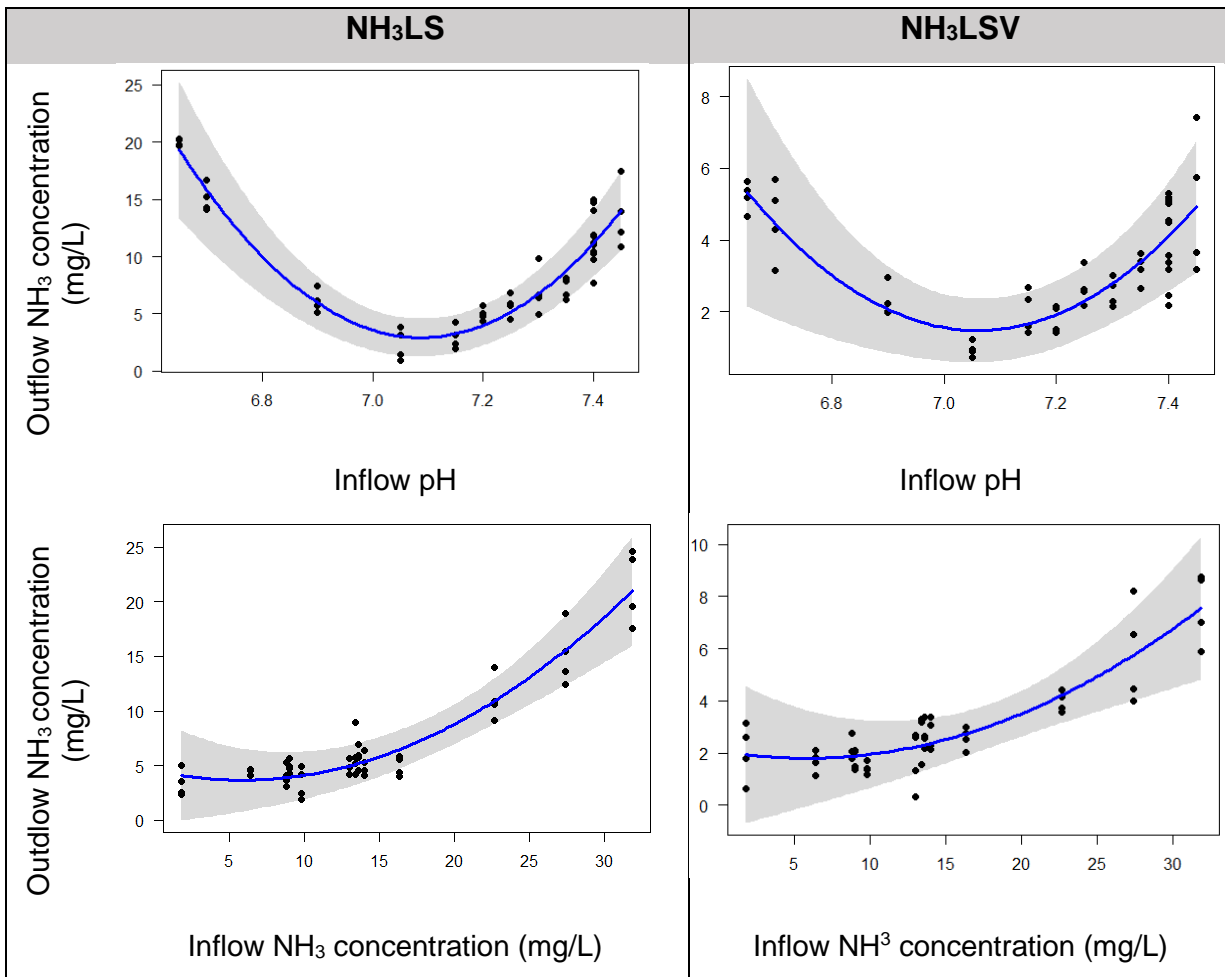
Figure 33: Visual representation of the partial relationships between outflow NH$_3$ concentration and significant predictors (p-value< 0.05) in both cells.

The slope for inflow NH$_3$ concentration becomes more positive as outflow NH$_3$ concentration increases in the NH$_3$LS model (Figure 33). However, the relationships between outflow NH$_3$ concentration and inflow water pH and temperature are not as straightforward. Initially, the slope for inflow pH becomes more negative as the outflow NH$_3$ concentration increases (Figure 33). The slope then reaches a minimum at a pH of 7.1 before it becomes increasingly positive (Figure 33

For inflow NH$_3$ concentration in the NH$_3$LSV model, the slope becomes more positive as outflow NH$_3$ concentration increases (Figure 33). However, the relationships between outflow NH$_3$ concentration and inflow water pH are also not as straightforward. Initially, the slope for inflow pH becomes more negative as the outflow NH$_3$ concentration increases (Figure 33). The slope then reaches a minimum at a pH of 7.1 before it becomes increasingly positive (Figure 33).

4.3.1.5. Discussion

The results show that evaporation, ET and rainfall did not influence outflow NH_3 concentrations significantly. Similar findings were made by Maniquiz et al. (2012) who found no significant correlation between the flow and pollutant mass balances of a biofiltration system. By comparison, other studies have shown that rainfall is not a significant source of N species, as rainfall depth and duration resulted in more dilution (Passeport and Hunt, 2009). However, higher rainfall amounts are also associated with higher nutrient loads, partly due to the build-up of pollutants and wash-off effects but could also be because rainfall is usually the main source of nutrients in urban areas (Pollman et al., 2002). Nevertheless, few rainfall events were captured during this study, which probably explains the lack of significance between rainfall and outflow NH_3.

Air temperature also had little effect on outflow NH_3. By comparison, other studies have shown that lower temperatures are associated with lower N removal rates (Passeport and Hunt, 2009). This is largely due to a reduction in the microbial activity and N removal processes, namely nitrification (Passeport et al., 2009). However, this study did not examine the effects of seasonal variation on outflow NH_3 and therefore captured a limited range of temperatures. This may explain the lack of significance between air temperature and outflow NH_3.

Despite initial predictions, HRT did not significantly influence outflow NH_3 concentrations. Similar findings were made by Lopez-Ponnada et al. (2020) who found that HRT had no significant effect on NO_x removal in field-scale biofiltration units with sand media. Jay et al. (2019) also showed that HRT did not have a significant relationship with TN removal in biofiltration column studies. The authors suggested that longer HRTs may have yielded more significant results. This could explain the lack of significance observed between HRT and NH_3 in this study, as previous research on the cells showed that HRT impacted the performance of the cells (Ghanashyam, 2018). Accordingly, HRTs of 7 and 14 days were associated with significant reductions of NH_3.

Inflow pH, temperature and NH_3 concentrations were found to significantly influence outflow NH_3 concentrations in both cells. An exponential increase in outflow NH_3 concentration was observed under exponentially increasing inflow NH_3 concentrations. By contrast, other studies have shown that increased N loading is associated with greater removal rates, within

tolerable limits (Lee and Scholz, 2007; Tunçsiper, 2009; Dan et al., 2011). However, Saeed and Sun (2011) noted that excessive inflow NH_3 concentrations could hamper the growth of certain wetland plants and biomass and result in reduced removal efficiencies. This could explain the positive relation between outflow and inflow NH_3 in the study.

There appears to be an 'optimal' relationship between outflow NH_3 concentration and inflow pH, whereby the outflow NH_3 reaches a minimum or maximum concentration depending on certain pH ranges. The results show that relations between pH and outflow NH_3 are generally negative under low values and positive under high values, whereas relations between temperature and outflow NH_3 are generally positive under low values and negative under high values (Figure 33). These results align with previous research which has shown that pH and temperature are major factors controlling denitrification (and thus, the removal) of N in biofilters (Garcia et al., 2010). According to the authors, denitrification is optimal between pH 6 and 8 but begins to slow down below pH 5, becoming almost negligible below pH 4 (Garcia et al., 2010).

4.3.2. Regression analysis for outflow Total Phosphate (TP)

4.3.2.1. Correlations

A Pearson's r correlation analysis was used to determine the statistical relationships between outflow TP concentration and several parameters, including HRT, air temperature, rainfall, evaporation, ET, inflow water pH, inflow water temperature and inflow TP concentration (Table 17).

Table 17: Pearson correlations between outflow TP concentration and selected parameters in both cells.

		HRT	Air Temp	Rainfall	Evaporation	ET	Inflow pH	Inflow Temp	Inflow TP Conc.
Outflow TP Conc. (LS)	Pearson Correlation	-0.32	0.2	-0.11	0.45	-	0.82	0.14	0.69
	Sig. (2-tailed)	0.82	0.17	0.45	<0.001	-	<0.001	0.31	<0.001
Outflow TP conc. (LSV)	Pearson Correlation	0.01	0.25	-0.05	-	0.56	0.86	0.29	0.66
	Sig. (2-tailed)	0.94	<0.1	0.73	-	<0.001	<0.001	<0.05	<0.001

*Indicates significant parameters ($p < 0.05$)

A Pearson's r correlation analysis showed that there is a moderate positive correlation between evaporation and outflow TP concentration (r= 0.45, p-value< 0.001) and a strong positive correlation between inflow pH and outflow TP concentration (r= 0.82, p-value< 0.001) and between inflow TP concentration and outflow TP concentration (r= 0.69, p-value< 0.001) in the LS cell (Table 13). However, no significant correlations were found between outflow TP concentration and HRT, air temperature, rainfall and inflow temperature (Table 13).

The Pearson's r correlation analysis showed that there is a weak negative correlation between air temperature and outflow TP concentration (r= 0.25, p-value< 0.1) and a weak positive correlation between inflow temperature and TP concentration (r= 0.29, p-value< 0.05) (Table 13). A moderate positive correlation between ET and outflow TP concentration (r= 0.56, p-value< 0.001) and a strong positive correlation between inflow pH and outflow TP concentration (r= 0.86, p-value< 0.001) and between inflow TP concentration and outflow TP concentration (r= 0.66, p-value< 0.001) was determined (Table 13). However, no significant correlations between outflow TP concentration and HRT and rainfall were found (Table 13).

4.3.2.2. Predictor variables

The variables listed in Table 18 were selected to predict the outflow TP concentration in both cells. HRT was included as a categorical variable with levels 1, 3, 5 and 7 days, while air

temperature, rainfall, evaporation, ET, inflow water pH, inflow water temperature and inflow TP concentrations were included as continuous variables. Evaporation was selected as a predictor variable for outflow TP concentration in the LS cell, whereas ET was selected as a predictor variable for outflow TP concentration in the LSV cell. This is because evaporation was the primary flow reduction pathway in the LS cell, whereas ET was the primary flow reduction pathway in the LSV cell.

Table 18: Variables used to describe output TP concentration in LS and LSV cells.

Predictor Variable	Type
HRT (day)	Categorical (levels = HRT 1, HRT 3, HRT 5, HRT 7)
Air Temperature (°C)	Continuous
Rainfall (mm)	Continuous
Evaporation (mm)/ ET (mm)	Continuous
Inflow Water pH	Continuous
Inflow Water Temperature (°C)	Continuous
Inflow TP Concentration (mg/L)	Continuous

Outcome variable: outflow TP concentration

4.3.2.3. Model summaries and goodness-of-fit

Multiple linear regression models were used to predict the outflow TP concentration in the LS and LSV cells based on seven predictor variables, namely HRT, air temperature, rainfall, evaporation/ET, inflow water pH, inflow water temperature and inflow TP concentration. Before developing the models, the outflow TP concentrations in the LS and LSV cells were plotted against the predictor variables to detect any non-linear relationships. Several non-linear relationships were detected, and thus polynomial terms of the predictor variables were added to give curvature to the models. This resulted in two polynomial regression models: TPLS (which predicted outflow TP concentration in the LS cell) and TPLSV (which predicted outflow TP concentration in the LSV cell).

A goodness-of-fit test was then used to determine the discrepancy between the observed values and those that would be expected of the model in a normal distribution case. This included a summary of the model outcomes (R, R^2 and adjusted R^2 values and Residual Sum of Error or RSE) (Table 19), an Analysis of Variance (ANOVA) test (Table 20), and graphs to illustrate the fitted relationship (i.e., the fitted vs observed values) (Figures 34 & 35). The

appropriateness of the fitted models was confirmed by testing the assumptions of linearity, constant error variance, independence and normality (see Figures B3 & 4 in Appendix B).

Table 19: Summary of TPLS and TPLSV models.

Model	R	R²	Adj R	RMSE
TPLS	0.87	0.78	0.68	0.10
TPLSV	0.90	0.82	0.74	0.05

Table 20: ANOVA results for TPLS and TPLSV models.

Model		SS	df	MS	F	p
TPLS	Regression	1.73	15	0.12	8.27	<0.001
	Residual	0.39	36	0.01		
	Total	2.12	41			
TPLSV	Regression	0.55	15	0.04	10.84	<0.001
	Residual	0.10	36	0.003		
	Total	0.65	41			
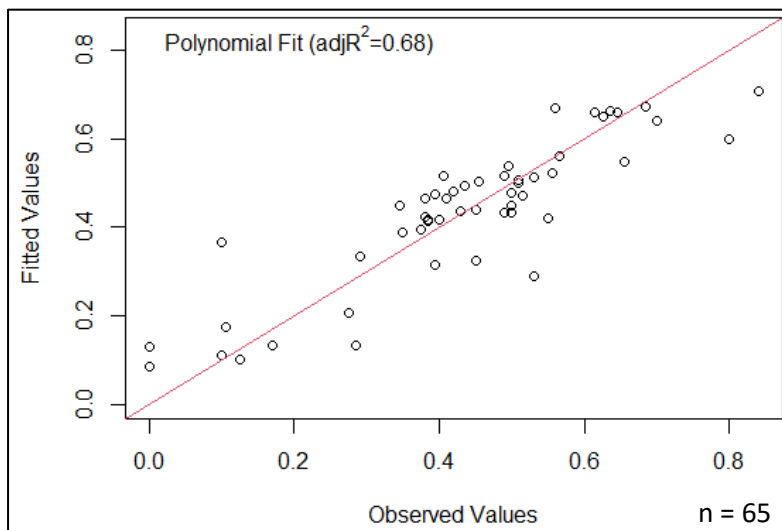
Figure 34: Fitted relationship (fitted vs observed values) of the TPLS model with adjusted R^2 value (n = 65).
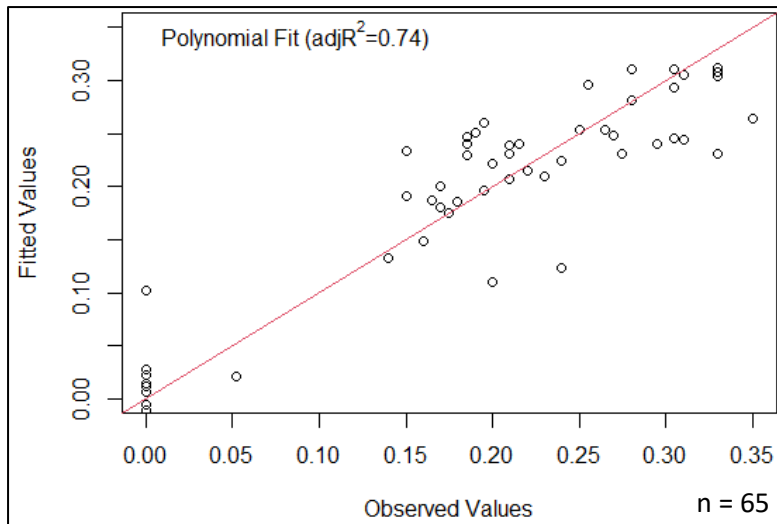
Figure 35: Fitted relationship (fitted vs observed values) of the TPLSV model with adjusted R^2 value (n = 65).

The results indicate that 68% of the variance in outflow TP concentration can be accounted for by the TPLS model, $F_{(0.1,36)} = 8.3$, p-value< 0.001 (Tables 15 & 16, Figure 34), whereas 68% of the variance in outflow TP concentration can be accounted for by the TPLSV model, $F_{(0.1,36)} = 10.8$, p-value< 0.001 (Tables 15 & 16, Figure 35). Thus, both models are relatively good predictors of outflow TP concentrations.

4.3.2.4. Model equations and coefficients

The model coefficients along with the summary statistics were calculated for each model (Table 21). These coefficients were incorporated into an equation that predicted outflow TP concentrations in the LS and LSV cells (Equations 3 & 4).

Table 21: Coefficients for TPLS and TPLSV models.

Model		β	SE	t	p
TPLS	(Intercept)	-41.764	29.864	-1.398	0.171
	HRT3	-0.021	0.046	-0.463	0.646
	HRT5	-0.051	0.046	-1.113	0.273
	HRT7	-0.027	0.043	-0.634	0.530
	AIRTEMP	0.109	0.077	1.420	0.164
	$I(AIRTEMP^2)$	-0.003	0.002	-1.404	0.169
	EP_LS	0.00003	0.0001	0.217	0.830
	$I(EP\_LS^2)$	0.00003	0.0000001	0.208	0.837
	RAIN	0.009	0.011	0.826	0.414
	$I(RAIN^2)$	0.00003	0.0003	-0.938	0.354
	PH_IN	11.585	10.514	1.102	0.278
	$I(PH\_IN^2)$	-0.775	0.736	-1.053	0.299
	TEMP_IN	-0.125	0.885	-0.142	0.888
	$I(TEMP\_IN^2)$	0.002	0.018	0.102	0.920
	TP_IN	-0.187	0.312	-0.599	0.553
	$I(TP\_IN^2)$	0.055	0.089	0.623	0.537
TPLSV	(Intercept)	-22.464	14.130	-1.590	0.121
	HRT3	0.006	0.023	0.262	0.795
	HRT5	0.004	0.026	0.176	0.862
	HRT7	-0.010	0.023	-0.427	0.672
	AIRTEMP	0.014	0.040	0.344	0.733
	$I(AIRTEMP^2)$	-0.0004	0.001	-0.448	0.657
	ET_LSV	0.0007	0.00009	0.803	0.427
	$I(ET\_LSV^2)$	0.0000003	0.0002	-0.525	0.603
	RAIN	-0.006	0.005	-1.032	0.309
	$I(RAIN^2)$	0.0002	0.0002	1.180	0.246
	PH_IN	8.896	5.038	1.766	0.086
	$I(PH\_IN^2)$	-0.611	0.353	-1.732	0.092
	TEMP_IN	-0.796	0.448	-1.778	0.084
	$I(TEMP\_IN^2)$	0.016	0.009	1.775	0.084
	TP_IN	0.087	0.138	0.626	0.535
	$I(TP\_IN^2)$	-0.022	0.041	-0.536	0.595

The following equation was used to predict outflow TP in the LS cell:

$$TP\_OUT = -41.764 - (0.021 * HRT3) - (0.051 * HRT5) - (0.027 * HRT7) + (0.109 * AIRTEMP) - (0.003 * AIRTEMP^2) + (0.00003 * EP\_LS) + (0.00003 * EP\_LS^2) + (0.009 * RAIN) + (0.00003 * RAIN^2) - (11.585 * PH\_IN) - (0.755 * PH\_IN^2) - (0.125 * TEMP\_IN) + (0.002 * TEMP\_IN^2) - (0.186 * TP\_IN) - (0.055 * TP\_IN^2)$$

Equation 3

where TP_OUT is outflow TP-N concentration (in mg/L) in the LS cell; HRT is hydraulic retention time (with four levels: 1, 3, 5, and 7 days); AIRTEMP is the air temperature (in °C),

AIRTEMP^2 is the polynomial term of AIRTEMP, RAIN is rainfall (in mm), RAIN^2 is the polynomial term of RAIN; EP_LS is evaporation in LS cell (in mm); EP_LS^2 is the polynomial term of EP_LS; PH_IN is the inflow water pH; PH_IN^2 is the polynomial term of PH_IN; TEMP_IN is the inflow water temperature (in °C); TEMP_IN^2 is the polynomial term of TEMP_IN; TP_IN is the inflow TP concentration; TP_IN^2 is the polynomial term of TP_IN.

The following equation was calculated to predict outflow TP concentration in the LSV cell:

$$TP\_OUT = -22.464 + (0.006*HRT3) - (0.004*HRT5) - (0.010*HRT7) +$$ | Equation 4

$$(0.014*AIRTEMP) - (0.0003*AIRTEMP^2) + (0.00007*ET\_LSV) + (0.0000003*ET\_LSV^2) -$$
$$(0.006*RAIN) - (0.000*RAIN^2) + (8.896*PH\_IN) - (0.611*PH\_IN^2) - (0.796*TEMP\_IN) +$$
$$(0.016*TEMP\_IN^2) + (0.087*TP\_IN) - (0.022*TP\_IN^2)$$

where TP_OUT is outflow TP concentration (in mg/L) in the LSV cell; HRT is hydraulic retention time (with four levels: 1, 3, 5, and 7 days); AIRTEMP is the air temperature (in °C), AIRTEMP^2 is the quadratic term of AIRTEMP, RAIN is rainfall (in mm), RAIN^2 is the polynomial term of RAIN; EP_LS is evaporation in LS cell (in mm); EP_LS^2 is the polynomial term of EP_LS; PH_IN is the inflow water pH; PH_IN^2 is the polynomial term of PH_IN; TEMP_IN is the inflow water temperature (in °C); TEMP_IN^2 is the polynomial term of TEMP_IN; TP_IN is the inflow TP concentration (in mg/L); and TP_IN^2 is the polynomial term of TP_IN.

Table 21 shows that none of the variables contributed significantly to the TPLS and TPLSV models. Therefore, the influence of these variables on the outflow TP concentrations was not analysed further.

4.3.2.5. Discussion

The correlation analysis showed that outflow TP had a positive linear relationship with evaporation and ET, however, results from the polynomial regression model indicated that neither evaporation nor ET significantly influenced outflow TP. Similarly, no significant relationship was found between outflow TP and rainfall. These results align with the findings from Maniquiz et al.'s (2012) study, whereby no significant correlation was found between the flow and pollutant mass balances. The relation between outflow TP and HRT was also insignificant. This contradicts previous research which showed that TP reductions increased with longer HRTs (Wu et al., 2013). A reason for this observation could be that TP was absorbed onto the surface of the media, and therefore, was unaffected by HRT.

The results showed inflow pH, temperature and TP concentrations were positively correlated with outflow TP concentration in LSV cell, while inflow pH and TP concentration were positively correlated with outflow TP concentration in the LS cell. However, results from the polynomial regression models show that none of these variables significantly influenced outflow TP. This contrasts with previous research which has shown some effects, mostly unfavourable, from varying runoff pHs (Davis et al., 2006). For example, Barrow (1983) conducted experiments to show that P sorption decreased slightly with pH under acidic conditions, however, there was little dependence on pH in the neutral regime. Nevertheless, studies have shown that increasing temperature can cause P concentrations to decrease in vegetated biofilters (Gardner and Jones, 2008). These observations were attributed to increased sorption, which suggested that higher plant-available P was available at lower temperatures. Moreover, plant P uptake might decrease at low temperatures due to decreased plant activity. However, this did not seem to be the case in the LSV cell in this study.

CHAPTER 5: CONCLUSION

5.1.   Key findings

This study addressed the primary objectives of (1) analysing the performance of two field-scale biofiltration cells (one vegetated and one non-vegetated) that are batch-fed with surface water runoff from an upstream informal settlement, (2) determining the effects of various operating conditions (HRT), design parameters (presence of vegetation) and environmental factors (rainfall, temperature, evaporation/ET and inflow water quality) on the performance of the cells and (3) developing a multiple linear regression model for predicting the outflow ammonia (NH_3) and Total Phosphate (TP) concentrations in the cells under varying conditions.

The results showed that vegetated (LSV) and non-vegetated large stone (LS) cells effectively removed NH_3, TP and *Escherichia coli* (*E. coli*) from the infiltrating runoff, however, an overall increase in outflow nitrate (NO_3^-) and (NO_2^-) was observed. The net decrease in NH_3 and the net increase in NO_3^- and NO_2^- suggests that nitrification was the predominant nitrogen (N) removal process in the cells. Furthermore, the negligible difference between the cells indicates that plant uptake played a comparatively small role in removing pollutants.

Percentage NH_3 reductions were greater in the LSV cell than in the LS cell under higher inflow NH_3 concentrations. This suggests that vegetation was important for promoting nitrification in the cell. Furthermore, the LSV cell showed a more consistent removal of TP over time, which indicates that vegetation minimised the accumulation of phosphate in the media. Thus, vegetation may be an important factor controlling the lifespan of biofiltration media.

Hydraulic retention time (HRT), rainfall, temperature, evaporation and ET had no significant effect on the performance of the cells. However, inflow water quality parameters, including inflow water pH, temperature and NH_3 concentration significantly influenced outflow NH_3 in both cells. Outflow NH_3 increased exponentially with increasing inflow NH_3, while outflow NH_3 was lowest within certain pH and temperature ranges. The same effects were not observed for outflow TP, as outflow TP was not significantly influenced by any parameter.

The percentage of infiltrating runoff lost via ET was relatively high (26% average) compared to the percentage lost via evaporation (6% average) in the LSV cell. Therefore, vegetation played a significant role in reducing infiltrating runoff volumes. However, evaporation was

high in the LS cell (19% average), and therefore made a substantial contribution to the reduction of infiltrating runoff.

Lastly, the study shows that both cells effectively reduced N and EC concentrations to meet the minimum water quality requirements for irrigational reuse. The pH of the treated waters was also suitable for irrigation. However, there is insufficient evidence to show that the treated water is safe from faecal contamination.

5.2. Concluding remarks

This study has strengthened the understanding of the extent to which biofilters can be used to clean and reuse contaminated surface water runoff from upstream informal settlements. The water quality and quantity analyses confirmed that the cells were able to effectively reduce the pollutant concentrations and volume of infiltrating surface water runoff. These results align with previous studies which show that biofilters can be used to treat domestic sewage (Mburu et al., 2013; Zhai et al., 2011), agricultural wastewater (Lee et al., 2004), industrial wastewater (Chen et al., 2006, Maine et al., 2007), stormwater runoff (Sim et al., 2008) and landfill leachate (Nahlik and Mitsch, 2006) in developing countries.

The study also confirmed that HRT, rainfall, temperature, evaporation and ET do not have significant impacts on the performance of the cells. Instead, inflow water quality offers more insight into the performance of the cells, as inflow water pH, temperature and NH_3 concentrations can significantly influence outflow NH_3 concentrations. These results can be used to determine the performance of the cells under varying inflow water quality conditions. This is crucial for improving the design and/or operation of the cells, and hence, can ensure the performance and continued viability of the biofilter.

Lastly, the study confirmed the reuse potential of biofilters for irrigating vegetables. Although N, EC and pH levels were suitable for irrigational reuse, faecal contamination still poses a significant threat to human health and safety. It is therefore recommended that additional disinfection be required to mitigate any health-related risks. Alternatively, more research should be conducted to improve the design and/or operation of the cells for removing *E. coli*.

5.3. Recommendations for future study

This study demonstrates the extent to which biofilters can be used to clean and reuse contaminated surface water runoff from informal settlements. However, it also highlights some key aspects for future research:

- To determine how N removal can be improved.
- To determine the extent to which biofilters can be used to remove other pollutants, such as contaminants of emerging concerns (CECs) and heavy metals, from surface water runoff.
- To analyse the performance of the biofilters under a continuous flow regime.
- To evaluate the performance of the biofilters during the winter season and thus determine the effects of rainfall on the outflow water quality of the cells.
- To improve the accuracy of ET estimates by incorporating crop specific factors.

REFERENCES

Adhikari, R. A., Bal Krishna, K. C. & Sarukkalige, R. 2016. Evaluation of phosphorus adsorption capacity of various filter materials from aqueous solution. *Adsorption Science & Technology,* 34**,** 320-330.

Ahiablame, L. and Shakya, R., 2016. Modeling flood reduction effects of low impact development at a watershed scale. *Journal of Environmental* Management*, 171,* pp.81-91.

Akratos, C. S. & Tsihrintzis, V. A. 2007. Effect of temperature, HRT, vegetation and porous media on removal efficiency of pilot-scale horizontal subsurface flow constructed wetlands. *Ecological Engineering,* 29**,** 173-191.

Allen, R. G., Pereira, L. S., Raes, D. & Smith, M. 1998. Crop evapotranspiration-Guidelines for computing crop water requirements-FAO Irrigation and drainage paper 56. *Fao, Rome,* 300**,** D05109.

Arden, S. & Ma, X. 2018. Constructed wetlands for greywater recycle and reuse: A review. *Science of the Total Environment,* 630**,** 587-599.

Armitage, N. P., Winter, K., Spiegel, A. & Kruger, E. 2009. Community-focused greywater management in two informal settlements in South Africa. *Water, Science & Technology,* 59**,** 2341-50.

Babatunde, A. O., Zhao, Y. Q. & Zhao, X. H. 2010. Alum sludge-based constructed wetland system for enhanced removal of P and OM from wastewater: concept, design and performance analysis. *Bioresource Technology,* 101**,** 6576-9.

Barrow, N. 1983. A mechanistic model for describing the sorption and desorption of phosphate by soil. *Journal of soil science,* 34**,** 733-750.

Beebe, D. A., Castle, J. W., Molz, F. J. & Rodgers, J. H. 2014. Effects of evapotranspiration on treatment performance in constructed wetlands: Experimental studies and modeling. *Ecological Engineering,* 71**,** 394-400.

Bertino, G., Menconi, F., Zraunig, A., Terzidis, E. & Kisser, J. 2018. Innovative Circular Solutions and Services for New Buildings and Refurbishments. *Eco-Architecture VII: Harmonisation between Architecture and Nature.*

Blecken, G.-T., Zinger, Y., Deletić, A., Fletcher, T. D., Hedström, A. & Viklander, M. 2010. Laboratory study on stormwater biofiltration: Nutrient and sediment removal in cold temperatures. *Journal of Hydrology,* 394**,** 507-514.

Boano, F., Caruso, A., Costamagna, E., Ridolfi, L., Fiore, S., Demichelis, F., Galvao, A., Pisoeiro, J., Rizzo, A. & Masi, F. 2020. A review of nature-based solutions for greywater treatment: Applications, hydraulic design, and environmental benefits. *Science of the Total Environment,* 711**,** 134731.

Bojcevska, H. & Tonderski, K. 2007. Impact of loads, season, and plant species on the performance of a tropical constructed wetland polishing effluent from sugar factory stabilization ponds. *Ecological Engineering,* 29**,** 66-76.

Borin, M. & Salvato, M. 2012. Effects of five macrophytes on nitrogen remediation and mass balance in wetland mesocosms. *Ecological Engineering,* 46**,** 34-42.

Borin, M. & Tocchetto, D. 2007. Five year water and nitrogen balance for a constructed surface flow wetland treating agricultural drainage waters. *Science of the Total Environment,* 380**,** 38-47.

Bradford, S. A., Simunek, J. & Walker, S. L. 2006. Transport and straining ofE. coliO157:H7 in saturated porous media. *Water Resources Research,* 42.

Brander, K. E., Owen, K. E. & Potter., K. W. 2009. Modeled impacts of development type on runoff volume and infiltration performance. *Journal of the American Water Resources Association,* 40**,** 8.

Bratieres, K., Fletcher, T. D., Deletic, A. & Zinger, Y. 2008. Nutrient and sediment removal by stormwater biofilters: a large-scale design optimisation study. *Water Research,* 42**,** 3930-40.

Brears, R. C. 2018. *Blue and green cities: the role of blue-green infrastructure in managing urban water resources*, Springer.

Brown, R., Zhang, Z., Comeau, L.-P. & Bedard-Haughn, A. 2017. Effects of drainage duration on mineral wetland soils in a Prairie Pothole agroecosystem. *Soil and Tillage Research,* 168**,** 187-197.

Brown, R. A. & Hunt, W. F. 2011. Impacts of Media Depth on Effluent Water Quality and Hydrologic Performance of Undersized Bioretention Cells. *Journal of Irrigation and Drainage Engineering,* 137**,** 132-143.

Bulc, T. G. 2006. Long term performance of a constructed wetland for landfill leachate treatment. *Ecological Engineering,* 26**,** 365-374.

Bunce, J. T., Ndam, E., Ofiteru, I. D., Moore, A. & Graham, D. W. 2018. A Review of Phosphorus Removal Technologies and Their Applicability to Small-Scale Domestic Wastewater Treatment Systems. *Frontiers in Environmental Science,* 6.

Carden, K., Armitage, N., Fisher-Jeffes, L., Winter, K., Mauck, B., Sanya, T., Bhikha, P., Mallett, G., Kanyerere, T. & Gxokwe, S. 2018. Challenges and opportunities for implementing Water Sensitive Design in South Africa. South Africa: Water Research Commission.

Carden, K., Armitage, N., Sichone, O. & Winter, K. 2007. The use and disposal of greywater in the non-sewered areas of South Africa: Part 2 – Greywater management options. *Water SA,* 33.

Carpenter, D. D. & Hallam, L. 2010. Influence of planting soil mix characteristics on bioretention cell design and performance. *Journal of Hydrologic Engineering,* 15**,** 14.

Caselles-Osorio, A. & Garcia, J. 2007. Impact of different feeding strategies and plant presence on the performance of shallow horizontal subsurface-flow constructed wetlands. *Science of the Total Environment,* 378**,** 253-62.

Cerezo, G. R., Suarez, M. L. & Vidal-Abarca, M. R. 2001. The performance of a multi-stage system of constructed wetlands for urban wastewater treatment in a semiarid region of SE Spain. *Ecological Engineering,* 16.

Chandrasena, G., Deletic, A., Ellerton, J. & McCarthy, D. T. 2012. Evaluating Escherichia coli removal performance in stormwater biofilters: a laboratory-scale study. *Water, Science & Technology,* 66**,** 1132-1138.

Chandrasena, G. I., Deletic, A. & McCarthy, D. T. 2016. Biofiltration for stormwater harvesting: Comparison of Campylobacter spp. and Escherichia coli removal under normal and challenging operational conditions. *Journal of Hydrology,* 537**,** 248-259.

Chandrasena, G. I., Pham, T., Payne, E. G., Deletic, A. & McCarthy, D. T. 2014. E. coli removal in laboratory scale stormwater biofilters: Influence of vegetation and submerged zone. *Journal of Hydrology,* 519**,** 814-822.

Chen, T. Y., Kao, C. M., Yeh, T. Y., Chien, H. Y. & Chao, A. C. 2006. Application of a constructed wetland for industrial wastewater treatment: a pilot-scale study. *Chemosphere,* 64**,** 497-502.

Chen, Y., Chen, R., Liu, Z., Yu, X., Zheng, S. & Yuan, S. 2021. Nitrogen process in stormwater bioretention: the impact of alternate drying and rewetting on nitrogen migration and transformation. *Environmental Science Pollution Research International*.

Cho, K. W., Yoon, M. H., Song, K. G. & Ahn, K. H. 2011. The effects of antecedent dry days on the nitrogen removal in layered soil infiltration systems for storm run-off control. *Environmental Technology,* 32**,** 747-55.

Chung, J., Amin, K., Kim, S., Yoon, S., Kwon, K. & Bae, W. 2014. Autotrophic denitrification of nitrate and nitrite using thiosulfate as an electron donor. *Water Research,* 58**,** 169-78.

Chung, Y. C., Ho, K. L. & Tseng, C. P. 2007. Two-stage biofilter for effective NH3 removal from waste gases containing high concentrations of H2S. *Journal of Air and Watste Management Association,* 57**,** 337-47.

Cohen-Shacham, E., Walters, G., Janzen, C. & Maginnis, S. 2016. Nature-based solutions to address global societal challenges. *IUCN: Gland, Switzerland,* 97.

Commission, E. 2015. Final Report of the Horizon 2020 Expert Group on 'Nature-Based Solutions and ReNaturing Cities'. *Directorate-General for Research and Innovation–Climate Action, Environment, Resource Efficiency and Raw Materials,* 74.

Craft, C. B., Vymazal, J. & Richardson, C. J. 1995. Response of everglades plant communities to nitrogen and phosphorus additions. *Wetlands,* 15**,** 258-271.

Cunqi, L., Jianjian, L. & Hepeng, L. 2007. Landward changes of soil enzyme activities in a tidal flat wetland of the Yangtze River Estuary and correlations with physico-chemical factors. *Acta Ecologica Sinica,* 27**,** 3663-3669.

Dan, T. H., Quang, L. N., Chiem, N. H. & Brix, H. 2011. Treatment of high-strength wastewater in tropical constructed wetlands planted with Sesbania sesban: Horizontal subsurface flow versus vertical downflow. *Ecological Engineering,* 37**,** 711-720.

Davies, T. & Cottingham, P. 2020. Phosphorus removal from wastewater in a constructed wetland. *Constructed wetlands for water quality improvement.* CRC Press.

Davis, A. P. 2008. Field performance of bioretention: hydrology impacts. *Journal of Hydrologic Engineering,* 13**,** 5.

Davis, A. P., Shokouhian, M., Himanshu, S. & Minami, C. 2001. Laboratory Study of Biological Retention for Urban Stormwater Management. *Water environment research,* 73**,** 9.

Davis, A. P., Shokouhian, M., Sharma, H. & Minami, C. 2006. Water quality improvement through bioretention media: nitrogen and phosphorus removal. *Water environment research,* 78**,** 284-93.

Davis, A. P., Traver, R. & Hunt, W. F. 2010. Improving Urban Stormwater Quality: Applying Fundamental Principles. *Journal of Contemporary Water Research & Education***,** 7.

Decamp, O. & Warren, A. 2001. Abundance, biomass and viability of bacteria in wastewaters: impact of treatment in horizontal subsurface flow constructed wetlands. *Water Research,* 35**,** 3496-3501.

De Clercq, W., Ellis, F., Fey, M., van Meirvenne, M., Engelbrecht, H. and de Smet, G. 2006. Research on Berg River Management: Summary of Water Quality Information System and Soil Quality Studies. Available at: https://scholar.sun.ac.za/handle/10019.1/40809 [Accessed April 5, 2017].

Demin, O. A. & Dudeney, A. W. L. 2003. Nitrification in Constructed Wetlands Treating Ochreous Mine Water. *Mine, Water and the Environment,* 22**,** 6.

Denich, C. & Bradford, A. 2010. Estimation of Evapotranspiration from Bioretention Areas Using Weighing Lysimeters. *Journal of Hydrologic Engineering,* 15**,** 8.

Dietz, M. E. & Clausen, J. C. 2005. A field evaluation of rain garden flow and pollutant treatment. *Water, Air, & Soil Pollution,* 167**,** 15.

Dumitru, A. & Wendling, L. 2021. Evaluating the Impacts of Nature-based Solutions: A Handbook for Practitioners.

DWAF 1996. South African Water Quality Guidelines (second edition). *In:* FORESTRY, D. O. W. A. A. (ed.) 2 ed. Pretoria, South Africa: Department of Water Affairs and Forestry.

Ebrahimian, A., Wadzuk, B. & Traver, R. 2019. Evapotranspiration in green stormwater infrastructure systems. *Science of the Total Environment,* 688**,** 797-810.

EPA, U. 2000. Low Impact Development (LID): A Literature Review. . United States Environmental Protection Agency.

Erickson, A. J., Gulliver, J. S. & Weiss, P. T. 2012. Capturing phosphates with iron enhanced sand filtration. *Water Research,* 46**,** 3032-42.

Fell, J. 2018. *An analysis of surface water from an informal settlement, Langrug, Franschhoek: down a slippery slope.* MSc, University of Cape Town.

Ferguson, C., Husman, A. M. d. R., Altavilla, N., Deere, D. & Ashbolt, N. 2003. Fate and Transport of Surface Water Pathogens in Watersheds. *Critical Reviews in Environmental Science and Technology,* 33**,** 299-361.

Fletcher, T. D., Shuster, W., Hunt, W. F., Ashley, R., Butler, D., Arthur, S., Trowsdale, S., Barraud, S., Semadeni-Davies, A., Bertrand-Krajewski, J.-L., Mikkelsen, P. S., Rivard, G., Uhl, M., Dagenais, D. & Viklander, M. 2014. SUDS, LID, BMPs, WSUD and more – The evolution and application of terminology surrounding urban drainage. *Urban Water Journal,* 12**,** 525-542.

Fonder, N. & Headley, T. 2013. The taxonomy of treatment wetlands: A proposed classification and nomenclature system. *Ecological Engineering,* 51**,** 203-211.

García, J., Aguirre, P., Barragán, J., Mujeriego, R., Matamoros, V. & Bayona, J. M. 2005. Effect of key design parameters on the efficiency of horizontal subsurface flow constructed wetlands. *Ecological Engineering,* 25**,** 405-418.

Garcia, J., Rousseau, D. P. L., MoratÓ, J., Lesage, E. L. S., Matamoros, V. & Bayona, J. M. 2010. Contaminant Removal Processes in Subsurface-Flow Constructed Wetlands: A Review. *Critical Reviews in Environmental Science and Technology,* 40**,** 561-661.

Gardner, B. R. & Jones, J. P. 2008. Effects of temperature on phosphate sorption isotherms and phosphate desorption. *Communications in Soil Science and Plant Analysis,* 4**,** 83-93.

Gerardi, M. H. 2003. *Nitrification and denitrification in the activated sludge process*, John Wiley & Sons.

Gervin, L. & Brix, H. 2001. Removal of nutrients from combined sewer overflows and lake water in a vertical-flow constructed wetland system. *Water, Science & Technology,* 44.

Ghanashyam, A. 2018. *The use of biofiltration cells to filter contaminated water flowing from a slum settlement in South Africa.* MSc, University of Cape Town.

Glaister, B. J., Fletcher, T. D., Cook, P. L. M. & Hatt, B. E. 2017. Interactions between design, plant growth and the treatment performance of stormwater biofilters. *Ecological Engineering,* 105**,** 21-31.

Gonzalez-Merchan, C., Barraud, S. & Bedell, J. P. 2014. Influence of spontaneous vegetation in stormwater infiltration system clogging. *Environmental Science and Pollution Research International,* 21**,** 5419-26.

Guo, X., Drury, C. F., Yang, X., Daniel Reynolds, W. & Fan, R. 2014. The Extent of Soil Drying and Rewetting Affects Nitrous Oxide Emissions, Denitrification, and Nitrogen Mineralization. *Soil Science Society of America Journal,* 78**,** 194-204.

Hart, T. 2017. *Root-enhanced Infiltration in Stormwater Bioretention Facilities in Portland, Oregon.* Doctor of Philosophy, Portland State University.

Hathaway, J. M., Hunt, W. F., Graves, A. K. & Wright, J. D. 2011. Field Evaluation of Bioretention Indicator Bacteria Sequestration in Wilmington, North Carolina. *Journal of Environmental Engineering,* 137**,** 1103-1113.

Hatt, B. E., Fletcher, T. D. & Deletic, A. 2007. Treatment performance of gravel filter media: implications for design and application of stormwater infiltration systems. *Water Research,* 41**,** 2513-24.

Hatt, B. E., Fletcher, T. D. & Deletic, A. 2009. Pollutant removal performance of field-scale stormwater biofiltration systems. *Water, Science & Technology,* 59**,** 1567-76.

Henderson, C., Greenway, M. & Phillips, I. 2007. Removal of dissolved nitrogen, phosphorus and carbon from stormwater by biofiltration mesocosms. *Water, Science & Technology,* 55**,** 183-91.

Hermawan, A. A., Talei, A., Salamatinia, B. & Chua, L. H. C. 2020. Seasonal performance of stormwater biofiltration system under tropical conditions. *Ecological Engineering,* 143.

Hickman, J., John, Wadzuk, B. & Traver, R. Evaluating the role of evapotranspiration in the hydrology of a bioinfiltration basin using a weighing lysimeter. World Environmental and Water Resources Congress 2011: Bearing Knowledge for Sustainability, 2011. 3601-3609.

Huang, J., Reneau, R. B. & Hagedorn, C. 2000. Nitrogen removal in constructed wetlands employed to treat domestic wastewater. *Water Research,* 34**,** 6.

Huett, D. O., Morris, S. G., Smith, G. & Hunt, N. 2005. Nitrogen and phosphorus removal from plant nursery runoff in vegetated and unvegetated subsurface flow wetlands. *Water Research,* 39**,** 3259-72.

Hunt, W. F., Jarret, A. R., Smith, J. T. & Sharkey, L. J. 2006. Evaluating Bioretention Hydrology and Nutrient Removal at Three Field Sites in North Carolina. *Journal of Irrigation and Drainage Engineering,* 132.

Hunt, W. F., Smith, J. T., Jadlocki, S. J., Hathaway, J. M. & Eubanks, P. R. 2008. Pollutant removal and peak flow mitigation by a bioretention cell in urban Charlotte, N.C. *Journal of Environmental Engineering,* 134.

Information, N. G.-s. 2021. River catchments [Shape file, January 2021]. National Geo-spatial Information. South Africa: National Geo-spatial Information.

Isidima. 2017. *The Water Hub Project* [Online]. Available: https://www.isidima.net/ [Accessed].

Jay, J. G., Brown, S. L., Kurtz, K. & Grothkopp, F. 2017. Predictors of Phosphorus Leaching from Bioretention Soil Media. *Journal of environmental quality,* 46**,** 1098-1105.

Jay, J. G., Tyler-Plog, M., Brown, S. L. & Grothkopp, F. 2019. Nutrient, metal, and organics removal from stormwater using a range of bioretention soil mixtures. *Journal of environmental quality,* 48**,** 493-501.

Jenkins, J. K. G., Wadzuk, B. M. & Welker, A. L. 2010. Fines accumulation and distribution in a storm-water rain garden nine years postconstruction. *Journal of Irrigation and Drainage Engineering,* 136**,** 7.

Jenssen, P. D., Mæhlum, T., Krogstad, T. & Vråle, L. 2005. High performance constructed wetlands for cold climates. *Journal of Environmental Science and Health,* 40**,** 1343-1353.

Jiang, C., Li, J., Li, H. & Li, Y. 2019. An improved approach to design bioretention system media. *Ecological Engineering,* 136**,** 125-133.

Jiang, C., Li, J., Li, H., Li, Y. & Chen, L. 2017. Field Performance of Bioretention Systems for Runoff Quantity Regulation and Pollutant Removal. *Water, Air, & Soil Pollution,* 228.

Jing, D.-b. & Hu, H.-y. 2010. Chemical Oxygen Demand, Nitrogen, and Phosphorus Removal by Vegetation of Different Species in Pilot-Scale Subsurface Wetlands. *Environmental Engineering Science,* 27**,** 247-253.

Jones, J. E. & Hunt, W. F. 2009. Bioretention Impact on Runoff Temperature in Trout Sensitive Waters. *Journal of Environmental Engineering,* 135.

Juang, T. C., Wang, M. K., Chen, H. J. & Tan, C. C. 2001. Ammonia fixation by surface soils and clays. *Soil Science,* 166.

Jurries, D. 2003. Biofilters (bioswales, vegetative buffers, & constructed wetlands) for storm water discharge pollution removal.

Kadlec, R. H. & Reddy, K. R. 2001. Temperature Effects in Treatment Wetlands. *Water environment research,* 73**,** 14.

Kadlec, R. H., Tanner, C. C., Hally, V. M. & Gibbs, M. M. 2005. Nitrogen spiraling in subsurface-flow constructed wetlands: implications for treatment response. *Ecological Engineering,* 25**,** 365-381.

Kadlec, R. H. & Wallace, S. 2008. *Treatment Wetlands*, CRC Press.

Kandel, S., Vogel, J., Penn, C. & Brown, G. 2017. Phosphorus Retention by Fly Ash Amended Filter Media in Aged Bioretention Cells. *Water,* 9.

Kandra, H. S., Deletic, A. & McCarthy, D. 2014. Assessment of Impact of Filter Design Variables on Clogging in Stormwater Filters. *Water Resources Management,* 28**,** 1873-1885.

Katayon, S., Fiona, Z., Megat Mohd Noor, M. J., Abdul Halim, G. & Ahmad, J. 2008. Treatment of mild domestic wastewater using subsurface constructed wetlands in Malaysia. *International Journal of Environmental Studies,* 65**,** 87-102.

Kim, H., Seagren, E. A. & Davis, A. P. 2003. Engineered Bioretention for Removal of Nitrate from Stormwater Runoff. *Water environment research,* 75.

Kisser, J., Wirth, M., De Gusseme, B., Van Eekert, M., Zeeman, G., Schoenborn, A., Vinnerås, B., Finger, D. C., Kolbl Repinc, S., Bulc, T. G., Bani, A., Pavlova, D., Staicu, L. C., Atasoy, M., Cetecioglu, Z., Kokko, M., Haznedaroglu, B. Z., Hansen, J., Isteni̇č, D., Canga, E., Malamis, S., Camilleri-Fenech, M. & Beesley, L. 2020. A review of nature-based solutions for resource recovery in cities. *Blue-Green Systems,* 2**,** 138-172.

Kivaisi, A. 2001. The potential for constructed wetlands for wastewater treatment and reuse in developing countries: a review. *Ecological Engineering,* 16**,** 5.

Konnerup, D., Koottatep, T. & Brix, H. 2009. Treatment of domestic wastewater in tropical, subsurface flow constructed wetlands planted with Canna and Heliconia. *Ecological Engineering,* 35**,** 248-257.

Laber, J., Perfler, R. & Haberl, R. 1997. Two strategies for advanced nitrogen elimination in vertical flow constructed wetlands. *Water, Science and Technology,* 35.

Langergraber, G. 2007. Simulation of the treatment performance of outdoor subsurface flow constructed wetlands in temperate climates. *Science of the Total Environment,* 380**,** 210-9.

Le Coustumer, S., Fletcher, T. D., Deletic, A. & Barraud, S. 2007. Hydraulic performance of biofilters for stormwater management: first lessons from both laboratory and field studies. *Water, Science & Technology,* 56**,** 93-100.

Le Coustumer, S., Fletcher, T. D., Deletic, A., Barraud, S. & Poelsma, P. 2012. The influence of design parameters on clogging of stormwater biofilters: a large-scale column study. *Water Research,* 46**,** 6743-52.

Lee, B.-H. & Scholz, M. 2007. What is the role of Phragmites australis in experimental constructed wetland filters treating urban runoff? *Ecological Engineering,* 29**,** 87-95.

Lee, C. Y., Lee, C. C., Lee, F. Y., Tseng, S. K. & Liao, C. J. 2004. Performance of subsurface flow constructed wetland taking pretreated swine effluent under heavy loads. *Bioresource Technology,* 92**,** 173-9.

LeFevre, G. H., Paus, K. H., Natarajan, P., Gulliver, J. S., Novak, P. J. & Hozalski, R. M. 2015. Review of Dissolved Pollutants in Urban Storm Water and Their Removal and Fate in Bioretention Cells. *Journal of Environmental Engineering,* 141.

Leitner, S., Minixhofer, P., Inselsbacher, E., Keiblinger, K. M., Zimmermann, M. & Zechmeister-Boltenstern, S. 2017. Short-term soil mineral and organic nitrogen fluxes during moderate and severe drying–rewetting events. *Applied Soil Ecology,* 114**,** 28-33.

Li, H. & Davis, A. P. 2009. Water Quality Improvement through Reductions of Pollutant Loads Using Bioretention. *Journal of Environmental Engineering,* 135.

Li, H., Sharkey, L. J., Hunt, W. F. & Davis, A. P. 2009. Mitigation of Impervious Surface Hydrology Using Bioretention in North Carolina and Maryland. *Journal of Hydrologic Engineering,* 14.

Li, J. & Davis, A. P. 2016. A unified look at phosphorus treatment using bioretention. *Water Research,* 90**,** 141-155.

Li, Y., Li, H., Sun, T. & Wang, X. 2011. Study on nitrogen removal enhanced by shunt distributing wastewater in a constructed subsurface infiltration system under intermittent operation mode. *Journal of Hazardous Materials,* 189**,** 336-41.

Lin, Y.-F., Jing, S.-R., Lee, D.-Y. & Wang, T.-W. 2002. Nutrient removal from aquaculture wastewater using constructed wetlands system. *Aquaculture,* 209**,** 15.

Liu, J. & Davis, A. P. 2014. Phosphorus speciation and treatment using enhanced phosphorus removal bioretention. *Environmental Science & Technology,* 48**,** 607-14.

Liu, J., Yue, P., He, Y. & Zhao, M. 2020. Removal of E. coli from stormwater by bioretention system: parameter optimization and mechanism. *Water, Science & Technology,* 81**,** 1170-1179.

Lopez-Ponnada, E. V., Lynn, T. J., Ergas, S. J. & Mihelcic, J. R. 2020. Long-term field performance of a conventional and modified bioretention system for removing dissolved nitrogen species in stormwater runoff. *Water Research,* 170**,** 115336.

Lu, S. Y., Wu, F. C., Lu, Y. F., Xiang, C. S., Zhang, P. Y. & Jin, C. X. 2009. Phosphorus removal from agricultural runoff by constructed wetland. *Ecological Engineering,* 35**,** 402-409.

Lucas, W. & Greenway, M. 2008. Nutrient Retention in Vegetated and Nonvegetated Bioretention Mesocosms. *Journal of Irrigation and Drainage Engineering,* 134.

Lucas, W. & Greenway, M. 2011. Phosphorus Retention by Bioretention Mesocosms Using Media Formulated for Phosphorus Sortion: Response to Accelerated Loads. *Journal of Irrigation and Drainage Engineering,* 137.

Lynn, T. J., Yeh, D. H. & Ergas, S. J. 2015. Performance of denitrifying stormwater biofilters under intermittent conditions. *Environmental Engineering Science,* 32**,** 796-805.

Maine, M. A., Sune, N., Hadad, H. & Sanchez, G. 2007. Temporal and spatial variation of phosphate distribution in the sediment of a free water surface constructed wetland. *Science of the Total Environment,* 380**,** 75-83.

Maniquiz, M. C., Kim, L.-H., Lee, S. & Choi, J. 2012. Flow and mass balance analysis of eco-bio infiltration system. *Frontiers of Environmental Science & Engineering,* 6**,** 612-619.

Masi, F., Rizzo, A. & Regelsberger, M. 2018. The role of constructed wetlands in a new circular economy, resource oriented, and ecosystem services paradigm. *Journal of Environmental Management,* 216**,** 275-284.

Matheson, F. E. & Sukias, J. P. 2010. Nitrate removal processes in a constructed wetland treating drainage from dairy pasture. *Ecological Engineering,* 36**,** 1260-1265.

Mayo, A. W. & Mutamba, J. 2004. Effect of HRT on nitrogen removal in a coupled HRP and unplanted subsurface flow gravel bed constructed wetland. *Physics and Chemistry of the Earth, Parts A/B/C,* 29**,** 1253-1257.

Mburu, N., Tebitendwa, S. M., Rousseau, D. P., Van Bruggen, J. J. A. & Lens, P. N. 2013. Performance evaluation of horizontal subsurface flow–constructed wetlands for the treatment of domestic wastewater in the tropics. *Journal of Environmental Engineering,* 139**,** 9.

McNett, J. K., Hunt, W. F. & Davis, A. P. 2011. Influent Pollutant Concentrations as Predictors of Effluent Pollutant Concentrations for Mid-Atlantic Bioretention. *Journal of Environmental Engineering,* 137**,** 790-799.

Milandri, S. G., Winter, K. J., Chimphango, S. B. M., Armitage, N. P., Mbui, D. N., Jackson, G. E. & Liebau, V. 2012. The performance of plant species in removing nutrients from stormwater in biofiltration systems in Cape Town. *Water SA,* 38.

Moene, A. F. & Van Dam, J. C. 2014. *Transport in the atmosphere-vegetation-soil continuum*, Cambridge University Press.

Muerdter, C., Wong, C. & Le Fevre, G. 2018. Emerging investigator series: The Role of Vegetation in Bioretention for Stormwater Treatment in the Built Environment: Pollutant Removal, Hydrologic Function, and Ancillary Benefits. *Environmental Science: Water Research & Technology.*

Municipality, S. 2011. Stellenbosch Municipality Annual Report. *In:* MUNICIPALITY, S. L. (ed.). Stellenbosch.

Muthanna, T. M., Viklander, M., Blecken, G. & Thorolfsson, S. T. 2007. Snowmelt pollutant removal in bioretention areas. *Water Research,* 41**,** 4061-72.

Nahlik, A. M. & Mitsch, W. J. 2006. Tropical treatment wetlands dominated by free-floating macrophytes for water quality improvement in Costa Rica. *Ecological Engineering,* 28**,** 246-257.

Navarro-García, F., Casermeiro, M. Á. & Schimel, J. P. 2012. When structure means conservation: Effect of aggregate structure in controlling microbial responses to rewetting events. *Soil Biology and Biochemistry,* 44**,** 1-8.

Nivala, J., Hoos, M. B., Cross, C., Wallace, S. & Parkin, G. 2007. Treatment of landfill leachate using an aerated, horizontal subsurface-flow constructed wetland. *Science of the Total Environment,* 380**,** 19-27.

Nocco, M. A., Rouse, S. E. & Balster, N. J. 2016. Vegetation type alters water and nitrogen budgets in a controlled, replicated experiment on residential-sized rain gardens planted with prairie, shrub, and turfgrass. *Urban Ecosystems,* 19**,** 1665-1691.

Norton, R. A., Harrison, J. A., Kent Keller, C. & Moffett, K. B. 2017. Effects of storm size and frequency on nitrogen retention, denitrification, and N2O production in bioretention swale mesocosms. *Biogeochemistry,* 134**,** 353-370.

O'Luanaigh, N. D., Goodhue, R. & Gill, L. W. 2010. Nutrient removal from on-site domestic wastewater in horizontal subsurface flow reed beds in Ireland. *Ecological Engineering,* 36**,** 1266-1276.

Oral, H. V., Carvalho, P., Gajewska, M., Ursino, N., Masi, F., Hullebusch, E. D. v., Kazak, J. K., Exposito, A., Cipolletta, G., Andersen, T. R., Finger, D. C., Simperler, L., Regelsberger, M., Rous, V.,

Radinja, M., Buttiglieri, G., Krzeminski, P., Rizzo, A., Dehghanian, K., Nikolova, M. & Zimmermann, M. 2020. A review of nature-based solutions for urban water management in European circular cities: a critical assessment based on case studies and literature. *Blue-Green Systems,* 2**,** 112-136.

Pappalardo, V., La Rosa, D., Campisano, A. & La Greca, P. 2017. The potential of green infrastructure application in urban runoff control for land use planning: A preliminary evaluation from a southern Italy case study. *Ecosystem Services,* 26**,** 345-354.

Paredes, D., Kuschk, P., Mbwette, T. S. A., Stange, F., Müller, R. A. & Köser, H. 2007. New Aspects of Microbial Nitrogen Transformations in the Context of Wastewater Treatment – A Review. *Engineering in Life Sciences,* 7**,** 13-25.

Passeport, E. & Hunt, W. F. 2009. Asphalt Parking Lot Runoff Nutrient Characterization for Eight Sites in North Carolina, USA. *Journal of Hydrologic Engineering,* 14.

Passeport, E., Hunt, W. F., Smith, R. & Brown, R. A. 2009. Field Study of the Ability of Two Grassed Bioretention Cells to Reduce Storm-Water Runoff Pollution. *Journal of Irrigation and Drainage Engineering,* 135.

Pathan, S. M., Barton, L. & Colmer, T. D. 2007. Evaluation of a soil moisture sensor to reduce water and nutrient leaching in turfgrass (Cynodon dactylon cv. Wintergreen). *Australian Journal of Experimental Agriculture,* 47.

Payne, E. G. I., Fletcher, T. D., Cook, P. L. M., Deletic, A. & Hatt, B. E. 2014. Processes and Drivers of Nitrogen Removal in Stormwater Biofiltration. *Critical Reviews in Environmental Science and Technology,* 44**,** 796-846.

Pearlmutter, D., Theochari, D., Nehls, T., Pinho, P., Piro, P., Korolova, A., Papaefthimiou, S., Mateo, M. C. G., Calheiros, C., Zluwa, I., Pitha, U., Schosseler, P., Florentin, Y., Ouannou, S., Gal, E., Aicher, A., Arnold, K., Igondová, E. & Pucher, B. 2020. Enhancing the circular economy with nature-based solutions in the built urban environment: green building materials, systems and sites. *Blue-Green Systems,* 2**,** 46-72.

Pollman, C., Landing, W., Perry Jr, J. & Fitzpatrick, T. 2002. Wet deposition of phosphorus in Florida. *Atmospheric Environment,* 36**,** 2309-2318.

Qiu, F., Zhao, S., Zhao, D., Wang, J. & Fu, K. 2019. Enhanced nutrient removal in bioretention systems modified with water treatment residuals and internal water storage zone. *Environmental Science: Water Research & Technology,* 5**,** 993-1003.

Rahman, M. Y. A., Nachabe, M. H. & Ergas, S. J. 2020. Biochar amendment of stormwater bioretention systems for nitrogen and Escherichia coli removal: Effect of hydraulic loading rates and antecedent dry periods. *Bioresource Technology,* 310**,** 123428.

Read, J., Fletcher, T. D., Wevill, T. & Deletic, A. 2010. Plant traits that enhance pollutant removal from stormwater in biofiltration systems. *International Journal of Phytoremediation,* 12**,** 34-53.

Read, J., Wevill, T., Fletcher, T. & Deletic, A. 2008. Variation among plant species in pollutant removal from stormwater in biofiltration systems. *Water Research,* 42**,** 893-902.

Reddy, K. R., Patrick, W. H. & Broadbent, F. E. 2009. Nitrogen transformations and loss in flooded soils and sediments. *CRC Critical Reviews in Environmental Control,* 13**,** 273-309.

Rodda, N., Carden, K. and Armitage, N., 2010. Sustainable use of greywater in small-scale agriculture and gardens in South Africa. Water Research Commission, Cape Town, South Africa. ISBN, 1790667908.

Roseen, R. M., Ballestero, T. P., Houle, J. J., Avellaneda, P., Briggs, J., Fowler, G. & Wildey, R. 2009. Seasonal performance variations for storm-water management systems in cold climate conditions. *Environmental Engineering,* 135.

Roy-Poirier, A., Champagne, P., Asce, A. M. & Filion, Y. 2010. Review of Bioretention System Research and Design: Past, Present, and Future. *Journal of Environmental Engineering*.

Rusciano, G. M. & Obropta, C. C. 2007. Bioretention Column Study: Fecal Coliform and Total Suspended Solids Reductions. *Transactions of the ASABE*.

Russell, C. A., Fillery, I. R. P., Bootsma, N. & McInnes, K. J. 2007. Effect of temperature and nitrogen source on nitrification in a sandy soil. *Communications in Soil Science and Plant Analysis,* 33**,** 1975-1989.

Rycewicz-Borecki, M., McLean, J. E. & Dupont, R. R. 2017. Nitrogen and phosphorus mass balance, retention and uptake in six plant species grown in stormwater bioretention microcosms. *Ecological Engineering,* 99**,** 409-416.

Saeed, T. & Sun, G. 2011. Enhanced denitrification and organics removal in hybrid wetland columns: comparative experiments. *Bioresource Technology,* 102**,** 967-74.

Saeed, T. & Sun, G. 2012. A review on nitrogen and organics removal mechanisms in subsurface flow constructed wetlands: Dependency on environmental parameters, operating conditions and supporting media. *Journal of Environmental Management*.

Sharkey, L. J. 2006. *The performance of bioretention areas in North Carolina: A study of water quality, water quantity, and soil media.* Master of Science, North Carolina State University.

Shi, P., Chen, C., Srinivasan, R., Zhang, X., Cai, T., Fang, X., Qu, S., Chen, X. & Li, Q. 2011. Evaluating the SWAT Model for Hydrological Modeling in the Xixian Watershed and a Comparison with the XAJ Model. *Water Resources Management,* 25**,** 2595-2612.

Sim, C. H., Yusoff, M. K., Shutes, B., Ho, S. C. & Mansor, M. 2008. Nutrient removal in a pilot and full scale constructed wetland, Putrajaya city, Malaysia. *Journal of Environmental Management,* 88**,** 307-17.

Skorobogatov, A., He, J., Chu, A., Valeo, C. & van Duin, B. 2020. The impact of media, plants and their interactions on bioretention performance: A review. *Science of the Total Environment,* 715**,** 136918.

Smith, E. H., Abumaizar, R. J., Halff, A. H. & Skipwith, W. E. 2001. Simple mass balance approach for assessment of flood control sumps in an urban watershed: case study of heavy metal loading. *Water, Science & Technology,* 43.

Søberg, L. C., Viklander, M., Blecken, G.-T. & Hedström, A. 2019. Reduction of Escherichia coli, Enterococcus faecalis and Pseudomonas aeruginosa in stormwater bioretention: Effect of drying, temperature and submerged zone. *Journal of Hydrology* 3.

Stander, E. K. & Borst, M. 2010. Hydraulic test of a bioretention media carbon amendment. *Journal of Hydrologic Engineering,* 15**,** 5.

Stottmeister, U., Wiessner, A., Kuschk, P., Kappelmeyer, U., Kastner, M., Bederski, O., Muller, R. A. & Moormann, H. 2003. Effects of plants and microorganisms in constructed wetlands for wastewater treatment. *Biotechnology Advances,* 22**,** 93-117.

Strecker, E. W., Quigley, M. M., Urbonas, B. R., Jones, J. E. & Clary, J. K. 2001. Determing urban stormwater BMP effectiveness. *Journal of Water Resources Planning and Management,* 127.

Subramaniam, D., Mather, P., Russell, S. & Rajapakse, J. 2016. Dynamics of Nitrate-Nitrogen Removal in Experimental Stormwater Biofilters under Intermittent Wetting and Drying. *Journal of Environmental Engineering,* 142.

Subramaniam, D. N., Logeswaran, T., Tharshikka, V. & Nilakshan, B. 2018. Dynamics of Clay Particles in Non-vegetated Stormwater Biofilters. *Water, Air, & Soil Pollution,* 229.

Sun, G., Gray, K. R. & Biddlestone, A. J. 1998a. Treatment of Agricultural and Domestic Effluents in Constructed Downflow Reed Beds Employing Recirculation. *Environmental Technology,* 19**,** 529-536.

Sun, G., Gray, K. R. & Biddlestone, A. J. 1998b. Treatment of Agricultural Wastewater in Downflow Reed Beds: Experimental Trials and Mathematical Model. *Journal of Agricultural Engineering Research,* 69**,** 8.

Sun, G., Zhao, Y., Allen, S. & Cooper, D. 2006. Generating "Tide" in Pilot-Scale Constructed Wetlands to Enhance Agricultural Wastewater Treatment. *Engineering in Life Sciences,* 6**,** 560-565.

Szota, C., McCarthy, M. J., Sanders, G. J., Farrell, C., Fletcher, T. D., Arndt, S. K. & Livesley, S. J. 2018. Tree water-use strategies to improve stormwater retention performance of biofiltration systems. *Water Research,* 144**,** 285-295.

Tanner, C. 2004. Nitrogen removal processes in constructed wetlands. *Wetlands & Ecosystems in Asia.* Elsevier.

Trang, N. T. D., Konnerup, D., Schierup, H.-H., Chiem, N. H., Tuan, L. A. & Brix, H. 2010. Kinetics of pollutant removal from domestic wastewater in a tropical horizontal subsurface flow constructed wetland system: Effects of hydraulic loading rate. *Ecological Engineering,* 36**,** 527-535.

Tunçsiper, B. 2009. Nitrogen removal in a combined vertical and horizontal subsurface-flow constructed wetland system. *Desalination,* 247**,** 466-475.

Virahsawmy, H., Stewardson, M., Vietz, G. & Fletcher, T. D. 2014. Factors that affect the hydraulic performance of raingardens: Implications for design and maintenance. *Water, Science and Technology,* 69.

Vymazal, J. 1999. Removal of BOD5 in constructed wetlands with horizontal sub-surface flow: cech experience. *Water, Science & Technology,* 40.

Vymazal, J. 2005a. Horizontal sub-surface flow and hybrid constructed wetlands systems for wastewater treatment. *Ecological Engineering,* 25**,** 478-490.

Vymazal, J. 2005b. Horizontal sub-surface flow and hybrid constructed wetlands systems for wastewater treatment. *Ecological Engineering*.

Vymazal, J. 2007. Removal of nutrients in various types of constructed wetlands. *Science of the Total Environment,* 380**,** 48-65.

Wan, Z., Li, T. & Liu, Y. 2018. Effective nitrogen removal during different periods of a field-scale bioretention system. *Environmental Science and Pollution Research International,* 25**,** 17855-17861.

Wang, C., Wang, F., Qin, H., Zeng, X., Li, X. & Yu, S.-L. 2018. Effect of Saturated Zone on Nitrogen Removal Processes in Stormwater Bioretention Systems. *Water,* 10.

Woods-Ballard, B., Kellagher, R., Martin, P., Jefferies, C., Bray, R. & Shaffer, P. 2007. *The SUDs Manual,* London, Ciria.

Wu, H., Zhang, J., Li, C., Fan, J. & Zou, Y. 2013. Mass Balance Study on Phosphorus Removal in Constructed Wetland Microcosms Treating Polluted River Water. *CLEAN - Soil, Air, Water,* 41**,** 844-850.

Wu, S., Zhang, D., Austin, D., Dong, R. & Pang, C. 2011. Evaluation of a lab-scale tidal flow constructed wetland performance: Oxygen transfer capacity, organic matter and ammonium removal. *Ecological Engineering,* 37**,** 1789-1795.

Xiong, J., Ren, S., He, Y., Wang, X. C., Bai, X., Wang, J. & Dzakpasu, M. 2019. Bioretention cell incorporating Fe-biochar and saturated zones for enhanced stormwater runoff treatment. *Chemosphere,* 237**,** 124424.

Zachritz, W. H., Hanson, A. T., Sauceda, J. A. & Fitzsimmons, K. M. 2008. Evaluation of submerged surface flow (SSF) constructed wetlands for recirculating tilapia production systems. *Aquacultural Engineering,* 39**,** 16-23.

Zhang, D. Q., Jinadasa, K. B., Gersberg, R. M., Liu, Y., Ng, W. J. & Tan, S. K. 2014. Application of constructed wetlands for wastewater treatment in developing countries--a review of recent developments (2000-2013). *Journal of Environmental Management,* 141**,** 116-31.

Zhang, D. Q., Tan, S. K., Gersberg, R. M., Zhu, J., Sadreddini, S. & Li, Y. 2012. Nutrient removal in tropical subsurface flow constructed wetlands under batch and continuous flow conditions. *Journal of Environmental Management,* 96**,** 1-6.

Zhang, L., Seagren, E. A., Davis, A. P. & Karns, J. S. 2010. The capture and destruction of Escherichia coli from simulated urban runoff using conventional bioretention media and iron oxide-coated sand. *Water environment research,* 82**,** 701-14.

Zhao, Y. J., Liu, B., Zhang, W. G., Ouyang, Y. & An, S. Q. 2010. Performance of pilot-scale vertical-flow constructed wetlands in responding to variation in influent C/N ratios of simulated urban sewage. *Bioresource Technology,* 101**,** 1693-700.

Zinger, Y., Fletcher, T. D., Deletic, A. & Wong, T. 2011. A Dual-mode Biofilter System: Case Study in Kfar Sava, Israel. *12th International Conference on Urban Drainage.* Porto Alegre/Brazil.

APPENDIX A

Table A.1: Weather data recorded between November 2020 and March 2021 for the batch experiment.

Batch	Date	Avg. temp (°C)	High temp (°C)	Low temp (°C)	Rainfall (mm)	Avg. wind speed (km/hr)	Relative humidity (%)
1	2020/11/23	15.5	19.4	13	0	2.7	60
	2020/11/24	13.5	16.3	11	8.2	2.4	61
	2020/11/25	14.4	20.3	10.8	0	2.1	63
	2020/11/26	16.3	20.8	12.1	0	7.4	58
	2020/11/27	19.7	27.4	14.9	0	8	66
	2020/11/28	19.3	23.6	15.1	0	8.7	49
	2020/11/29	19.3	26.6	14.2	0	6.3	62
2	2020/12/07	19.1	21.8	16.2	13.2	5.5	69
	2020/12/08	18.7	25.4	14.7	0	1.3	77
	2020/12/09	19.2	24.5	16.4	1.6	3.2	61
	2020/12/10	19.8	25.8	14.1	0	2.1	64
	2020/12/11	15.7	19.8	11.3	2.2	0.8	77
	2020/12/12	16.7	21.7	11.1	0.2	4	60
	2020/12/13	19.9	28.9	12.7	0	2.6	49
3	2021/01/04	26	34.7	20.8	0	3.5	62
	2021/01/05	20.9	23.9	18.6	0	8.4	66
	2021/01/06	21.4	27.6	16.6	0	6.4	61
	2021/01/07	23.6	32.7	17.8	0	5.8	61
	2021/01/08	22.4	28.9	18.4	0	7.7	55
	2021/01/09	22.2	28.2	16.2	0	3.4	67
	2021/01/10	18.9	22.2	15.2	0	8.9	55
4	2021/01/11	22.2	28.9	17.6	0	8.7	51
	2021/01/12	23.7	29.1	20.3	0	8	57
	2021/01/13	24	28.6	20.8	0	8.4	55
	2021/01/14	26.3	36.1	18.3	0	3.1	56
	2021/01/15	18.7	22.1	17.2	5	2.3	80
	2021/01/16	18.9	24.3	16.3	1	1.1	73
	2021/01/17	22.3	29.8	16.2	0	4.8	60
5	2021/01/18	24.8	34.4	17.4	0	3.1	54
	2021/01/19	20.4	26.1	15.9	0	5.3	60
	2021/01/20	23.1	31.7	17.5	0	7.4	50
	2021/01/21	24.3	36.6	16.2	0	4.3	64
	2021/01/22	26.9	35.5	19	0	2.1	68
	2021/01/23	21.3	27.9	15.4	0	3.5	68
	2021/01/24	19.9	25.4	15.7	0	10.1	52

Batch	Date	Avg. temp (°C)	High temp (°C)	Low temp (°C)	Rainfall (mm)	Avg. wind speed (km/hr)	Relative humidity (%)
6	2021/02/01	18.5	23.6	14.6	0.2	10	48
	2021/02/02	24.7	34.2	15	0	2.3	42
	2021/02/03	23.7	32.2	17.6	0	4	65
	2021/02/04	22.2	29	18.2	0	7.9	68
	2021/02/05	23.9	31.5	19	0	6.1	68
	2021/02/06	24.3	32.4	18.4	0	3.7	70
	2021/02/07	20.7	24.8	17.6	0	7.7	56
7	2021/02/08	21.6	28.7	16.3	0	8.4	62
	2021/02/09	23.5	31	18.2	0	6.6	67
	2021/02/10	25.2	33.2	18.5	0	6.3	70
	2021/02/11	26.6	36.6	18.9	0	4.3	68
	2021/02/12	25.7	33.6	20.4	0	3.4	76
	2021/02/13	23.6	30.2	18.7	0	2.7	69
	2021/02/14	19.2	22.3	16.9	0.4	1.9	74
8	2021/02/16	21.3	28.7	16.9	0	8.2	43
	2021/02/17	21.6	28.9	14.4	0	3.2	56
	2021/02/18	18.6	24.8	13.5	0	2.9	60
	2021/02/19	19.9	27.8	15.4	0	5.5	56
	2021/02/20	18.8	23.8	14.7	0	2.9	49
	2021/02/21	17.1	21.9	12.8	0	4.7	57
	2021/02/22	19.8	28.7	11.6	0	3.9	53
9	2021/02/23	19.7	27.5	12.3	0	2.3	58
	2021/02/24	20.8	28.7	17.5	0	6.9	62
	2021/02/25	20.1	25.7	16.8	0	10	55
	2021/02/26	21.8	27.6	17.9	0	10	51
	2021/02/27	22.2	29.3	17.3	0	8.9	47
	2021/02/28	26.1	35	19.7	0	6.8	50
	2021/03/01	24.3	30.3	18.6	0.4	1.3	50
10	2021/03/02	21.2	29.3	16.1	0	3.1	67
	2021/03/03	20.6	29.2	13.6	0	1.6	67
	2021/03/04	19.3	24.2	16.4	0	4.2	67
	2021/03/05	21.7	29.4	16.6	0	4.5	50
	2021/03/06	19.9	26.4	15.7	0	2.3	64
	2021/03/07	17.9	24.4	14.1	0	3.5	81
	2021/03/08	17.4	23.7	12.7	0	2.6	50
11	2021/03/09	15.9	20.1	11.4	4.6	4.3	60
	2021/03/10	18.2	19.6	15.6	36.8	6.4	92
	2021/03/11	19.4	25	16	0.6	2.3	61
	2021/03/12	18.3	30.8	14.9	0	0.2	53
	2021/03/13	17.3	26.2	14.2	0	2.7	68
	2021/03/14	18.8	19.7	16.8	0.2	5.3	70
	2021/03/15	21	19.1	16.1	1.2	4.8	86

Batch	Date	Avg. temp (°C)	High temp (°C)	Low temp (°C)	Rainfall (mm)	Avg. wind speed (km/hr)	Relative humidity (%)
12	2021/03/16	18.8	23.8	15.5	0	6.9	61
	2021/03/17	21	28.1	14.7	0	2.3	59
	2021/03/18	18.9	25.6	14.9	0	2.1	74
	2021/03/19	18.1	22.2	16.2	0	6.3	59
	2021/03/20	17.9	21	15.9	0	7.7	62
	2021/03/21	19.3	24.5	16.6	0	7.9	50
	2021/03/22	21.1	27.1	16.7	0	7.1	51
13	2021/03/24	22.8	28.7	17	0	5	57
	2021/03/25	23.4	32.2	15.9	0	1	53
	2021/03/26	18	22.3	15.9	0.6	3.1	65
	2021/03/27	17	20.6	14.5	2.6	5.1	67
	2021/03/28	20.3	26.3	13.9	0	2.7	54
	2021/03/29	23.1	31.8	16.2	0	1	49
	2021/03/30	17.8	24.7	11.9	0	1.9	69

APPENDIX B

This section of the Appendices contains analyses of several key assumptions for the NH$_3$LS, NH$_3$LSV, TPLS and TPLSV models.
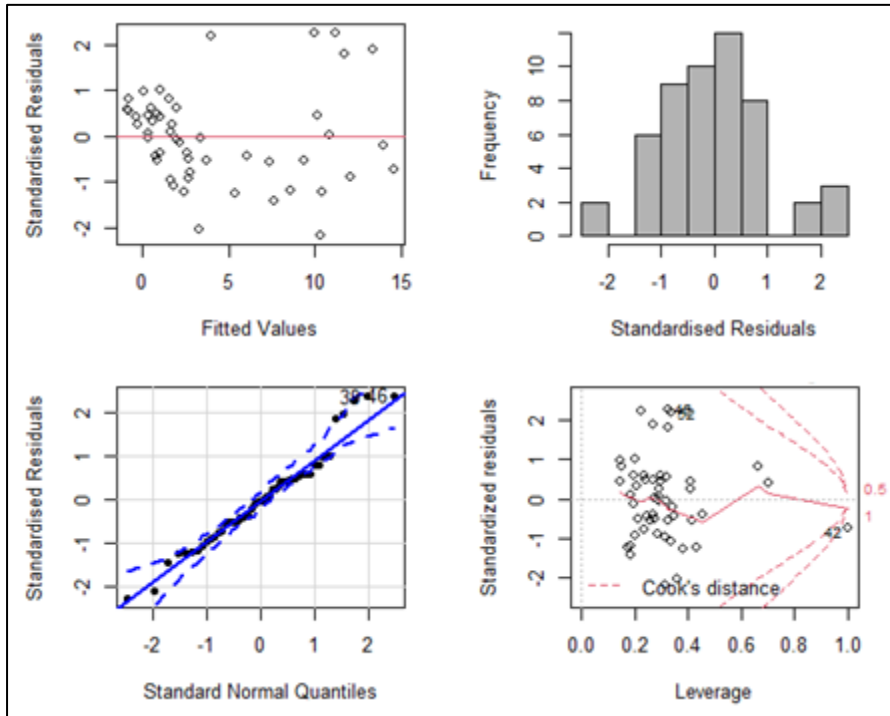

Figure B.1: Residual plots for NH$_3$LS model for outflow NH$_3$ concentration.
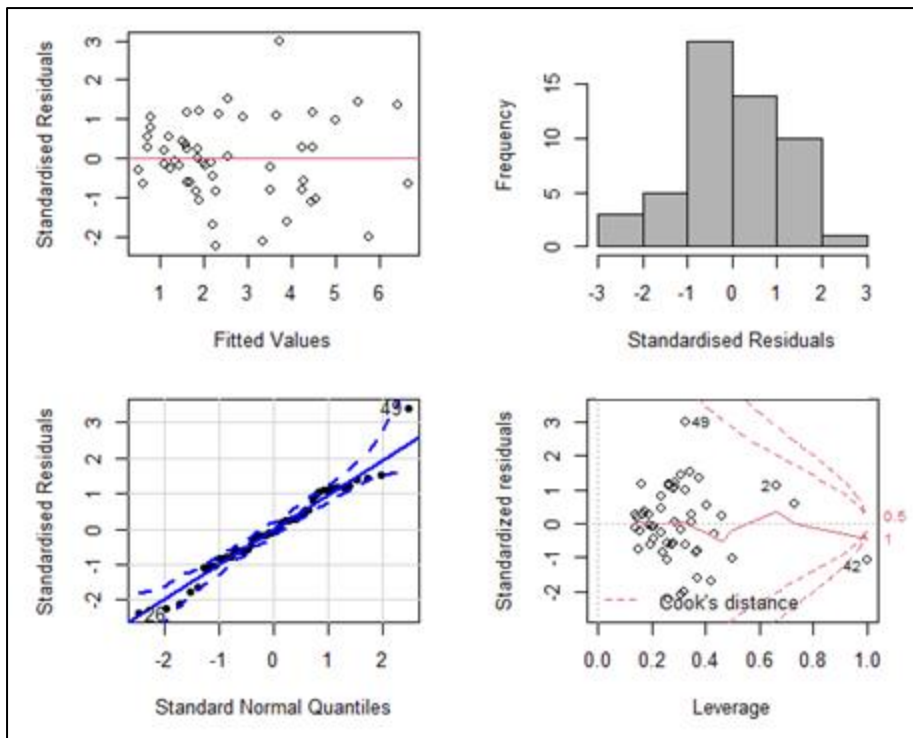

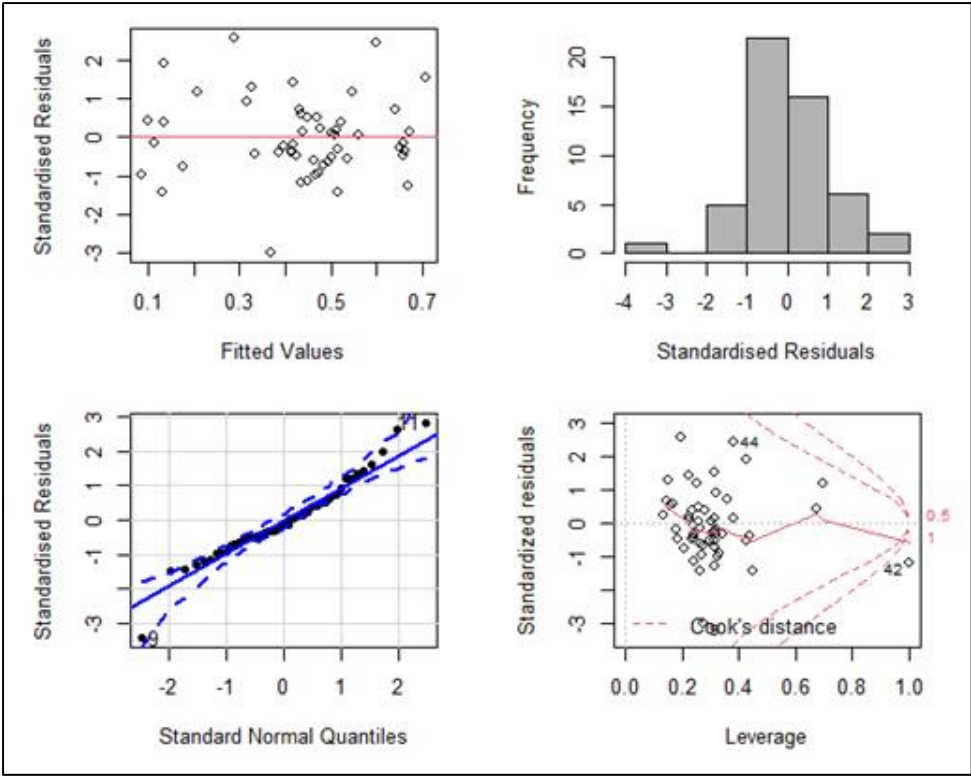Figure B.2: Residual plots for NH$_3$LSV model for outflow NH$_3$ concentration.

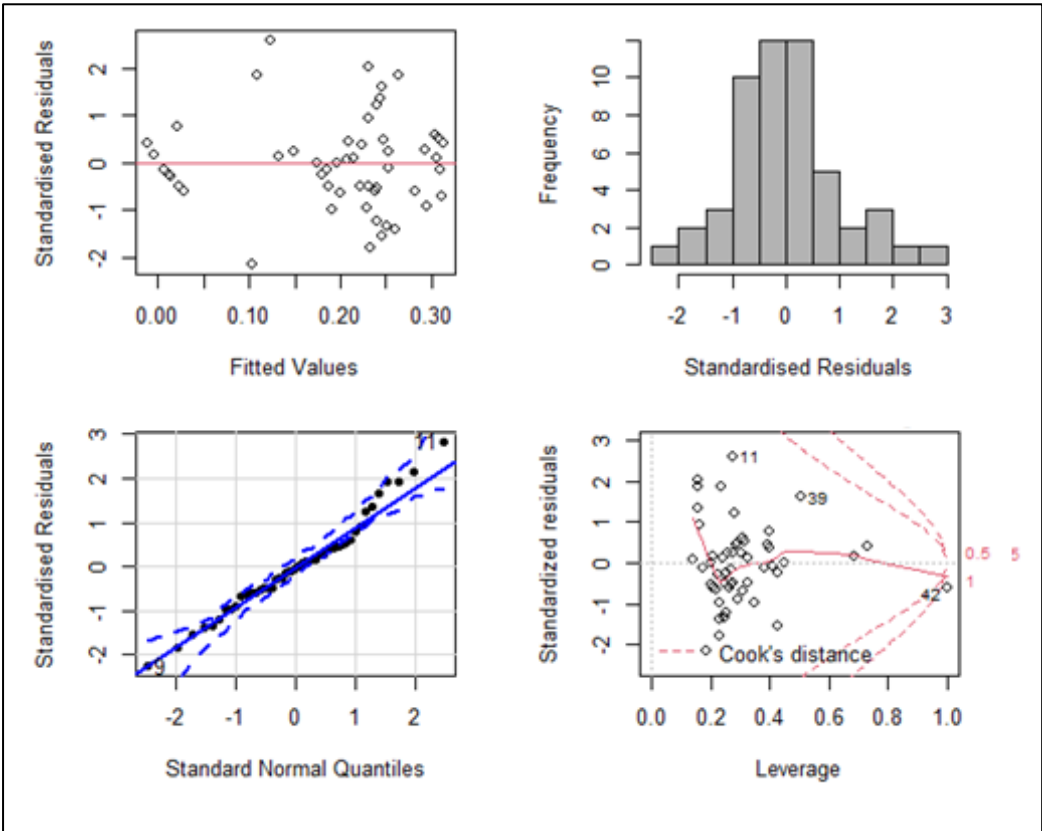Figure B.3: Residual plots for TPLS model for outflow TP concentration.

Figure B.4: Residual plots for TPLSV model for outflow TP concentration.